Novel regulators of the cell division cycle

Phd Thesis

Sigrid Bratlie Thoresen

Centre for Cancer Biomedicine, Faculty of Medicine, University of Oslo

Department of Biochemistry, Institute for Cancer Research, Oslo University Hospital

UiO : Faculty of Medicine
University of Oslo

Centre for Cancer Biomedicine

HELSE SØR-ØST

Series of dissertations submitted to the
Faculty of Medicine, University of Oslo
No. 1758

ISBN 978-82-8264-838-7

Cover: Inger Sandved Anfinsen.
Printed in Norway: AIT Oslo AS.

Produced in co-operation with Akademika Publishing.
The thesis is produced by Akademika Publishing merely in connection with the thesis defence. Kindly direct all inquiries regarding the thesis to the copyright holder or the unit which grants the doctorate.

-My PhD- the short version

Table of contents

Acknowledgements 6

Abbreviations 8

Publications included in this thesis 11

Introduction 14

The cell division cycle 14

Cell cycle checkpoints – key regulatory mechanisms of the cell division cycle 16

PtdIns3P and the ESCRT machinery regulate membrane remodelling events during cell cycle entry and exit 23

PtdIns3P, ESCRTs and VPS4 in growth factor receptor degradation 30

PtdIns3P, ESCRTs and VPS4 in cytokinesis 32

Knowledge is key 35

Summary of the included papers 39

Discussion 42

Differential roles of the PI3K-III complex 42

PtdIns3P as a positive regulator of cytokinesis 44

Positive vs negative regulation of cytokinesis – both can lead to abscission failure 45

ANCHR (ZFYVE19) – a previously uncharacterized protein 46

ANCHR as a regulator of the abscission checkpoint 47

ANCHR in G2/M checkpoint regulation 51

Implications for cancer: PtdIns3P and ANCHR 56

Experimental considerations 62

Conclusions and future perspectives 68

Reference List 70

Acknowledgements

This work was carried out at the Department of Biochemistry, Institute for Cancer Research at the Norwegian Radium Hospital in the laboratory of Professor Harald Stenmark between Nov. 2008 and Feb. 2014. The funding received from Helse Sør-Øst and the Centre for Cancer Biomedicine (CCB) is gratefully acknowledged.

First and foremost I would like to thank my supervisor Professor Harald Stenmark for giving me the opportunity to do such exciting and cutting edge work! Not only have you been a constant support and helped me navigate the treacherous waters of experimental science and publishing, but have also allowed me to develop my own ideas and decide the direction of all my projects. I could not have asked for a better supervisor.

Special thanks also to Coen Campsteijn, who has proved a bottomless well of knowledge about everything from cell cycle regulation to British comedy. Your neverending enthusiasm and insightful input have been substantial contributors to the success of these projects, and a source of inspiration for me throughout these last years.

Also many thanks to Nina Marie Pedersen and Camilla Raiborg for introducing me to the intricate world of HeLa cells and the workings of the lab. I further wish to thank all my other collaborators for their significant effort, excellent work and essential guidance, including Kay O. Schink, Marina Vietri, Hilde Abrahamsen, Knut Liestøl and Jens Andersen. Great discussions and technical expertise was also to be found at the Department of Radiation Biology, in particular from Randi Syljuåsen, Trond Stokke, Kirsti Solberg Landsverk and Idun Dale Rein, and Lina Cekaite at the Department of Cancer Prevention.

Thanks also to everyone in the Stenmark group and at the Department of Biochemistry, past and present, for providing such a great working environment, encouraging scientific discussions and collaboration, and many laughs. Special thanks

to Nadja Katheder and Marina Vietri for many scientific (and not-so-scientific) discussions over the years, and for being such great office mates through good times and bad! A well deserved thanks also to Chema, our IT-expert, for always being at hand to solve every thinkable computer problem and for excellent DJ-ing services. Many thanks also to the department technical staff, the expertise and efforts of whom have made this work possible.

To end, I wish to acknowledge my family. Thanks to my parents for always encouraging me to be curious (nosy), an independent thinker (opinionated) and perseverant (stubborn), traits that have all proved useful during the pursuit of a PhD. Thanks also to my daughter Helene for unconditional love, and for leaving my things alone during hectic periods of working from home. And last, but certainly not least, this work would not have been possible without the neverending love and support of my husband, Ole, who has endured years of attempted explanations of what on earth I am spending so many of my hours doing. The faith you have in me has always spurred me on and inspired me to do well.

Abbreviations

ALIX – Alg2-interacting Protein X

AMBRA1 – Activating Molecule in Beclin 1-Regulated Autophagy

AML – Acute Myeloid Leukemia

ANCHR – Abscission / NoCut Checkpoint Regulator

ATG14 - Autophagy-related protein 14-like protein

ATM – Ataxia Telangiectasia Mutated

ATR – Ataxia Telangiectasia and Rad3-related protein

BIF-1 – Endophilin B1

BORA – Aurora A kinase activator

CDC – Cell Division Cycle

CDK – Cyclin Dependent Kinase

CEP – Centrosomal Protein

CHK – Checkpoint Kinase

CHMP – Chromatin Modifying Protein / Charged MVB Protein

CK – Caseine Kinase

CLL – Chronic Lymphocytic Leukemia

CPC – Chromosomal Passenger Complex

DAG - Diacylglycerol

DNA – Deoxyribonucleic Acid

DSB – Double-Strand Break

EE - Early endosome

EEA – Early Endosome Antigen

EGF – Epidermal Growth Factor

EGFR – Epidermal Growth Factor Receptor

ER – Endoplasmic Reticulum

ESCRT - Endosomal Sorting Complex Required for Transport

FYVE - Fab1, YOTB, Vac1 and EEA1

FYVE-CENT - FYVE domain containing centrosomal protein

G1 – Growth / Gap phase 1

G2 – Growth / Gap phase 2

GFP – Green Fluorescent Protein

HRS – Hepatocyte growth factor regulated tyrosine kinase substrate

ILV – Intraluminal Vesicle

IR – Ionizing Radiation

IST – Increased Sodium Tolerance

KIF – Kinesin superfamily of proteins

LIP – LYST-interacting Protein

M - Mitosis

MIM – MIT-interacting Motif

MIT – Microtubule Interaction and Transport

MKLP – Mitotic Kinesin-like Protein

MLL – Mixed Lineage Leukemia

MVB – Multivesicular body

MYT – Myelin Transcription Factor

NEK - NIMA (Never In Mitosis)-Related Kinase

NHEJ – Non-Homologous End Joining

PI - Phsophoinositide

PI3K-III – Phosphatidylinositol 3-kinase class III complex

PIN – Peptidyl-prolyl cis-trans Isomerase NIMA-interacting

PLK – Polo-Like Kinase

PtdIns - Phosphatidylinositol

PX - Phox homology

RAB – Ras-related Protein

RNA – Ribonucleic Acid

ROS – Reactive Oxygen Species

RTK – Receptor Tyrosine Kinase

RUBICON – Run domain Beclin 1 interacting and cysteine-rich containing protein

S – DNA Synthesis phase

SCF/β-TrCP – Skp, Cullin, F-box containing complex / β-transducin repeat-containing Protein

SDS-PAGE – Sodium Dodecyl Sulfate Polyacrylamide Gel Electrophoresis

siRNA – Short interfering RNA

STAM – Signal Transducing Adapter Molecule

TSG – Tumour Susceptibility Gene

TTC – Tetratricopeptide Repeat Domain

UVRAG - UV radiation resistance-associated gene

VPS – Vacuolar Protein Sorting

WEE – Wee Kinase

ZFYVE – FYVE-family of Zinc Fingers

Publications included in this thesis

I. A phosphatidylinositol 3-kinase class III sub-complex containing VPS15, VPS34, Beclin 1, UVRAG and BIF-1 regulates cytokinesis and degradative endocytic traffic.

Thoresen SB, Pedersen NM, Liestøl K, Stenmark H.

Exp. Cell Res., 2010 Dec 10; 316(20): 3368-78

II. ANCHR mediates Aurora B-dependent abscission checkpoint control via retention of VPS4.

Thoresen SB, Campsteijn C, Vietri M, Schink KO, Liestøl K, Andersen JS, Raiborg C, Stenmark H.

Submitted for publication

III. ANCHR is required for G2/M DNA damage checkpoint function

Thoresen SB, Campsteijn C, Abrahamsen H, Andersen JS, Stenmark H.

Manuscript

Related publications not included in this thesis:

Nedd4-dependent lysine-11-linked polyubiquitination of the tumour suppressor Beclin 1. Platta HW, Abrahamsen H, Thoresen SB, Stenmark H. *Biochem J., 2012 Jan 1; 441(1): 399-406*

"Pluck any atom from your body, and it is no more alive than is a grain of sand. It is only when they come together within the nurturing refuge of a cell that these diverse materials can take part in the amazing dance that we call life."

–Bill Bryson, "A Short History of Nearly Everything"

Introduction

The cell constitutes one of the fundamental building blocks of life, with trillions of cells making up a human body. All cells are subject to a large number of regulatory mechanisms to maintain normal cell division, growth and function. This involves the complex interplay of macromolecules such as lipids and proteins, which make up vast signalling networks in the cell that ultimately determine cell fate. The complexity of these networks and the diverse functions of proteins and lipids are still not fully understood. However, it is becoming increasingly apparent that many play key roles in multiple processes, where they differentially participate in a context-dependent manner, depending on subcellular compartmentalization, timing, chemical modifications and availability of other macromolecules that in concert control their function. It is perhaps not surprising, in an evolutionary sense, that macromolecules are functionally diverse, since many cellular processes depend on similar mechanisms. For instance, membrane trafficking and deformation are central to several processes such as endocytic transport of membrane-bound vesicles, membrane scission during the separation of two dividing daughter cells (cytokinesis) and virus budding from the plasma membrane. Here, many key molecular events and factors are shared, including lipid signalling and protein-mediated membrane remodelling. The multifaceted interplay between different proteins and lipids and their differential context-dependent functions are recurring themes throughout this thesis, and I will summarize and discuss my findings in this perspective.

The cell division cycle

Cell proliferation is the fundamental process supporting life, and drives both development, normal tissue homeostasis and pathological conditions such as cancer. When a cell receives stimuli to divide such as growth factors, the cell embarks on a

precisely controlled journey through the cell cycle, where DNA is replicated and equally transmitted into two nascent daughter cells (Figure 1).

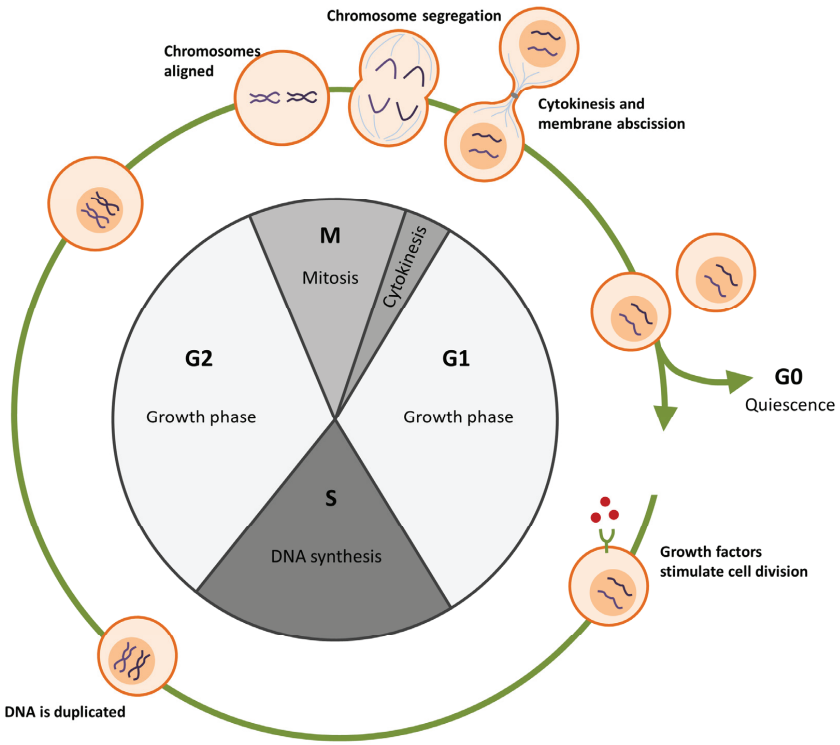

Figure 1: Schematic representation of cell division. Upon stimulation by proliferative signals such as growth factors, the cell progresses through the cell cycle where the DNA is duplicated and segregated into two daughter cells.

The eukaryotic cell cycle can be divided into several sequential phases; An initial growth / gap phase (G1), a DNA synthesis phase (S), a second growth / gap phase (G2) and finally mitosis (M), where the duplicated DNA is condensed and segregated equally into the two nascent daughter cells (Norbury and Nurse, 1992). Cytokinesis is the final step of mitosis and starts with the formation and contraction of an actomyosin ring, forming a continuously ingressing cleavage furrow between daughter cells and their segregating DNA. At the centre of the developing intercellular bridge is the protein-

dense midbody ring that together with interconnecting microtubule spindle defines the midbody, a structure that harbours many regulators of cell division. Cytokinesis culminates in membrane abscission where the two daughter cells are physically separated. Subsequently, the cell either progresses through another round of cell division or exits the cell cycle to enter a non-dividing, quiescent state known as G0.

Cell cycle progression is controlled by the concerted action of multiple proteins and other macromolecules, which are subjected to many regulatory mechanisms. Firstly, control of transcription and degradation impacting on protein abundance help establish cell cycle irreversibility. Moreover, protein activity is often dependent on phosphorylation status which is regulated by vast networks of protein kinases and phosphatases. These are particularly important for prevention of cell cycle progression in the presence of DNA aberrations, and regulate phase-specific signalling pathways that are collectively termed cell cycle checkpoints.

Cell cycle checkpoints – key regulatory mechanisms of the cell division cycle

As the cell progresses through the cell cycle, several checkpoints function to monitor the integrity of the DNA and inhibit transition to the next phase if it is compromized, thereby ensuring fidelity of cell division (Hartwell and Weinert, 1989). If aberrations are detected, the cell cycle arrests until they are resolved, or, if they are too extensive, the cell undergoes programmed cell death (apoptosis). First, the G1/S checkpoint induces arrest prior to DNA replication if DNA is damaged or in the absence of proliferative signals such as growth factors. Second, the intra-S checkpoint slows cell cycle progression in the case of DNA replication errors. Next, the G2/M checkpoint is activated prior to mitosis in the presence of DNA damage. During mitosis, the spindle checkpoint prevents separation of sister chromatids until they are all properly attached to the spindle machinery. And finally, the recently identified abscission (NoCut) checkpoint functions to prevent DNA aberrations and multinucleation during cytokinesis (Figure 2).

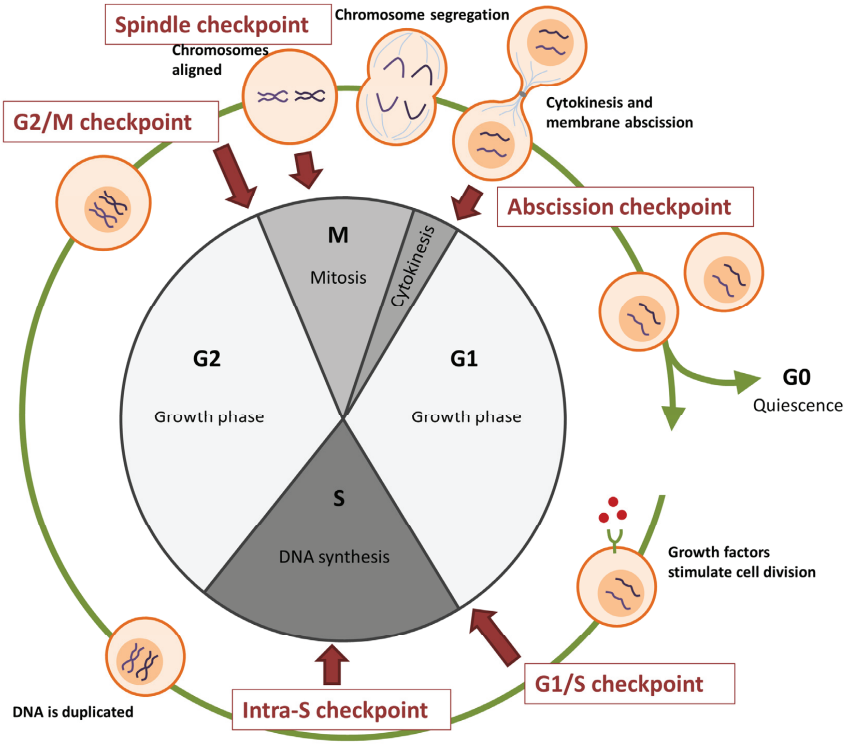

Figure 2: Cell cycle checkpoints. As the cell progresses through the cell cycle, several checkpoints operate to monitor the integrity of the DNA, including the G1/S checkpoint, the intra-S checkpoint, the G2/M checkpoint, the spindle checkpoint and the recently identified abscission checkpoint.

While all checkpoints serve important functions, this thesis will focus on the two checkpoints governing mitotic entry and completion, namely the G2/M checkpoint and the abscission checkpoint, respectively. Here, compromized checkpoint signalling may have catastrophic consequences for the maintenance of DNA integrity, and has been linked to development of cancer.

The G2/M checkpoint

The cell is constantly subjected to a plethora of external and internal stresses, many of which can damage DNA. These include reactive oxygen species (ROS) as a by-product of cell metabolism, ionizing radiation (IR), chemical agents and ultraviolet light. Of all the possible outcomes, double-strand DNA breaks (DSBs) are known as the most toxic type of DNA lesion (Ward, 1990). Prior to mitosis, the G2/M DNA damage checkpoint arrests the cell cycle to allow time for repair of the damaged DNA or to initiate apoptotic cell death if DNA repair is unsuccessful. These responses both constitute important tumour suppressive mechanisms (Jackson and Bartek, 2009). Cells that fail to arrest in G2 upon DNA damage progress through mitosis with DNA lesions, which can lead to missegregation and subsequent chromosomal instability and aneuploidy in daughter cells, both of which are critical contributors to cancer development (Fenech et al., 2011; Chow and Poon, 2010).

Several parallel signalling pathways converge on the central Cyclin B/CDK1 complex which is pivotal in regulating transition from G2 to mitosis. In G2, CDK1 is maintained in an inactive phosphorylated state by the kinases WEE1 and MYT1 (Parker and Piwnica-Worms, 1992; Booher et al., 1997), but as cells approach mitosis, the phosphatase CDC25 dephosphorylates CDK1, leading to its activation (Karlsson-Rosenthal and Millar, 2006). Once active, the Cyclin B/CDK1 complex promotes several early mitotic events such as chromosome condensation, spindle pole formation and disassembly of the nuclear envelope (Andersen, 1999; Nigg, 1995; Heald and McKeon, 1990; Kimura et al., 1998). Upon accumulation of DNA lesions, G2/M checkpoint signalling is initiated by DSB-sensing protein complexes that recruit and promote the activation of the kinases ATM/ATR (Lee and Paull, 2004). A positive feedback loop involving ATM-mediated phosphorylation of the histone variant H2AX, yielding γH2AX, causes further accumulation of ATM and extensive signal propagation at DNA damage foci (Stucki and Jackson, 2006). Signals are relayed via the ATM/ATR targets CHK1/CHK2, which in turn inactivate CDC25 (Donzelli and Draetta, 2003).

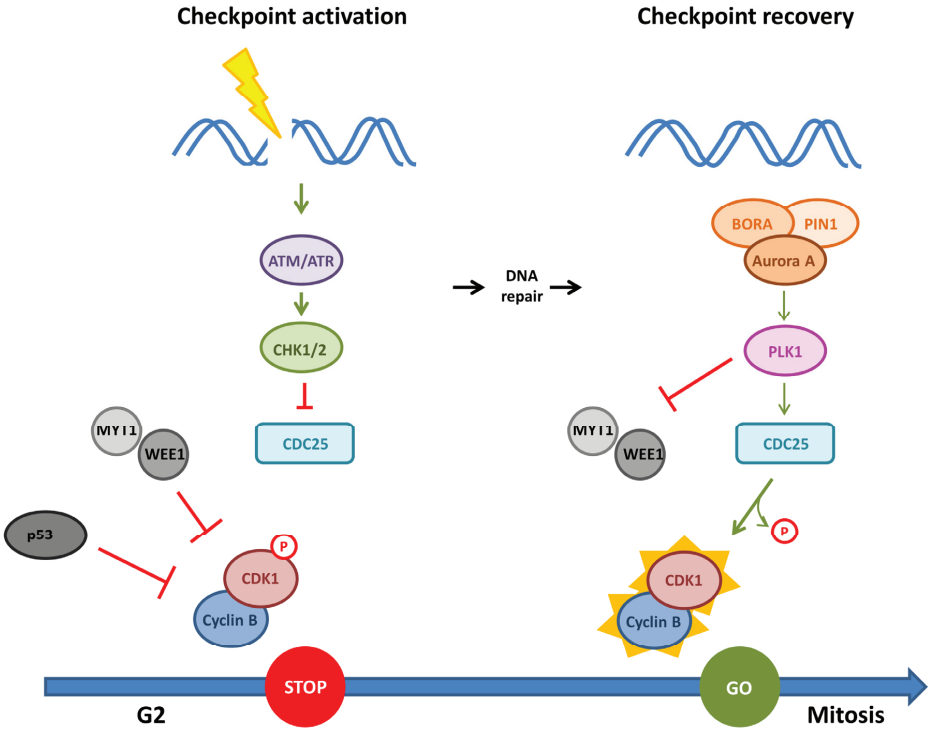

Figure 3: Activation and recovery of the G2/M checkpoint. Upon DNA damage, Cyclin B/CDK1 is inactivated by inhibition of CDC25 by a signalling cascade involving ATM/ATR and CHK1/2, causing a G2 arrest. Following repair of DNA lesions, the cell cycle resumes through Aurora A/PLK1-dependent checkpoint recovery.

A parallel signalling cascade involves the tumour suppressor p53, mainly through transcriptional regulation of target genes, that ultimately serves to inhibit and dissociate the Cyclin B/CDK1 complex (Taylor and Stark, 2001). Once DNA lesions have been repaired, the cell is ready to resume cell cycle progression and enter mitosis through the process of checkpoint recovery. This involves positive regulation of the Cyclin B / CDK1 complex by PLK1-mediated activation of CDC25 (van Vugt et al., 2004). PLK1 itself is activated by Aurora A kinase together with its cofactor BORA (Macurek et al., 2008; Seki et al., 2008b). However, some cells are able to exit G2 arrest and enter mitosis before the damaged DNA has been fully repaired. This is termed adaptation, and involves premature PLK1-dependent checkpoint recovery (Syljuasen et al., 2006).

The G2/M checkpoint is schematically represented in Figure 3. Deregulation or mutation of G2/M checkpoint signalling factors can result in failure to maintain G2 arrest upon DNA damage. This leads to mitotic entry in the presence of damaged DNA, a known cause of genomic instability.

The abscission checkpoint:

During mitotic exit, the cell needs to faithfully and equally segregate sister chromatids into each daughter cell, followed by reformation of the nuclear envelope. Pioneering work in both yeast and mammalian cells has recently identified the existence of an abscission checkpoint (also termed the NoCut checkpoint) that delays cytokineic membrane abscission in the presence of lagging chromatin spanning the intercellular bridge or when nuclear architecture is disrupted. This is controlled by the kinase Aurora B, the sustained activity of which is required for maintenance of cytokinesis arrest. Aurora B can be activated either by incompletely formed nuclear envelopes (Mackay et al., 2010), the details of which are still not fully elucidated, or by chromatin-mediated signalling. The latter is supported by obervations that chromatin bridges, but not a mechanical barrier such as asbestos fibers spanning the intracellular bridge, can activate Aurora B (Steigemann et al., 2009). Furthermore, at least in yeast, Aurora B-dependent NoCut activation requires chromatin passenger complex (CPC)-facilitated sensing of acetylated chromatin (Mendoza et al., 2009).

Prevention of untimely abscission is crucial to avoid chromosomal damage, cleavage furrow regression and multinucleation (Steigemann et al., 2009; Carlton et al., 2012). Here, Aurora B signalling plays a dual role in the execution of cytokinesis arrest. Firstly, it phosphorylates midbody-localized MKLP1 to stabilize the interaction between the ingressed cleavage furrow and the midbody to prevent furrow regression in the presence of chromosome bridges. Secondly, it targets components of the Endosomal Sorting Complex Required for Transport (ESCRT) machinery to prevent premature abscission. Specifically, Aurora B can phosphorylate CHMP4C, an ESCRT-III subunit

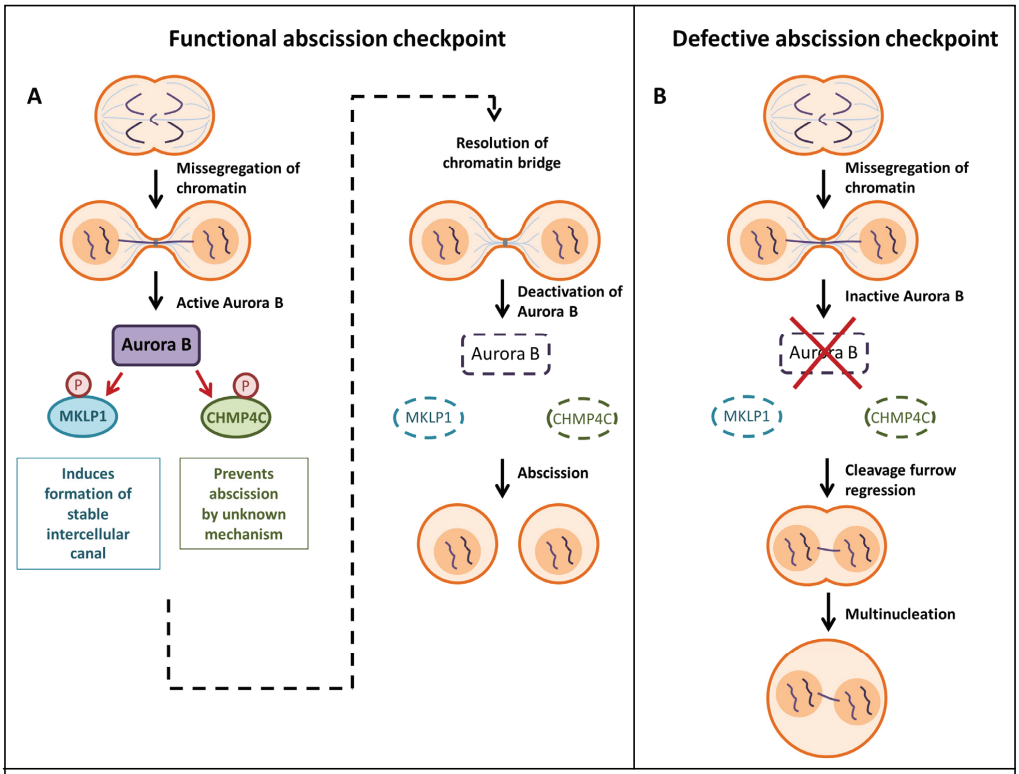

Figure 4: The abscission checkpoint. (A) In the presence of lagging chromatin, Aurora B-dependent cytokinesis arrest is executed by I) MKLP-mediated stabilization of the intercellular canal and II) CHMP4C-mediated abscission delay by an unknown mechanism. Upon resolution of the chromatin bridge, Aurora B is deactivated and abscission proceeds. **(B)** Deregulated abscission checkpoint function results in cleavage furrow regression and multinucleation.

that is required for maintenance of the abscission checkpoint in mammals (Carlton et al., 2012). Figure 4 illustrates abscission checkpoint function. It was shown that CHMP4C interacts with the CPC-subunit Borealin and, following phosphorylation by Aurora B, relocalizes from the midbody arms to the midbody ring. Moreover, mutation of the Aurora B target residue abolished cytokinesis delay induced by overexpression of CHMP4C. In contrast, another study found that mutation of the CHMP4C Aurora B target sites rather increased cytokinetic arrest and multinucleation, but not its localization pattern (Capalbo et al., 2012). Thus, the mechanism by which CHMP4C induces abscission delay is unknown, and conflicting observations suggest alternative

modes of action. The roles of the ESCRT machinery in abscission will be described later. Although the importance of coordinating chromatin segregation with abscission timing is largely appreciated, the mechanistic details of abscission checkpoint regulation have only begun to be unravelled.

It is clear that checkpoint control of mitotic entry and completion rely heavily on the abundance and phosphorylation status of many regulatory factors. Here, the actions of kinases are particulary crucial, with key master regulators highlighted in figure 5.

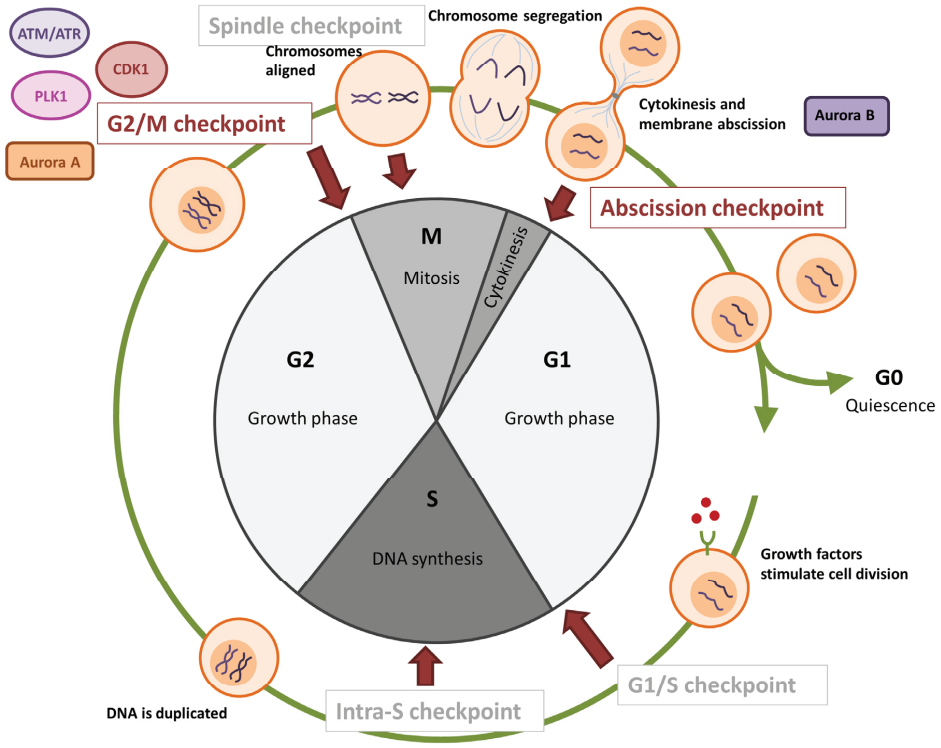

Figure 5: Kinases are important for checkpoint regulation during mitotic entry and completion. The G2/M checkpoint and mitotic entry are controlled by the kinases CDK1, ATM/ATR, Aurora A and PLK1. The abscission checkpoint during cytokinesis is controlled by the kinase Aurora B.

Like protein kinases, lipid kinases also play central roles in the regulation of multiple cellular processes. Their lipid targets are small organic molecules that act as structural components of cellular membranes, and are important for many signalling events. Of these, phosphoinositides (PIs), despite being low-abundant, play critical roles in the regulation of key processes. Here I will focus on the PI phosphatidylinositol-3-phosphate (PtdIns3P) and its effectors which control stress-response and nutrient scavenging (autophagy), growth factor (mitogenic) signalling, and cytokinesis. Importantly, the latter two functions are crucial during initiation and completion of the cell division cycle.

PtdIns3P and the ESCRT machinery regulate membrane remodelling events during cell cycle entry and exit

When a cell is stimulated by growth factors, proliferative signals are transmitted through cell surface receptors that activate intracellular signalling cascades. Consequently, the cell division cycle is initiated. To avoid uncontrolled proliferation, the signal must be terminated. This is achieved by engulfment of the receptor and its ligand through a process termed endocytosis, followed by lysosomal degradation. This process depends on a series of membrane remodelling events that, interestingly, are mechanistically similar to cytokinetic membrane abscission during cell cycle exit. Furthermore, these processes require many of the same regulatory factors, including PtdIns3P and its protein effectors such as the Endosomal Sorting Complex Required for Transport (ESCRT) machinery. The structure and function of these factors in endosomal membrane trafficking and cytokinesis will be described in greater detail.

PtdIns3P – a lipid regulating multiple cellular processes

Different PIs localize to specific subcellular organelles, thereby defining organelle identity. Furthermore, because they are important signalling molecules, their

biogenesis and turnover are subject to strict regulation. One important phosphoinositide is PtdIns3P, generated by phosphorylation of the hydroxyl group at the 3' position of the inositol head group of PtdIns by the PI3K (phosphatidylinositol 3-kinase) class III (PI3K-III) complex (Figure 6). PtdIns3P localizes mainly to early endosomes and on internal membranes of multivesicular bodies (MVBs), but has also been reported to reside within autophagosomes, smooth endoplasmic reticulum (ER) and golgi (Gillooly et al., 2000; Obara et al., 2008; Sarkes and Rameh, 2010). Importantly, PtdIns3P is involved in the regulation of several essential cellular processes, including endosomal membrane trafficking (degradation of growth factor receptors), autophagy (degradation of cytoplasmic content) and cytokinesis, the final step of cell division where two daughter cells separate. However, PtdIns3P-dependent functions need to be differentially regulated both temporally and spatially. Although this is not fully understood, it is achieved at least partly by differential composition and regulation of the lipid kinase complex required for PtdIns3P generation.

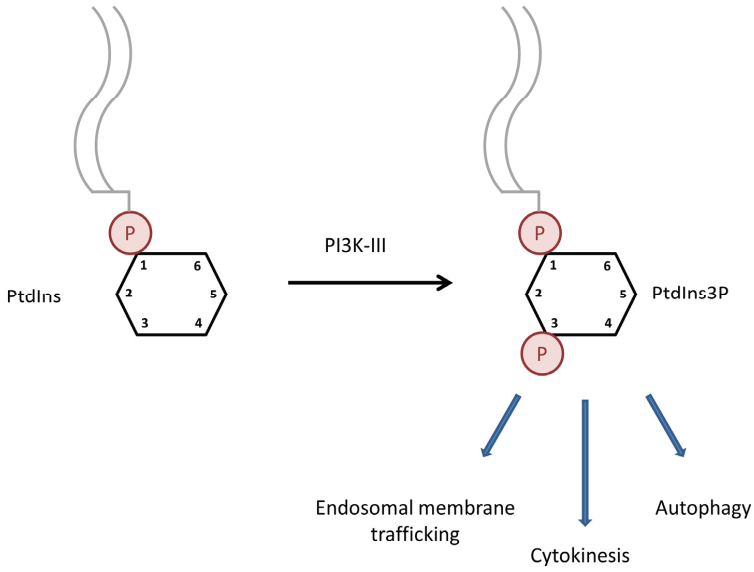

Figure 6: PtdIns3P. PtdIns3P is the catalytic product of the PI3K-III complex, and is generated by phosphorylation of the hydroxyl group at the 3' position of the inositol head group of PtdIns. PtdIns3P regulates endosomal membrane trafficking, cytokinesis and autophagy.

PI3K-III

The PI3K-III complex is a multisubunit lipid kinase protein complex that catalyses the formation of PtdIns3P. The phosphorylation event is carried out by the catalytic subunit VPS34, which is recruited to the complex by membrane-associated VPS15/p150 (Backer, 2008; Christoforidis et al., 1999; Murray et al., 2002; Panaretou et al., 1997). VPS34 is further positively regulated by its binding partner Beclin 1 (Atg6/Vps30), the third component of the core PI3K-III complex (Kihara et al., 2001a; Liang et al., 2006; Furuya et al., 2005) which is involved in all functions of PI3K-III. Beclin 1 further serves as a selective binding platform for other proteins that regulate the activity of the complex in a context-dependent manner. Importantly, UV radiation resistance-associated gene (UVRAG) or Autophagy-related protein 14-like protein (ATG14L) interact with Beclin 1 in a mutually exclusive manner, conferring functional specificity to PI3K-III; where UVRAG seems to play a role mainly in endocytic membrane trafficking, ATG14L seems to be predominantly involved in autophagy (Liang et al., 2006; Itakura et al., 2008; Itakura and Mizushima, 2009; Kihara et al., 2001b). Although some studies also suggest a role for UVRAG in autophagy, UVRAG and ATG14L seem to regulate different steps of this process (Itakura et al., 2008). Another protein, AMBRA 1, associates with Beclin 1 only in concert with ATG14L, suggesting it is specifically involved in autophagy. Through UVRAG, PI3K-III can also recruit endophilin B1 (BIF-1) or Run domain Beclin 1-interacting and cysteine-rich containing protein (RUBICON), positive and negative regulators of VPS34 activity, respectively (Takahashi et al., 2007; Zhong et al., 2009). The current knowledge about the context-dependent PI3K-III subcomplexes is summarized in Figure 7. In addition to endosomal membrane trafficking and autophagy, PtdIns3P was also recently shown to regulate cytokinesis, the final separation of two dividing daughter cells, where VPS34 and Beclin 1 are required for completion of membrane abscission (Sagona et al., 2011). However, the roles of the other PI3K-III subunits in this process have not yet been assessed.

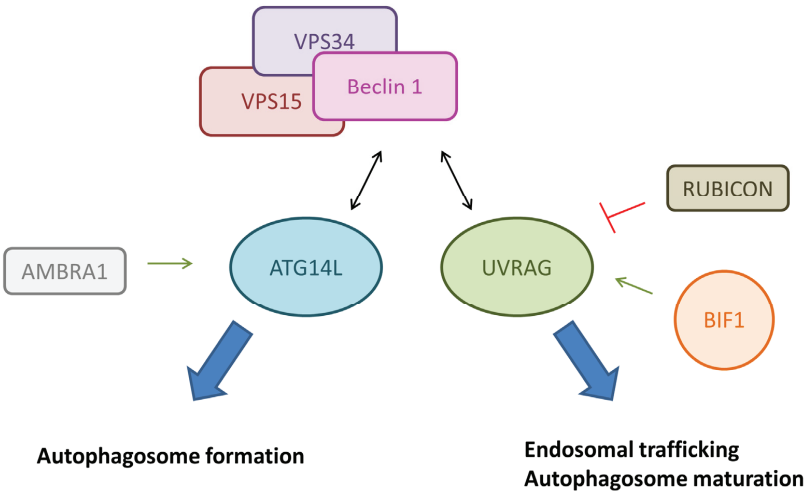

Figure 7: PI3K-III sub-complexes. The core PI3K-III complex consists of VPS15, VPS34 and Beclin 1. Research suggests that UVRAG and ATG14L can associate with Beclin 1 in a mutually exclusive and context-dependent manner. Additional factors can further control PI3K-III activity, through AMBRA1, a regulator of ATG14L, and RUBICON and BIF-1 that are negative and positive regulators of UVRAG, respectively. The specific sub-complexes are implicated in different PtdIns3P-dependent processes.

Although several aspects of PI3K-III function are known, many studies have been performed using yeast cells. Thus, although many subunit orthologues have been identified, the structure and functions of the PI3K-III complex in mammalian cells are less well-defined. Whereas functional studies have implicated all the identified PI3K-III subunits in autophagy, less is known about the specific sub-complexes involved in degradation of growth-factor receptors and cytokinesis. Importantly, although Beclin 1, UVRAG and BIF-1 have all been identified as tumour suppressors (Liang et al., 2006; Takahashi et al., 2007; Takahashi et al., 2005; Kim et al., 2008; Ionov et al., 2004; Goi et al., 2003; Bekri et al., 1997; Liang et al., 1999; Qu et al., 2003; Yue et al., 2003), no other bona fide tumour suppressors have been identified amongst the core autophagic machinery. This suggests that the tumour suppressive properties of the PI3K-III

complex may be related to control of receptor degradation and/or cytokinesis, and highlights the importance of fully characterizing the functional specificities of the different PI3K-III subunits in these processes.

PtdIns3P-binding proteins

PtdIns3P exerts its effects through downstream protein effectors which, although there are exceptions, typically bind the lipid through either a FYVE (Fab1, YOTB, Vac1 and EEA1) domain or a PX (Phox homology) domain. Whereas proteins with PX domains are somewhat promiscuous as they can bind a few different PIs and other proteins, most FYVE domain proteins exclusively bind to PtdIns3P (Gaullier et al., 1998; Burd and Emr, 1998; Patki et al., 1998). PX domains interact with PtdIns3P through a conserved structural conformation based on specific protein folds with little sequence conservation, while FYVE domains contain several conserved residues, including key cysteines that bind Zn^{2+} ions that allow interaction with PtdIns3P (Cheever et al., 2001; Kutateladze and Overduin, 2001). Many PtdIns3P effectors have been identified, although many are still not fully characterized. These play important roles in all PtdIns3P regulated pathways, with key factors described below.

ESCRTs and VPS4

The Endosomal Sorting Complex Required for Transport (ESCRT) machinery constitute important PtdIns3P effectors, and are required for several essential cellular processes, including endosomal membrane trafficking, viral egress, and cytokinesis. The ESCRT machinery comprise at least four subcomplexes (ESCRT-0, -I, -II and -III) (Katzmann et al., 2002; Raiborg and Stenmark, 2009), which are recruited in a consecutive and interdependent manner. While the first three are preassembled, the final ESCRT-III complex is assembled on site. The ESCRT-0 complex consists of the subunits HRS and STAM, both of which contain domains for ubiquitin- and clathrin-

binding (Hofmann and Falquet, 2001; Raiborg et al., 2001; McCullough et al., 2006). Additionally, HRS contains a PtdIns3P-binding FYVE-domain. The ESCRT-I complex is made up of four subunits, namely TSG101, VPS28, VPS37 and MVB12, that together mediate binding to both ESCRT-0 and ESCRT-II (Kostelansky et al., 2007). ESCRT-II is composed of one VPS22, one VPS36 and two VPS25 subunits (Hierro et al., 2004). This complex bridges ESCRT-I and ESCRT-III, and additionally binds ubiquitin and PtdIns3P via an unusual GLUE domain found in VPS36 (Slagsvold et al., 2005). Most mammalian ESCRT-III components are commonly known as CHMPs, initially as an abbreviation for 'chromatin modifying proteins', which reflects the predicted function of the first identified gene of the family, *CHMP1A*, in regulating chromatin structure during gene transcription (Stauffer et al., 2001). However, the CHMP family is more commonly associated with their known functions in endosomal membrane trafficking, thereby designated 'charged MVB proteins'. To date, 11 mammalian ESCRT-III proteins are known, including different CHMP isoforms (CHMP1-7) and IST1, which is also classified as ESCRT-III due to its similar N-terminal fold (Xiao et al., 2009). Although there is some functional redundancy between CHMP isoforms, there may also be certain isoform-specific functions. In general, ESCRT-III subunits come together to form higher-order multimeric filaments that mediate membrane scission events. Although the details are not yet fully understood, current models suggest that ESCRT-III filaments form a spiral structure that bring opposing membranes together to allow membrane scission to occur (Fabrikant et al., 2009; Hanson et al., 2008). First, CHMP6 nucleates the assembly of CHMP4 spirals that are then capped by CHMP3 and CHMP2. While these comprise the core ESCRT-III complex, other ESCRT-III proteins play regulatory roles (Babst et al., 2002; Hurley and Hanson, 2010; Wollert et al., 2009). Finally, ESCRT-III-mediated membrane scission is dependent on the catalytic action of the AAA ATPase VPS4 (vacuolar protein sorting 4). Functional VPS4 has a multimeric structure and drives ESCRT-III disassembly through hydrolysis of Adenosine triphosphate (ATP) (Babst et al., 1997; Scott et al., 2005). Importantly, VPS4 contains an N-terminal MIT (microtubule interaction and transport) domain that interacts with specific motifs found

in all CHMPs termed MIMs (MIT-interacting motifs) (Stuchell-Brereton et al., 2007). There are several types of MIMs identified, where MIM1 and MIM2 are the best characterized. Importantly, these are capable of interacting with one MIT simultanously as they can bind on diametrically opposite surfaces of the MIT domain (Kieffer et al., 2008) (Figure 8). The assembly and recruitment of VPS4 to the core ESCRT-III complex are also regulated by several other ESCRT-III-like proteins, including IST1, CHMP1, CHMP2, CHMP5 and LIP5, most of which are also dependent on MIM-MIT interactions (Adell and Teis, 2011). Here, IST1 and CHMP1 are involved in the recruitment of VPS4 to ESCRT-III, although IST1 is also thought to inhibit VPS4 by preventing the mulitmerization of VPS4 subunits into a functional multimeric form (Dimaano et al., 2008; Xiao et al., 2009; Rue et al., 2008). LIP5 on the other hand is a positive regulator of VPS4 assembly and ATPase activity, and forms a multimeric complex together with VPS4 multimers independently of its MIT-domain (Lottridge et al., 2006; Yu et al., 2008). Furthermore, LIP5 also contains two MIT-domains that can interact with CHMP1, thought to contribute to the recruitment of VPS4, and CHMP5, a less well characterized regulator of VPS4 (Skalicky et al., 2012). It is clear that MIM-MIT interactions are important for how the ESCRT-III proteins and VPS4 with its accessory regulators come together to regulate membrane scission. Moreover, different MIM-MIT affinities are important for interaction selectivity and competition.

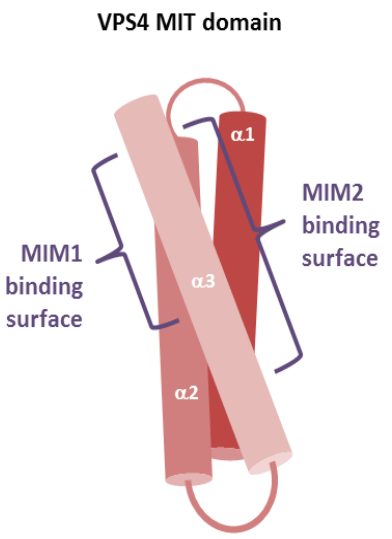

Figure 8: The VPS4 MIT domain. The VPS4 MIT domain contains binding sites for both MIM1 and MIM2, which are on diametrically opposite surfaces, facilitating simultaneous interactions (adapted from Babst et al., 2011).

PtdIns3P, ESCRTs and VPS4 in growth factor receptor degradation

Extrinsic stimuli, in particular growth-factor mediated signalling, play pivotal roles in normal cellular functions as well as pathogenesis, including cancer. Upon activation of their respective receptor tyrosine kinases (RTKs), growth factors stimulate intracellular signalling cascades that alter gene transcription that positively influences cell survival, growth and proliferation. The amplitude and kinetics of growth factor signalling is largely determined by the ability of a cell to engulf and transport activated RTKs via endocytic membrane trafficking for subsequent degradation in lysosomes (schematically represented in figure 9). Here, the PI3K-III complex and PtdIns3P play instrumental roles. In fact, the first characterized functions of the yeast orthologues of VPS34 and VPS15 were those associated with endosomal membrane trafficking and vacuolar protein sorting (Schu et al., 1993; Herman et al., 1991). Although there are different types of cargo and several mechanisms of endocytosis known, this overview will focus on the Epidermal Growth Factor Receptor (EGFR), the prototypic RTK, and clathrin-mediated endocytosis as the canonical endocytic mechanism.

Initially, ligand-activated EGFR accumulates in dynamically forming invaginations on the plasma membrane, known as clathrin-coated pits. Receptors are then enveloped by a portion of the plasma membrane which pinches off to form an endocytic vesicle in the cytosol. Subsequently, endocytic vesicles fuse with compartments known as early endosomes (EEs). This tethering and fusion process is mediated by several vesicular proteins, including the small GTPase RAB5, its FYVE-domain-containing effectors EEA1 and Rabenosyn-5, and the fusion-mediator VPS45 (Nielsen et al., 2000; Simonsen et al., 1998). Furthermore, RAB5 also binds VPS15, thereby providing a recruitment platform for the PI3K-III complex and concomitant generation of PtdIns3P necessary for recruitment of its effectors (Christoforidis et al., 1999; Murray et al., 2002).

From early endosomes, cargo is either recycled back to the plasma membrane or, as in the case of EGFR, internalized into intraluminal vesicles (ILVs). This process

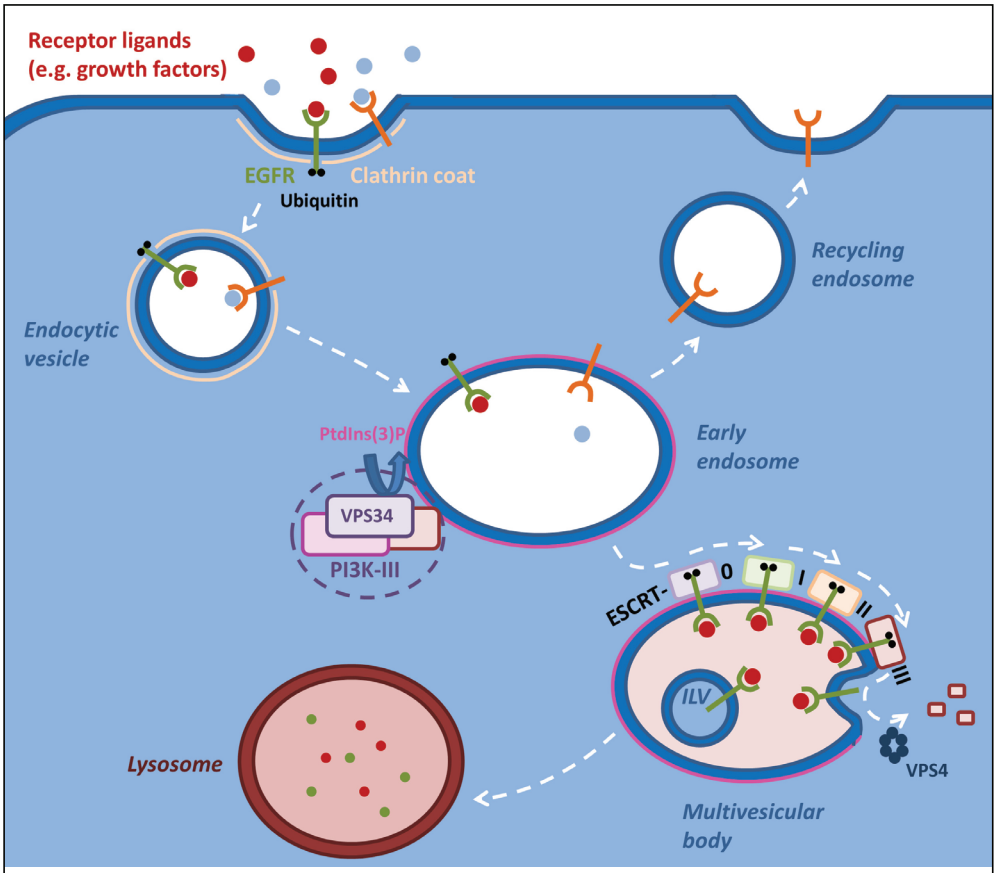

Figure 9: Epidermal growth factor receptor (EGFR) degradation. Ligand-bound receptor accumulates in clathrin-coated pits, and is ubiquitinated and endocytosed. Endocytic vesicles subsequently fuse with PtdIns3P-rich early endosomes, where cargo is sorted for recycling, or, in the case of active EGFR, for degradation. Sorting of EGFR into intraluminal vesicles (ILVs) in multivesicular bodies (MVB) is mediated by the ESCRT machinery in sequential order by ESCRT-0, -I, -II and –III, and the ATPase VPS4 which disassembles ESCRT-III. Finally, fusion with acidic lysosomes leads to degradation of the recetor and ligand.

requires PI3K-III, since interfering with VPS34 function results in enlarged endosomes lacking ILVs (Fernandez-Borja et al., 1999; Futter et al., 2001). This PtdIns3P-dependency can be explained by the concerted action of the ESCRT machinery. First, ESCRT-0 is recruited to endosomal membranes via binding of the FYVE-domain of the HRS subunit to PtdIns3P. Concurrently, ESCRT-0 sequesters EGFR modified with a

ubiquitin moiety which acts as a tag to direct the cargo for degradation. Subsequently, ESCRT-I and -II are thought to receive cargo from ESCRT-0 via ubiquitin-binding domains, and also serve to form membrane invaginations into which cargo can be sorted. Next, ESCRT-III filaments are recruited to mediate scission of the forming ILV from the limiting membrane of the endosome. Finally, and crucially, the AAA ATPase VPS4 mediates dissociation of the ESCRT-III filaments, a step necessary for ILV formation and termination of growth factor receptor signalling (Hanson and Whiteheart, 2005; Landsberg et al., 2009). Here, VPS4 function is regulated by IST1, LIP5, CHMP1 and CHMP5. A successively increasing amount of ILVs correlates with maturation of the early endosome into an MVB. Finally, the MVB will fuse with acidic lysosomes where cargo is degraded, defining the terminal step of the receptor degradation pathway.

PtdIns3P, ESCRTs and VPS4 in cytokinesis

Cytokinesis is the final step of cell division, where the two daughter cells are physically divided through membrane abscission. Towards the end of cytokinesis, following cleavage furrow ingression and establishment of the midbody, the intercellular bridge undergoes a secondary ingression in which it narrows from approx. 1-2 μm to about 100 nm, juxtaposed ~1 μm at either or both sides of the midbody. This defines the abscission zone where, following microtubule severing, the final membrane fission event is thought to occur (Elia et al., 2011; Guizetti et al., 2011). Accumulating evidence shows that cytokinesis and abscission are highly regulated processes involving many different proteins and lipids, including ESCRTs, VPS4 and PtdIns3P.

Regulation of cytokinesis appears to be the ancestral function of the ESCRT machinery (Lindas et al., 2008; Samson et al., 2008). Initially, deactivation of the kinase PLK1 promotes midbody targeting of CEP55 via MKLP1, which subsequently recruits ESCRT-I (TSG101) and ALIX proteins (Lee et al., 2008a; Morita et al., 2007; Carlton and Martin-Serrano, 2007). Next, ESCRT-III factors are recruited and form

concentric ring-like filaments that spiral outwards from the midbody. Although these filaments contain a variety of ESCRT-III subunits, including CHMP4B and CHMP2A (Morita et al., 2007; Guizetti et al., 2011), the precise makeup of these filaments remains to be determined. Other ESCRT-III components such as

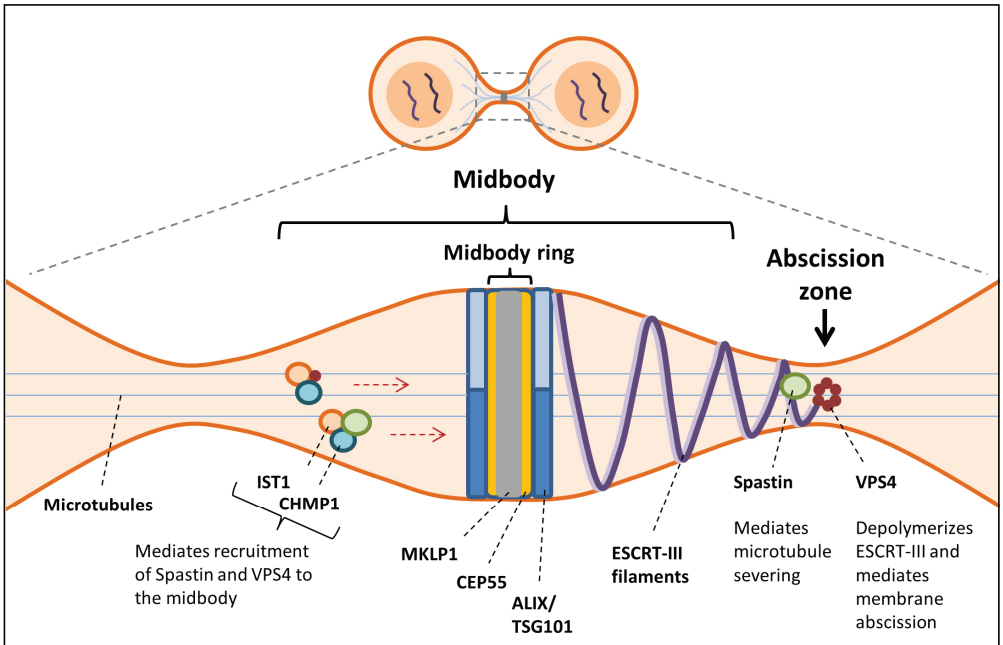

Figure 10: Organization of the midbody during cytokinesis and abscission. Cytokinesis proceeds through the sequential recruitment and action of multi-protein complexes at the midbody. First, CEP55 is recruited to the midbody ring by MKLP1, and further recruit the ESCRT-I protein TSG101 and the adaptor protein ALIX. Subsequent recruitment of ESCRT-III factors polymerize into filamentous spirals or rings that drive membrane constriction and formation of a secondary ingression defining the abscission zone. Although CHMP4B is a central component of these filaments, and other ESCRT-III factors such as CHMP2 and CHMP3 are known to associate with them, their exact makeup is not clear. Finally, IST1 and CHMP1 mediate recruitment of the enzymes Spastin and VPS4 to the midbody. At the abscission zone, Spastin mediates microtubule severing while VPS4 is required for membrane abscission which is thought to occur through disassembly of ESCRT-III polymers.

CHMP1 and IST1 then mediate recruitment of the MIT-domain proteins Spastin, an ATPase required for microtubule severing, and VPS4 to the midbody and abscission zone immediately preceeding abscission (Reid et al., 2005; Elia et al., 2011; Yang et al., 2008). Figure 10 illustrates midbody organization during cytokinesis. Importantly, VPS4 is required for abscission, since interfering with endogenous VPS4 leads to accumulation of cytokinetic and multinuclear cells (Carlton and Martin-Serrano, 2007; Morita et al., 2007). The mechanism by which VPS4 mediates membrane scission is not fully elucidated, but is thought to involve ESCRT-III disassembly, similar to its role in ILV formation and viral budding. Interestingly, recruitment of VPS4 to the midbody could only be observed when the intercellular bridge was particularly thin, suggesting it acts specifically during the final stages of cytokinesis (Morita et al., 2010). Another MIT-domain protein recruited by ESCRT-III during cytokinesis is MITD1 which negatively regulates the IST1-VPS4 interaction at the midbody, suggesting that it thereby positively influences VPS4 function (Lee et al., 2012; Hadders et al., 2012). Although not fully understood, it is clear that cytokinesis abscission is regulated by a complex network of MIM and MIT-domain-containing protein interactions, many of which involve VPS4.

It is interesting to note that the ESCRT machinery not only plays a role during the mechanistic process of cytokinetic abscission, but is also involved in regulation of the abscission checkpoint, as described above. Here, Aurora B-mediated phosphorylation of the ESCRT-III component CHMP4C is required for abscission delay upon checkpoint activation (Carlton et al., 2012). However, the exact mechanisms by which CHMP4C mediates abscission delay is unclear.

Several lipids have been implicated in the execution and regulation of cytokinesis abscission. Firstly, they are important constituents of vesicles that upon fusion with the plasma membrane allow progressive membrane constriction in the intercellular bridge. For instance, several studies have reported the accumulation of recycling endosomal vesicles in the intercellular bridge during telophase and cytokinesis (Goss and Toomre, 2008; Gromley et al., 2005). In particular, FIP3-positive

endosomes are required for the formation of the secondary ingression (Schiel et al., 2012). Although there is some controversy about the importance of vesicle transport during cytokinesis (Guizetti et al., 2011), the observation that fusion of secretory or endosomal vesicles with the plasma membrane immediately preceeds abscission lends credence to the notion that membrane transport during cytokinesis is involved in the thinning of the intercellular bridge. Secondly, vesicular transport and lipids are important for the recruitment of different proteins required for cytokinesis. For instance, FIP3 endosomes are required both for the coordination of actin dynamics during cytokinesis, and for recruitment of ESCRT-III to the abscission zone (Schiel et al., 2012). Also, there seems to be a role for PtdIns3P in the regulation of abscission (Sagona et al., 2010). Firstly, PtdIns3P was observed to localize close to the midbody during cytokinesis. Moreover, depletion of VPS34 or Beclin 1 resulted in cytokinetic arrest and accumulation of multinuclear cells. This PtdIns3P-dependent regulation of abscission was mediated by the PtdIns3P-effector FYVE-CENT and its binding partner TTC19, which in turn interacts with the ESCRT-III component CHMP4B. Although the details are not completely understood, these findings indicate a role for PtdIns3P-mediated signalling in the control of cytokinesis.

Knowledge is key

Although we are beginning to understand the process of cytokinesis and how it is regulated, much remains to be explored. However, accumulating evidence show it is dependent on many of the same mechanistic and regulatory factors as other processes, including endosomal membrane trafficking during downregulation of growth factor signalling (Figure 11). The complex interplay between different factors and their context-dependent functional roles highlight their importance in ensuring faithful progression through the cell division cycle, the deregulation of which can lead to uncontrolled cell proliferation. For instance, failure to terminate growth factor-mediated signalling through degradation of active receptors can result in cellular

hyperproliferation and cancer. Moreover, failure to properly engage and maintain cell cycle checkpoints, as well as failure of cytokinesis, can lead to chromosomal aberrations and aneuploidy in daughter cells which is often associated with cancer development. This underscores the importance of understanding the factors and mechanisms underlying the regulation of cell cycle progression. Although a lot is known, much is yet to be elucidated.

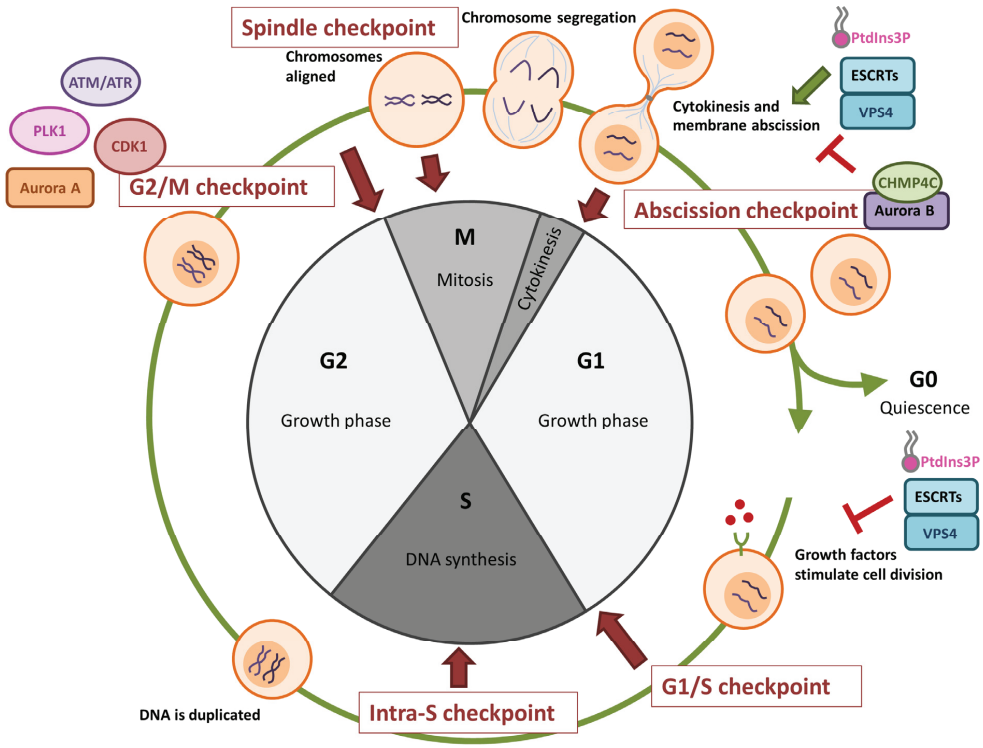

Figure 11: Growth factor receptor signalling during cell cycle entry and cytokinetic abscission during cell cycle exit are controlled by PtdIns3P, ESCRTs and VPS4.

Aims of the study

The overall aim of this study was to further our knowledge about context-dependent functions of the PI3K-III complex and effectors of its catalytic product PtdIns3P in intercellular membrane trafficking and cell division.

Paper I

A phosphatidylinositol 3-kinase class III sub-complex containing VPS15, VPS34, Beclin 1, UVRAG and BIF-1 regulates cytokinesis and degradative endocytic traffic

Previous studies suggest the existence of distinct PI3K-III sub-complexes that can confer functional specificity. However, most studies have focused on the role of PI3K-III subunits in autophagy. Our aim was to determine the individual roles of the different PI3K-III subunits specifically in endocytic growth factor receptor degradation and cyokinesis.

Paper II

ANCHR mediates Aurora B-dependent abscission checkpoint control via retention of VPS4

A screen for PtdIns3P-binding proteins involved in regulation of cytokinesis identified the previously uncharacterized protein ZFYVE19/ANCHR (Abscission / NoCut Checkpoint Regulator) as a potential candidate. In this paper, we sought to characterize the functional and molecular mechanisms underlying this observation.

Paper III

ANCHR is required for G2/M DNA damage checkpoint function

As part of our work in **paper II**, we had observed that ANCHR localized to centrosomes, structures that harbour many regulators of mitotic entry. Additionally, previous studies have identified ANCHR as a putative target of several kinases involved in G2/M checkpoint activation and mitotic entry control. We therefore set out to investigate whether ANCHR could play a role in regulating the G2 to M transition, specifically through G2/M checkpoint function.

Summary of the included papers

Paper I

A phosphatidylinositol 3-kinase class III sub-complex containing VPS15, VPS34, Beclin 1, UVRAG and BIF-1 regulates cytokinesis and degradative endocytic traffic

The catalytic product of the PI3K-III complex, PtdIns3P, regulates several essential cellular processes, including autophagy, endosomal membrane trafficking and cytokinesis. The PI3K-III complex consists of the core subunits VPS15, VPS34 and Beclin 1, where the latter provides a docking platform for UVRAG and ATG14L with which it associates in a mutually exclusive manner. BIF-1 further positively regulates UVRAG. Previous work has revealed that specific PI3K-III sub-complexes may function in a context-dependent manner, differentiated by the presence of UVRAG or ATG14L (Itakura et al., 2008; Itakura and Mizushima, 2009; Liang et al., 2006; Kihara et al., 2001b). Since most studies have focused on the role of PI3K-III in autophagy, we set out to determine the contribution of individual subunits specifically in degradative endocytic trafficking and cytokinesis. Firstly, siRNA-mediated depletion of PI3K-III subunits showed that there was interdependency between the different subunits to maintain complex stability, and outlined complex organization with recruitment of UVRAG or ATG14L to a core complex containing, in consecutive order, VPS15, VPS34 and Beclin 1. BIF-1 stability was independent of other subunits, suggesting that it might associate with the complex in a transient manner. High-content microscopy-based assays indicated that a specific sub-complex containing VPS15, VPS34, Beclin 1, UVRAG and BIF-1 regulates both growth factor receptor degradation and cytokinesis. The role of this complex in cytokinesis was further supported by localization of UVRAG and BIF-1 to the midbody. Importantly, our results open the possibility that the tumour suppressive functions of Beclin 1, UVRAG and BIF-1 may contribute to tumour suppression via downregulation of growth factor receptor signalling and / or prevention of cytokinesis failure and aneuploidy.

Paper II

ANCHR mediates Aurora B-dependent abscission checkpoint control via retention of VPS4

Cytokinesis is the final stage of cell division where two daughter cells and their genetic content are physically separated. The final membrane abscission event is mediated by the endosomal sorting complex required for transport (ESCRT) machinery through the activity of the ATPase VPS4 (Carlton and Martin-Serrano, 2007; Morita et al., 2007; Guizetti et al., 2011; Elia et al., 2011). Recent work has identified the existence of an Aurora B-dependent abscission checkpoint (also termed NoCut) that delays abscission to avoid DNA damage and aneuploidy in cells with chromosome segregation defects (Steigemann et al., 2009; Carlton et al., 2012). Although Aurora B-dependent phosphorylation of the ESCRT-III component CHMP4C has been implicated as a regulatory event (Carlton et al., 2012), how abscission delay occurs on a mechanistic level is largely unknown. An siRNA screen set up in the lab to assess the roles of PtdIns3P-binding proteins involved in cytokinesis identified a previously uncharacterized protein ZFYVE19, here renamed ANCHR (Abscission/NoCut Checkpoint Regulator), as important for the prevention of accumulation of multinucleate cells. We further show that ANCHR specifically inhibits cleavage furrow regression and multinucleation in cells with chromsome segregation defects. Endogenous and ectopically expressed ANCHR localizes to centrosomes and cytokinetic midbodies, where overexpression induces cytokinesis arrest independently of PtdIns3P. We show that ANCHR binds VPS4 through a classical MIM-MIT interaction, and that this is required for ANCHR-mediated cytokinesis arrest. Importantly, we show that ANCHR, in concert with CHMP4C, mediates abscission checkpoint function by retention of VPS4 on the midbody ring in an Aurora B-dependent manner, likely preventing VPS4 localization to the abscission zone. Together, our data establish ANCHR as a novel regulator of the abscission checkpoint, and provides the first mechanistic link between Aurora B-induced checkpoint activation and abscission delay.

Paper III

ANCHR is required for G2/M DNA damage checkpoint function

Cell cycle checkpoints operate at several stages of the cell cycle to monitor DNA integrity and to ensure fidelity of transmission of genetic material. During the G2 cell cycle phase, a complex network of proteins serves to delay mitotic entry in the presence of damaged DNA, specifically termed the G2/M checkpoint. We had previously shown that the abscission checkpoint regulator ANCHR was found to localize to centrosomes in HeLa cells (**paper II**), which are key structures harbouring many regulators of the G2 to M phase transition. Furthermore, ANCHR has also been reported as a putative target of several kinases involved in mediating DNA damage-induced G2 arrest and mitotic entry. Thus, we wanted to assess whether ANCHR could potentially be involved in G2/M checkpoint regulation. Accordingly, overexpression of ANCHR increased the G2 population in checkpoint-proficient U2OS cells, but not in HeLa cells which are known to have weak G2/M checkpoint induction. It also localized to centrosomes during both interphase and early mitosis in U2OS cells, as predicted. Importantly, depletion of ANCHR abrogated DNA damage-induced G2 arrest, indicating that it is required for proper G2/M checkpoint function. Induction of DNA damage also resulted in an increase in ANCHR protein levels over time, indicating either transcriptional level or increased protein stability. Bioinformatic analysis combined with mass spectrometry and in vitro kinase assays suggest that ANCHR may be a target for key G2/M checkpoint kinases such as CDK1, PLK1 and Aurora A. Phenotypic differences between HeLa and U2OS cell lines may reflect different p53-status, suggesting that ANCHR-mediated G2/M checkpoint function may be p53-dependent. Together, our data suggest a potential role for ANCHR in negative regulation of mitotic entry, specifically through control of the G2/M checkpoint. Future studies will hopefully uncover the mechanism by which ANCHR can induce G2 arrest.

Discussion

The work presented in this thesis has broadened our understanding of mechanisms regulating endsosomal membrane trafficking, cytokinesis and cell cycle checkpoints. Firstly, we have provided evidence that a specific sub-complex of PI3K-III is involved in positive regulation of both endosomal membrane trafficking and cytokinesis (**Paper I**). Since little is known about the role of PtdIns3P in regulation of cytokinesis, a subsequent siRNA-based screen was set up to identify PtdIns3P effectors involved in this process. Here, our results identified ANCHR as one of the most prominent candidates when scoring for the frequency of multinucleated cells (**Paper II**). However, we provide compelling evidence that ANCHR is a negative regulator of cytokinesis by specifically preventing cytokinetic abscission in missegregating cells through abscission checkpoint-mediated signalling, a function which may be PtdIns3P-independent. Our data also provide the first evidence of how the abscission checkpoint functions on a mechanistic level, where retention of VPS4 at the midbody ring by ANCHR and CHMP4C delays abscission in an Aurora B-dependent manner. Thirdly, we also provide data that ANCHR may function in the G2/M DNA damage checkpoint prior to mitotic entry (**Paper III**), establishing ANCHR as potentially a more general cell cycle checkpoint regulator and protector of genomic integrity.

Differential roles of the PI3K-III complex

Generation of PtdIns3P by the PI3K-III complex has been found to be essential for several intracellular processes. These include endosomal membrane trafficking, in particular with respect to degradation of growth factor receptors, degradation of cytoplasmic material through autophagy, and completion of cytokinesis. All of these processes are subject to regulation by both intrisic and extrinsic stimuli to ensure temporal and spatial specificity, such as nutrient availability, growth factor-mediated signalling, and process-specific post-translational modifications of various factors.

However, since PtdIns3P-mediated signalling is involved in multiple processes, and the roles of the different PI3K-III subunits in each of these have so far been debated, we speculated that differential PI3K-III subcomplexes may exist to confer additional specificity. In **paper I**, we show that a specific subcomplex containing VPS15, VPS34, Beclin 1, UVRAG and BIF-1, but not ATG14L, is required for both growth factor receptor degradation and cytokinesis. Thus, our results support the idea that there exist at least two distinct PI3K-III sub-complexes, containing either UVRAG (associated with BIF-1) or ATG14L which have been shown to be mutually exclusive (Itakura et al., 2008; Kihara et al., 2001b). This was supported by our observation that UVRAG and BIF-1, but not ATG14L, localize to the midbody region during cytokinesis. Similarly, UVRAG, but not ATG14L has previously been reported to localize to early endosomes. Also, although not entirely clear, accumulating evidence suggest the ATG14L-associated PI3K-III complex is the main regulator of autophagy.

The phenotypic penetrance following depletion of PI3K-III subunits, both in terms of inhibition of receptor degradation and cytokinesis, was relatively modest. This may, in part, be explained by potential residual levels / activity of subunits due to incomplete siRNA-mediated knockdown. Lack of penetrance was especially true for Beclin 1 depletion, perhaps surprisingly, since it forms an integral part of the core PI3K-III complex and has been reported to be the sole link between VPS34 and UVRAG (Liang et al., 2006). However, a recent report identified a mammal-specific Beclin 2 homologue, which was shown to have a role in autophagy and degradation of G-protein coupled receptors (GPCRs) (He et al., 2013). Although the authors speculate that Beclin 2 is not involved in growth factor receptor degradation, the lack of functional studies on this process means a role here cannot be formally excluded. Furthermore, Beclin 2 was shown to interact with several PI3K-III components incluing VPS34 and ATG14. If there is some functional redundancy, this might explain the relatively weak phenotypic effects upon depletion of Beclin 1 in our studies, should Beclin 2 be able to partially compensate for the lack of Beclin 1.

Although there may exist as yet unidentified differences in subunit composition, it is interesting that growth factor receptor degradation and cytokinesis are regulated by the same principle PI3K-III subcomplex, since they also rely on the action of other common factors such as ESCRTs and VPS4. One functional consequence may be coordination of events during cell cycle progression. However, this would also require differential regulation of the PI3K-III complex by cell cycle phase- and subcellular location-specific factors, to ensure temporal and spatial control of PtdIns3P-mediated signalling. For instance, autophagy-specific activation of PI3K-III occurs at autophagosomes by phosphorylation of Beclin1 by ULK1 (Russell et al., 2013). Furthermore, AMPK has been shown to specifically inactivate the UVRAG-associated PI3K-III subcomplex since it phosphorylates VPS34 only in the absence of ATG14L, thereby acting as a promotor of autophagy (Kim et al., 2013). Another study showed that during mitosis, VPS34 is phosphorylated by the kinase CDK1 during mitotic entry, resulting in inhibition of its catalytic activity and dissociation from Beclin 1 (Furuya et al., 2010). The functional implications of this is unclear, but may be to inhibit degradative events at a time when many cellular membranes are fragmented or disassembled, including the nuclear envelope, endoplasmic reticulum and golgi apparatus.

PtdIns3P as a positive regulator of cytokinesis

Although the role of PtdIns3P-mediated signalling in endosomal membrane trafficking and growth factor receptor degradation is well established, its role in the regulation of cytokinesis is a relatively recent discovery (Sagona et al., 2010), and so far less well characterized. It is likely to involve the PtdIns3P effector FYVE-CENT, which localizes to the midbody in a KIF13A-dependent manner. Furthermore, it interacts with TTC19 which also binds the ESCRT-III component CHMP4B. Whether or not PtdIns3P is involved in the regulation of CHMP4B through FYVE-CENT and TTC19 remains to be determined. Since depletion of VPS34 mainly arrested cells in

early cytokinesis, a stage which is presumably a lot earlier than when CHMP4B is thought to function, it may be that PtdIns3P rather functions to promote vesicular transport as a source of membrane or various cytokinetic factors to the ingressing cleavage furrow, in a similar manner to FIP3-positive vesicles (Simon and Prekeris, 2008; Schiel et al., 2012).

Positive vs negative regulation of cytokinesis – both can lead to abscission failure

It is becoming increasingly clear that cytokinesis is a highly complex process that involves multiple regulatory and mechanistic events. On one hand, successful abscission requires sequential recruitment and activation of many factors to the midbody, together comprising the cytokinetic positive regulatory network. These include PtdIns3P and the PI3K-III (**Paper I**), FYVE-CENT, midbody-based recruiters such as CEP55, core ESCRT-I and ESCRT-III components, the microtubule severing enzyme Spastin and finally, the ATPase VPS4. Deregulation of any of these factors will result in cytokinesis delay and/or failure in all cells progressing through the cell division cycle, the potential outcome of which is cleavage furrow regression and multinucleation.

Recent research shows that cytokinesis is also negatively regulated to avoid premature abscission in the presence of chromatin segregation errors or defects in nuclear envelope assembly. This abscission checkpoint regulatory network centres on the master regulator Aurora B which targets downstream factors to delay abscission, including MKLP1 which is involved in stablilising the intercellular bridge, and the ESCRT-III component CHMP4C. Although the mechanistic details of how abscission delay occurs have so far been unknown, it is clear that deregulation of this checkpoint can also result in cleavage furrow regression and multinucleation (Steigemann et al., 2009), specifically in cells with missegregating chromatin and/or disrupted nuclear envelopes. In normally segregating cells, failure of abscission checkpoint signalling

would not cause a cytokinesis delay, since its activation requires positive signals emanating from lagging chromatin or defective nuclear membranes.

ANCHR (ZFYVE19) – a previously uncharacterized protein

Since our research pinpoints the PI3K-III complex and its catalytic product PtdIns3Pas important regulators of cytokinesis (**Paper I**), a screen was set up to identify PtdIns3P effectors involved in this process (**Paper II**). Here, members of the FYVE-family of proteins were depleted by siRNA in HeLa cells, which were subsequently imaged by high-content microscopy and scored for multinucleation, indicative of failed cytokinesis. One of the highest scoring hits was ZFYVE19, which we later renamed ANCHR (**A**bscission/**N**oCut **Ch**eckpoint **R**egulator).

ANCHR is a 471 amino acid protein encoded by the *ZFYVE19* gene on chromosome 15 (15q15.1). It is classified as a FYVE-family protein based on its basic amino acid sequence which contains an N-terminal atypical FYVE-related zinc finger. Additionally, it contains a C-terminal BBOX type I zinc finger of unknown function. Further sequence analysis revealed the presence of two putative type I MIT-interacting motifs (MIMs), designated MIM1-A and MIM1-B. ANCHR also contains several putative binding sites and phosphorylation sites, many of which are targeted by known cell cycle regulators. These will be discussed later.

ANCHR is conserved in vertebrates, from *Danio rerio* (zebrafish) to *Homo sapiens* (human), although there is some sequence variation. There is a less well conserved orthologue in *Drosophila melanogaster* (fruit fly) that shows sequence conservation within the two zinc fingers, but otherwise little similarity. No orthologue is found in more primitive phyla such as the *Ascomycota* (yeast). In humans, ANCHR is ubiquitously expressed in all major tissue types, including immune cells, nervous tissue, muscle tissue, secretory tissue, reproductive tissue and tissues of many internal organs such as colon, kiney, lung and liver (Su et al., 2004; Wu et al., 2009).

Searching for ANCHR (ZFYVE19) on the PubMed database of life science and biomedical publications returns only three hits, all of which are clinical publications that report differential expression, or in one case, expression of an ANCHR fusion protein, in pathological conditions. Thus, we were intrigued to investigate this previously uncharacterized protein of potential function in the regulation of cytokinesis.

ANCHR as a regulator of the abscission checkpoint

In **paper II**, we identify ANCHR as a key regulator of the abscission checkpoint. We present evidence that VPS4 is a key target of the abscission checkpoint and is retained by ANCHR and CHMP4C at the midbody ring in an Aurora B-dependent manner. Thus, translocation of VPS4 to the abscission zone is prevented until checkpoint signalling terminates. Importantly, we provide the first reported mechanism for execution of cytoinesis abscission arrest.

VPS4 is a core component of the MIM-MIT interaction network that regulates cytokinesis

MIM-MIT interactions are central to the execution and regulation of cytokinesis. Moreover, since the MIT-domain protein VPS4 is crucial for the final step of abscission, it is perhaps not surprising that many of the known cytokinesis regulators impinge on VPS4. Known VPS4 interactors that are involved in cytokinesis include CHMP1, CHMP2, CHMP3, CHMP4 A/B/C, LIP5, IST1 and MITD1.

Here, we add ANCHR to the list of VPS4 interactors, and show that this binding is essential for abscission arrest during abscission checkpoint activation. We also show that ANCHR specifically binds the VPS4 MIT domain via its MIM1-A. The role of the MIM1-B is so far unclear, but may interact with other MIT-domain proteins. Furthermore, our results show that VPS4 retention at the midbody is achieved by

cooperative functions of ANCHR and CHMP4C. This synergism can be explained by their simultaneous binding to VPS4, forming a ternary complex, as suggested by our data. ANCHR and CHMP4C contain a type 1 and type 2 MIM, respectively, the binding sites for which are on the diametrically opposite surfaces of the MIT domain. Such dual binding has been demonstrated for other cytokinesis regulators such as IST1, which contains a MIM1 and a MIM2 that wrap around VPS4 to keep it in a monomeric and inactive state (Bajorek et al., 2009). In a similar way, IST1 can bind both interaction surfaces of MITD1 (Lee et al., 2012). Intriguingly, MIMs have previously only been found in ESCRTs and related proteins. Here, we present the first report of MIM occurrence in a non-ESCRT-related protein. This raises the possibility that the MIM-MIT network, and hence the complexity of regulation of cytokinesis and other processes, are more extensive than first thought. Detailed genomic sequence analysis could reveal additional candidate members of the MIM-MIT interaction network.

Linking Aurora B to abscission delay

Previously, only two factors implicated in abscission checkpoint maintenance downstream of Aurora B had been identified. One was MKLP1, which upon phosphorylation by Aurora B seems to play a role in stabilizing the intercellular bridge in the presence of lagging chromatin (Steigemann et al., 2009). The other was CHMP4C, which associates with the chromosomal passenger complex (CPC) and delays abscission in an Aurora B-dependent manner (Carlton et al., 2012). Although the authors did not provide any mechanism for CHMP4C-induced cytokinesis arrest, they speculated that Aurora B-mediated phosphorylation specifically directs CHMP4C to the midbody ring in late cytokinesis and that this could prevent the formation of CHMP4B filaments by competing for ALIX binding sites. This was supported by the observation that CHMP4C arrives at the midbody significantly earlier than CHMP4B. The contrasting results from Capalbo et al. (2012) showing that Aurora B-mediated phosphorylation of CHMP4C rather increased cytokinesis arrest and multinucleation

without changing its localization pattern led these authors to speculate that phosphorylated CHMP4C was kept in a 'closed' and inactive conformation that prevented its polymerization and formation of filaments required for abscission. Our data presented in **paper II** supports the former observation which pinpoints the midbody ring as the site for CHMP4C- (and ANCHR-) mediated abscission timing control, but identify the mechanism as retention of VPS4 rather than inhibition of filament formation. The study by Steigemann et al. (2009) showed that active Aurora B also localizes to the midbody ring during abscission checkpoint activation, again confirming this as a central hub for mediating cytokinesis delay.

We also tested whether ANCHR could be a target of Aurora B, since it contains several consensus target sites for Aurora Kinases. However, although in vitro kinase assays and mass spectrometric analyses confirmed that Aurora B could phosphorylate ANCHR at Serine 22 (S22) in vitro, there was no indication that this occurred in vivo (**paper II**, supplementary figure S11). Furthermore, a phospho-dead S22A mutant of ANCHR arrested cells in cytokinesis as effectively as the wild-type when overexpressed (data not shown), indicating that such a phosphorylation event is not required for ANCHR abscission checkpoint function. Thus, CHMP4C appears to be the key Aurora B target linking chromatin-mediated abscission checkpoint activation to ANCHR and VPS4. It is interesting to note that the Aurora B target site on CHMP4C is immediately downstream of the MIM2 element involved in VPS4 interaction, further supporting our model of abscission arrest.

Regulation of VPS4 during cytokinesis and abscission – a speculative model

Based on our data, in addition to previously published work, we can speculate about the dynamics of VPS4 localization and function during cytokinesis and abscission checkpoint activation. During early cytokinesis, VPS4 localizes to the intercellular bridge, but is absent from the midbody. At late cytokinesis, VPS4 is recruited to the midbody by ESCRT-III components such as CHMP1 and IST1 (Elia et al., 2011; Adell

and Teis, 2011). Interestingly, growth-phase dependent regulation of IST1 levels may determine cell fate, where high IST1 levels during rapid growth may direct VPS4 function towards cytokinesis through midbody recruitment and low IST1 levels found in stationary cells allow VPS4 localization to and function at multivesicular endosomes during membrane trafficking (Babst et al., 2011). Concurrently, IST1 binding through both a MIM1 and a MIM2 has been shown to keep VPS4 in a monomeric and hence inactive state, placing it as both a negative and positive regulator of VPS4 function during cytokinesis. Once at the midbody ring, VPS4 presumably undergoes a molecular hand-over from IST1/CHMP1 to ANCHR and CHMP4C, a process that may involve the protein MITD1 which has been implicated in negative regulation of the IST1-VPS4 interaction at the midbody (Lee et al., 2012; Hadders et al., 2012). Subsequently, VPS4 is retained on the midbody ring by ANCHR and CHMP4C until abscission checkpoint signalling is terminated. While our results indicate that VPS4 is not glued to the midbody ring upon ANCHR overexpression, its diffusion rate is significantly reduced, suggesting that ANCHR/CHMP4C-mediated retention of VPS4 involves competition with positive regulators of VPS4 through a shift in molecular dynamics and affinities. It is not unlikely that ANCHR and CHMP4C also keep VPS4 in an inactive state, since they may bind simultaneously to VPS4 monomers. Upon termination of the abscission checkpoint, inactivation of Aurora B and subsequent dephosphorylation of CHMP4C facilitates dissociation of the ANCHR/CHMP4C/VPS4 ternary complex and release of VPS4. It should be noted that VPS4 activation and translocation to the abscission zone, although currently not fully elucidated, entail a number of steps, such as multimerization and association with several cofactors. These steps have been shown to depend on several MIM-containing ESCRT-III proteins such as CHMP1B and CHMP2A (Adell and Teis, 2011), which may, as previously suggested, be out-competed by ANCHR/CHMP4C while abscission checkpoint signalling persists. According to current opinion, once at the abscission zone and after microtubule severing mediated by Spastin has occurred, multimeric VPS4 together with its cofactor LIP5 catalyzes disassembly of ESCRT-III (CHMP4B) filaments. This, in turn, leads to fusion of opposing membranes yielding two daughter cells. Although the details are still

unclear, the nature of VPS4 regulation and translocation is a complex and exciting topic which is subject to extensive research efforts in the field.

A role for PtdIns3P in regulation of ANCHR-mediated abscission delay?

Whereas previous results indicate a positive regulatory role for PtdIns3P in cytokinesis (**paper I** and (Sagona et al., 2010)), ANCHR is rather a negative regulator of this process. Although we could show that ANCHR could bind PtdIns3P through both liposome binding assays and localization of a FYVE-domain-containing ANCHR fragment to PtdIns3P-positive endosomes (**paper II**), interfering with PtdIns3P binding through mutation did not inhibit its ability to delay cytokinesis. If anything, there was a slight (but statistically insignificant) increase in the cytokinetic cell fraction (**paper II**, figure 1H). Thus, PtdIns3P binding is likely not essential for positive regulation of ANCHR function during cytokinesis. However, we cannot exclude that it may still contribute to negative regulation of ANCHR, consistent with the finding that PtdIns3P depletion causes cytokinesis arrest. Elucidation of PtdIns3P involvement in the regulation of ANCHR may also require further manipulation of auxilliary factors, especially CHMP4C given its similar role in VPS4 retention. It is interesting to note that the ANCHR FYVE domain has an atypical sequence, where key cysteine residues are conserved, but several other residues that form the core consensus sequence are not. This is intriguing, since very few atypical FYVE domains have been identified as functional PtdIns3P binders, and it has generally been thought that PtdIns3P binding relies heavily on the presence of conserved consensus residues.

ANCHR in G2/M checkpoint regulation

In **paper III** we uncover a role for ANCHR in maintaining G2 arrest upon DNA damage induction during G2/M checkpoint activation, to prevent premature mitotic entry. Not only does overexpression of ANCHR result in an increase in the G2

population in untreated U2OS cells, but depletion of ANCHR abrogates DNA damage-induced G2 arrest. Moreover, preliminary data suggest ANCHR could be regulated at the protein level and may be a target of several well known G2/M checkpoint kinases, including Aurora A, PLK1 and CDK1.

G2/M checkpoint function and regulation of mitotic entry are multifaceted processes. First, the cells must arrest the cell cycle through initial checkpoint activation, a signalling cascade that is dependent on mulitple kinases, phosphatases and other proteins such as ATM/ATR, CHK1/2, CDC25, culminating in the inhibition of Cyclin B / CDK1. Next, any damaged DNA must be repaired, before the cell cycle resumes through the process of checkpoint recovery. This latter event is also dependent on the action of many kinases and other proteins, including Aurora A, BORA and PLK1, which positively regulate the Cyclin B / CDK1 complex through activation of CDC25. If the DNA damage is too extensive for successful repair, the cell undergoes apoptosis.

G2/M checkpoint activation vs recovery

The precise role of ANCHR in G2/M checkpoint function is still unclear. Some findings support a role for ANCHR dutin checkpoint activation. Firstly, ANCHR is a putative target of the ATM/ATR kinases (Matsuoka et al., 2007) which are intstrumental during initiation of DNA-damage induced checkpoint signalling. Secondly, our mass spectrometric analysis, in addtition to previously published data (Olsen et al., 2010), revealed that ANCHR may also be differentially phosphorylated on serine 354 by the kinases NEK6 and/or CK2 upon DNA damage induction, both of which have been implicated in G2/M checkpoint activation (Lee et al., 2008b; Theis-Febvre et al., 2003; Zwicker et al., 2011). Thirdly, the enrichment of G2 cells upon overexpression of ANCHR in U2OS cells may reflect aberrant checkpoint activation. However, several observations argue for a role specifically in checkpoint recovery. Firstly, the initial lag in the rate of mitotic entry upon DNA damage induction in ANCHR-depleted U2OS cells suggests that they may have undergone checkpoint

activation, but failed to maintain a G2 arrest over time. Secondly, our *in vitro* kinase assays indicate that ANCHR is a putative target of several kinases specifically involved in checkpoint recovery, including PLK1 and Aurora A. In **paper II**, we found that phosphorylation of Serine 22 on ANCHR could be phosphorylated by Aurora B in vitro, but this phosphorylation event could not be verified in vivo, and did not seem to be required for ANCHR function in regulation of the abscission checkpoint. However, since Aurora A and Aurora B have identical sequence specificities, we speculate that phosphorylation of S22 could rather be an Aurora A target. Thirdly, if regulation of ANCHR abundance is essential for its role in G2/M checkpoint regulation, the relatively slow kinetics of protein level increase upon IR would argue for a role at later rather than earlier time points. To fully distinguish between checkpoint activation and recovery defects upon ANCHR depletion, abrogation of G2 arrest following DNA damage induction would have to be assessed at a higher time resolution, in particular at early timepoints, since activation occurs as early as 1-2 hours after IR (Menzel et al., 2011). Also, the use of kinase inhibitors would allow further temporal resolution and dissection of epistatic signalling relationships between ANCHR and other checkpoint regulators. Checkpoint activation and recovery regulation are of course not mutually exclusive processes, so it is not impossible that ANCHR plays a role in both. Regardless, it is not unlikely that ANCHR-mediated G2/M checkpoint control involves CDK1, since CDK1 is crucial for successful mitotic entry and is targeted by both activation and recovery regulators. This is supported by the observation that ANCHR can be phosphorylated by CDK1 in vitro. Moreover, ANCHR also contains two predicted binding sites for Cyclins that could mediate interaction with the Cyclin B / CDK1 complex in relation to CDK1-mediated phosphorylation, further supporting a potential functional relationship between these two. Interestingly, there is also a predicted binding site for PIN1 that directly overlaps with the CDK1 target phosphorylation site, a protein that has been shown to negatively regulate G2/M transition by interacting with the Aurora A - BORA complex (Lee et al., 2013). This suggests that differential phosphorylation status on this residue could affect the binding

of ANCHR to PIN1, should this be a *bona fide* interaction partner. However, further interaction-studies would be required to confirm this.

Is ANCHR-mediated G2/M checkpoint control p53 dependent?

Interestingly, overexpression of ANCHR caused enrichment of the G2 population in U2OS cells, but not in the HeLa cell line. One key difference between these two cell types is p53 status, where U2OS cells are p53-proficient (Florenes et al., 1994), while p53 function in HeLa cells is strongly repressed due to expression of the E6 and E7 proteins by oncogenic Human Papilloma Virus (HPV) (Villa, 1997). p53 is known as a master regulator of cell cycle progression and chromosomal stability, and has been found deregulated in most human cancers (Olivier et al., 2010). Furthermore, it is an integral part of the G2/M checkpoint maintenance network, mainly by acting as a transcriptional regulator of other checkpoint components and by inducing apoptosis. Moreover, HeLa cells are known to have weak G2/M checkpoint induction, partly due to inactivation of p53 (Bunz et al., 1998). The fact that p53 has been shown to be important for maintaining G2 arrest over time could be in accordance with our results suggesting that ANCHR-depleted cells may initially activate the G2/M checkpoint upon irradiation but rather recover prematurely, Moreover, the slow increase in ANCHR protein levels upon irradiation, should this be due to transcriptional regulation, may be attributed to p53 given its essential role as a tumour suppressive transcriptional regulator. Thus, the phenotypic difference between U2OS and HeLa cells upon ANCHR overexpression may reflect p53-dependency of ANCHR-mediated G2/M checkpoint function. It is also interesting to note that upon DNA damage induction by IR, the G1 population is reduced in ANCHR-depleted U2OS cells compared to cells treated with non-targeting siRNA. This could potentially reflect an ANCHR-dependent defect in G1 arrest and hence G1/S checkpoint signalling. Since this checkpoint is heavily reliant on p53, this observation also suggests that certain ANCHR-mediated checkpoint functions could be p53-dependent. However, the role of ANCHR in cell

cycle checkpoint signalling and its functional relationship with p53 need further investigation.

How does ANCHR function as a regulator of the G2/M checkpoint?

Our preliminary data place ANCHR as a regulator of the G2/M checkpoint, but the mechanism by which it functions to prevent aberrant mitotic entry is unknown. Firstly, our *in vitro* phosphorylation assays, mass spectrometric- and bioinformatic analysis suggest, together with previously published data, that ANCHR is a potential target for several kinases and other proteins implicated in checkpoint signalling. The observation that ANCHR is a putative phosphorylation target of CDK1 suggests that a functional relationship between these, should it exist, could underlie ANCHR-mediated G2/M checkpoint regulation. This might have implications for ANCHR localization, protein abundance or protein interactions. The increase in ANCHR protein levels during IR-induced G2 arrest suggests that it could either be transcriptionally upregulated or stabilized through inhibition of protein degradation, mechanisms which are both common for other regulators of the G2/M checkpoint. For instance, DNA damage is known to promote transcriptional regulation of many target genes, especially through p53-mediated transcriptional control (Taylor and Stark, 2001). Rapid alterations in protein levels can also be achieved through degradation. Well characterized examples include increased BRCA1-mediated proteasomal degradation of Cyclin B and CDC25 upon DNA damage induction (Shabbeer et al., 2013), and degradation of BORA as a requirement for mitotic progression, mediated by the SCF/β-TrCP ligase which targets it for proteolysis (Seki et al., 2008a). Interestingly, targeting of proteins for destruction is often preceeded by specific phosphorylation events, for instance by kinases such as PLK1 and CDK1 (Cardozo and Pagano, 2004). Since ANCHR harbour such target sites and seem to be phosphorylated by these kinases in vitro, it is not unlikely that this might contribute to regulation of ANCHR protein stability.

Whether G2/M checkpoint regulation by ANCHR could involve the ESCRT machinery and VPS4, as is the case during abscission checkpoint activation, remains to be determined. While these factors have well defined functions during cytokinesis and abscission, less is known about their roles during mitotic entry. Although several ESCRT components and VPS4 were implicated in centrosome and spindle maintenance and VPS4 could be detected at centrosomes during both interphase and early mitosis (Morita et al., 2010), no specific G2/M checkpoint functions have been described. Furthermore, no reports have linked PtdIns3P-mediated signalling to regulation of mitotic entry. Although a few reports highlight potential roles of lipids during the G2 to M transition, such as Diacylglycerol (DAG)-dependent disassembly of the nuclear envelope (Mall et al., 2012), this is a field that requires further study. There are also other as yet uncharacterized structural features of ANCHR which may have functional roles during checkpoint regulation. These include the C-terminal BBOX zinc finger, a type which is not well characterized, and the MIM1-B which may be involved in mediating interactions with MIT-domain protein(s). One interesting observation is that ANCHR is a putative target of PLK1, a kinase that is essential for regulating both the G2/M checkpoint and cytokinesis. Thus, this may represent a link between the two checkpoint functions of ANCHR.

It is clear that there is still a lot to be leared about the role of ANCHR in G2/M checkpoint regulation, and how this relates to its function in abscission checkpoint control. Nevertheless, **Paper II** and **III** suggest that ANCHR may be an important general checkpoint regulator.

Implications for cancer: PtdIns3P and ANCHR

Since normal cell function relies on the precise interplay of a multitude of cellular processes regulated both spatially and temporally, tumourigenesis can result from deregulation of many of these. Of the known hallmarks of cancer (Hanahan and Weinberg, 2011), sustained proliferative signalling, evasion of growth suppressors and

genomic instability constitute three of the crucial events driving cancer development. Thus, failure to properly degrade growth factors and their receptors, deregulation of checkpoint signalling and accumulation of mutations and aneuploidy are well known contributors to this process. Below, I will discuss how the findings presented in this thesis can be placed within the contextual framework of cancer development.

PI3K-III and PtdIns3P in tumour suppression

Several of the core PI3K-III subunits have been classified as tumour suppressors, including Beclin 1, UVRAG and BIF-1 (Liang et al., 2006; Takahashi et al., 2007; Takahashi et al., 2005; Kim et al., 2008; Ionov et al., 2004; Goi et al., 2003; Bekri et al., 1997; Liang et al., 1999; Qu et al., 2003; Yue et al., 2003). This was originally attributed to their roles in positive regulation of autophagy, since this is a tumour suppressive process through the scavenging of damaged organelles that can cause genomic instability through reactive oxygen species (ROS)-induced DNA damage (Mathew et al., 2007). However, only one other genuine tumour suppressor have so far been identified amongst the autophagic machinery, namely ATG4C (Marino et al., 2007). Furthermore, monoallelic deletions of UVRAG in colon cancer cells did not affect autophagy (Knaevelsrud et al., 2010). Thus, the tumour suppressive properties of the PI3K-III complex may be related to its function in growth factor receptor degradation and / or cytokinesis.

Arguing in favour of a tumour suppressive role for degradative endosomal trafficking is the observation that the endosomal fusion regulator, Rabenosyn, is a tumour suppressor in fruit flies (Morrison et al., 2008), as are several components of the ESCRT machinery that act downstream of PtdIns3P (Moberg et al., 2005; Vaccari and Bilder, 2005; Vaccari et al., 2009). However, the ESCRT-0 component HRS is not a tumour suppressor in flies, arguing against this idea.

Certain observations argue in favour of a tumour suppressive role of the PI3K-III complex and PtdIns3P through regulation of cytokinesis. Firstly, failure of cytokinesis is a source of aneuploidy through cleavage furrow regression and multinucleation, and may thus represent a step in oncogenesis (Sagona and Stenmark, 2010). Secondly, tumour suppressive ESCRTs such as TSG101 also play a role in cytokinesis (Carlton and Martin-Serrano, 2007). Thirdly, the PtdIns3P effector FYVE-CENT required for cytokinesis has been found frequently mutated in breast cancer (Sjoblom et al., 2006; Wood et al., 2007), although it remains to be determined whether this is a *bona fide* tumour suppressor. Interestingly, the PI3K-III subunit UVRAG may have an additional tumour suppressive function, since it has been shown to promote repair of damaged DNA through non-homologous end joining (NHEJ) (Zhao et al., 2012). This was found to be independent of Beclin 1. Thus, UVRAG could potentially protect against genomic instability through multiple mechanisms.

Dissection of the tumour suppressive roles of PI3K-III and PtdIns3P is challenging, since deregulation of any of the downstream processes may be tumourigenic. Nevertheless, PI3K-III may be a possible target for cancer therapy due to its enzymatic function which could be targeted by specific inhibitors. Furthermore, systematic analyses of expression profiles of PI3K-III tumour suppressors in cancers may provide a useful diagnostic tool.

Deregulation of checkpoint signalling during mitotic entry and cytokinesis contributes to cancer development

Cell cycle checkpoints represent crucial barriers to cell proliferation in the presence of genomic aberrations, the failures of which may lead to tumourigenesis. Failure to prevent mitotic entry in the presence of damaged DNA has been shown to trigger mitotic catastrophe, an oncosuppressive process where an attempt at aberrant chromosome segregation culminates in apoptotic cell death (Vitale et al., 2011). However, evasion of mitotic catastrophe is associated with increased chromosome

missegregation, a phenomenon often observed in cancer cells. Subsequent genomic instability arises from unequal distibution of chromosomes to daughter cells (aneuploidy and accumulation of micronulei), further DNA damage and structural chromosomal aberrations (e.g. translocations or deletions) (Janssen et al., 2011). Importantly, the recent discovery that chromosome bridges stemming from missegregating DNA can also cause cleavage furrow regression through failure of the abscission checkpoint establishes aberrant mitotic entry as a source of aneuploidy through multinucleation (Steigemann et al., 2009), closely linking the G2/M- and abscission checkpoints. It also highlights the importance of coordinating abscission timing with chromatin segregation, since roughly one percent of somatic cells show segregation defects, a rate which is even higher in transformed cells (Gisselsson et al., 2000; Cimini et al., 2003).

Tumour suppressive properties of G2/M checkpoint function and the DNA damage response are well established, where tumour suppressors and oncogenes are identified within all steps, including checkpoint activation (e.g. ATM, CHK2 and NEK6), DNA repair (e.g. BRCA1), checkpoint recovery (e.g. Aurora A and PLK1), and apoptosis (e.g. p53). (Liang et al., 2009; Lu et al., 2008; Lobrich and Jeggo, 2007; Lens et al., 2010; Nassirpour et al., 2010). Less is known about tumour suppression during activation of the abscission checkpoint, primarily because this is a new field of study with few regulatory factors described. The master regulator of the abscission checkpoint, Aurora B, has been linked to cancer development, although it is not clear if it functions primarily as an oncogene or as a tumour suppressor (Lens et al., 2010; Fu et al., 2007). This may reflect the diverse roles of Aurora B during mitosis, including chromatin modification, attachment of microtubules to chromosome kinetochores, spindle checkpoint function and cytokinesis. Since aneuploidy is strongly associated with cancer (Gordon et al., 2012), a role for abscission checkpoint as a tumour suppressive mechanism is not inconceivable.

ANCHR and cancer

Given the importance of both the G2/M- and abscission checkpoints in maintaining genomic stability, the dual roles of ANCHR in maintaining checkpoint-induced arrest both prior to mitotic entry and before completion of cytokinesis establishes it as a potential guardian of chromatin integrity (Figure 12). This, however, begs the question why ANCHR has not been observed frequently deregulated in cancers earlier? Perhaps ANCHR defects may generally have such detrimental effects on cell survival, for example through mitotic catastrophe or apoptosis, that they are not commonly detected in cancer screens. However, a preliminary analysis we conducted of normal and cancer tissues show that ANCHR is found differentially expressed is some cancers, in particular in certain blood cancers (unpublished data). Interestingly, of the three available clinical publications on ANCHR (ZFYVE19), they all relate to differential expression in blood cells, and two specifically relate to blood cancers. One study showed that ANCHR expression is upregulated in chronic lymphocytic leukemia (CLL) which elicited effective tumour immunity and subsequent remission in patients that received donor lymphocyte infusion (Marina et al., 2010). A second study showed that an ANCHR fragment recurred as a fusion with another protein MLL in acute myeloblastic leukemia (AML) (Chinwalla et al., 2003). Intriguingly, this ANCHR fragment lacked both the MIM1-B, FYVE- and BBOX domains, but retained the MIM1-A, suggesting that any tumourigenic effect of this fusion protein may involve VPS4. The limited data available

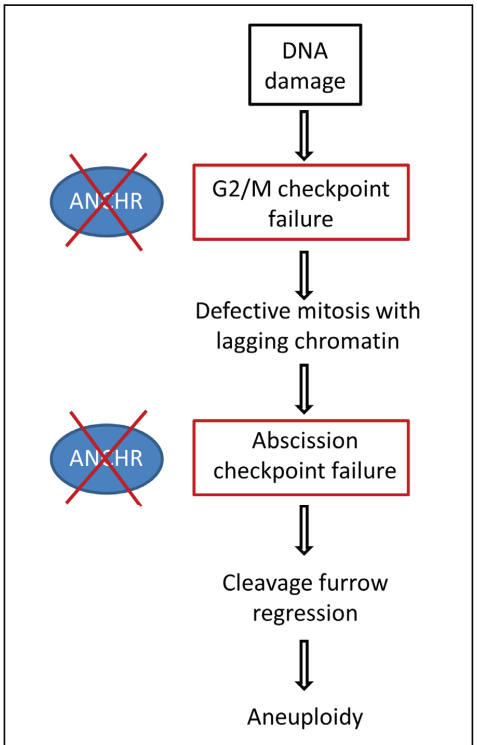

Figure 12: Deregulation of ANCHR may affect genomic stability and ploidy through multiple mechanisms.

on ANCHR highlight the need for further studies to get a more detailed understanding of its role as a checkpoint regulator and protector of genomic integrity in cancer development.

How alterations in ANCHR expression levels would impact on tumourigenesis remains to be determined. For instance, cleavage furrow regression and multinucleation can arise through failure of both positive and negative regulation of abscission. Thus, both up- and downregulation of ANCHR could potentially lead to aneuploidy and genomic instability, since normal cytokinesis is perturbed in both cases. Similarly, up- or downregulation of ANCHR during G2/M checkpoint signalling may both prove tumourigenic. On one hand, low ANCHR levels could allow cells to bypass the G2/M checkpoint, leading to increased chromosomal instability in the presence of DNA damage. On the other hand, since avoidance of apoptosis is a hallmark of cancer cells (Hanahan and Weinberg, 2011), persistent checkpoint activation by high ANCHR levels could lead to eventual adaptation and mitotic progression rather than cell death. Furthermore, since many cancer therapies exploit irradiation- or drug-induced DNA damage to initiate cell death through checkpoint-mediated apoptosis and/or mitotic catastrophe (Eriksson and Stigbrand, 2010), ANCHR status may impact on the outcome of such treatment. Accordingly, ANCHR expression level analysis could provide a potential prognostic marker for different cancer types, depending on genetic background, and their treatment.

Experimental considerations

Cell lines as model systems

Cell lines constitute essential research tools, since they provide a minimal human model in which to address fundamental biological questions. Unlike primary cells, immortalized cell lines can divide indefinitely, providing an unlimited supply of biological material. Furthermore, many such cell lines are easily manipulated, for example through transfections, and allow researchers to perform experiments in model systems with uniform and characterized genetic backgrounds. However, accumulation of mutations during many rounds of ex vivo growth may have made them considerably different from their original ancestors. Another disadvantage of using cell lines is the simplified picture of the biological process under study. In the human body, cells are part of a complex three-dimensional environment with which they interact, such as a wide range of cell types, growth factors, and nutrients in the blood stream. Many of these aspects of cell biology are absent in cell culture.

In the papers included in this thesis, we have utilized common immortal cell lines, including HeLa cervical cancer cell lines and an osteosarcoma U2OS cell line. The work in **paper I** was performed exclusively in the HeLa cell line, since this is a well established model to study both growth factor receptor degradation and cytokinesis. Similarly, this cell line formed the basis for the work on the role of ANCHR in the abscission checkpoint in **paper II**. In **paper III**, U2OS cells were more suited to study the role of ANCHR in the G2/M checkpoint, since they are known to be checkpoint-proficient, unlike HeLa cells which have a partially compromized checkpoint (Florenes et al., 1994; Bunz et al., 1998). In fact, the inherent difference in G2/M checkpoint proficiency between HeLa and U2OS cells was key to studying differential ANCHR checkpoint functions. Since ectopic overexpression of ANCHR appeared to induce a G2 arrest in U2OS cells, this would mask any downstream phenotypes. Since similar

overexpression in HeLa cells allowed mitotic progression and cytokinesis, we could utilize this to study ANCHR function in the abscission checkpoint. Moreover, since our results from **paper II** show that ANCHR specifically prevents multinucleation in cells with lagging chromatin, the identification of ANCHR in the initial siRNA screen (scoring for multinucleate cells) was possible only because the HeLa cells used in this study display a high basal rate of chromosome missegregation. Finally, G2/M checkpoint deficiency in HeLa cells would prohibit the study of ANCHR function during this process. These observations highlight the importance of caution in generalizing across different biological systems, but more importantly the value of utilizing different cell lines to study different processes.

siRNA-mediated depletion of proteins

Gene silencing by siRNA has become a standard technique to study protein function. However, there are a few pitfalls that must be considered when deciding an experimental setup. Firstly, the transfection reagent used together with the siRNA oligo can itself be toxic to the cells. Secondly, the siRNA oligo may itself produce both toxic and non-specific effects due to either activation of the interferon response or silencing additional genes from sequence overlap with other RNA transcripts (off-target effects). When studying the PI3K-III subunits in **paper I**, we used primarily siRNA sequences that had been used in previously published studies. Extra steps were taken to reduce off-target effects when studying the previously uncharacterized protein ANCHR, firstly by using two individual siRNA oligos targeting different sequences, and also by rescue assays where depletion-induced phenotypes were reversed by stable expression of moderate levels of siRNA-resistant ANCHR. Thirdly, efficiency of siRNA-depletion can vary between different oligos and also between experiments. Measuring protein levels by western blotting (whole cell protein levels) and /or immunofluoresence microscopy (site-specific levels) is commonly used to verify depletion, where antibodies recognizing endogenous proteins are available.

Screening for regulators of cytokinesis

Identification of ANCHR as a regulator of cytokinesis was achieved through an image-based siRNA screen targeting FYVE-domain (PtdIns3P-binding) proteins. Here, the use of unbiased high-content microscopy and multiple experiment repeats limited the rate of false positives and negatives. Also, we employed the use of smart-pool siRNAs, where each pool contain a mix of four different siRNA oligos targeting the same protein. This increases the probability of efficient knock-down of target proteins, thereby reducing the rate of false negatives. However, it also increases the rate of off-target effects, highlighting the importance of caution during analysis, and the need for validation of results during follow-up studies.

Ectopic expression of proteins

To study the function of proteins of interest or to assess the effect of mutations or truncations in those, we have utilized transient transfection of cells and stably transfected cell lines. The use of tagged proteins provides a useful tool for easy visualization in cases where detection of endogenous proteins by antibodies is not feasible, because antibodies are either not available (e.g. for CHMP4C) or not suitable (e.g. for live microscopy). Stably transfected cell lines are very useful to study protein dynamics over time, and can be manipulated to express proteins at homogenous and moderate or near-endogenous levels. However, generating stable cell lines is a time-consuming process. Transient transfections are extensively used, fast and easily performed, but also have their caveats. Firstly, transfection efficiency and expression levels may be highly heterogeneous between cells, potentially giving large variation in phenotypic outcome. Furthermore, significant overexpression of proteins may have dominant negative effects, and may induce effects that are not physiologically relevant, such as altered protein interaction affinities and mislocalization. Here, complementary studies, for instance by protein depletion and mutation, are useful to distinguish between artefacts and true protein function. However, overexpression may sometimes

prove particularly useful in the study of protein function, as was the case for ANCHR, since moderate expression levels did not induce proper cytokinesis arrest (**paper II**). Nevertheless, it is important to be cautious when interpreting phenotypic effects based on protein overexpression.

High content image analysis, confocal and live microscopy

Quantitation of cytokinetic and multinuclear cells (**paper I, II** and **III**), degradation of EGF (**paper I**) and cells in G2 phase (**paper III**) was based on image acquisition by high-content microscopy. Subsequently, images were analysed either automatically by software packages that allowed identification of individual cells and spot intensity (EGF and G2 cells), or manual scoring of cells stained with additional markers (cytokinetic and multinucleate cells). The main advantages of using this setup are firstly the ability to analyse large datasets acquired at a high speed, reducing the need for manual labour. Also, the automated nature of image acquisition allows unbiased imaging of a large number of random cells.

For qualitative assessment of subcellular localization and protein levels, we utilized confocal microscopy. This is based on the principle of signal exclusion from outside the focal plane, resulting in highly resolved images in the x-, y- and z-axes. As long as precautions are taken to avoid artefacts such as bleed-through and signal saturation, confocal microscopy provides a powerful tool for the detailed dissection of protein localization, co-localization and abundance.

The confocal microscope was also employed for photoconversion experiments assessing VPS4 diffusion at the midbody in **paper II**. Here, a photoconvertable form of GFP (mEOS) fused to VPS4 was illuminated at the region of interest (midbody), switching it from green to red fluoresence. This allowed measurement of signal intensities and thus the half-life of photoconverted fluorophores specifically. This was compared between untransfected cells and GFP-ANCHR transfected cells. The

drawback here is that the GFP-ANCHR itself may influence the efficiency of photoconversion and / or signal detection of photoconverted VPS4. Thus, these experiments should ideally be performed with untagged ANCHR, or with a tagged protein that also localizes to the midbody but does not influence VPS4 diffusion as a control. However, these also present significant technical challenges, such as the difficulty of detection of ANCHR-transfected non-fixed cells and avoiding artefacts induced by overexpression of midbody proteins.

For the study of protein dynamics over time (**paper II**), we utilized live microscopy of cells stably expressing different tagged protein markers. This is also useful for analysing cell fate following various treatments, such as siRNA or protein inhibitors.

Protein-protein interaction studies

Many of the findings presented in **paper II** are based on novel protein-protein interactions. These were primarily based on two methods, namely GFP-trap immunoprecipitation and mass spectrometry. The GFP-trap system utilizes antibodies that recognize and immunoprecipitate ectopically expressed GFP-tagged proteins and concommittantly their interaction partners. The resulting lysate could then be analysed by either biochemical methods such as western blotting, or mass spectrometric analysis. In the latter case, protein peptides were identified based on their molecular and chemical composition. Thus, classical mass spectrometry is a robust way of detecting the presence of protein peptides and, althought not inherently quantitative, it can to a certain extent say something about protein expression levels through the frequency of peptide occurrence.

Bioinformatic analyses of domains, motifs and phospho sites

The use of bioinformatic software to analyse protein sequences and predict domains, motifs and post-translational modifications is becoming more and more widely used. This is based on sequence alignments and defined consensus sequences to find conservation and similarities with known structural elements. We have employed such methods to identify potential target phosphorylation sites and protein interaction sites on ANCHR in **paper II** and **III**. While bioinformatic analyses provide useful tools to indicate potential features of interest, the relevance of these in a biological context is unknown. Thus, bioinformatic data should always be verified experimentally. Since different software employ different algorithms, they can give differing results. Another source of uncertainty stems from natural sequence variation (e.g. single nucleotide polymorphisms) or sequencing errors resulting in wrongly annotated protein sequences. These issues highlight the importance of carefully selecting software and identification of the protein sequence of interest.

In vitro and in vivo phosphorylation

In **paper III**, we have analysed phosphorylation of ANCHR by different methods. The first is *in vitro* phosphorylation where purified proteins are incubated with active kinases that catalyses the incorporation of radioactive phosphate groups on target peptides. This can be analysed by subsequent SDS-PAGE and autoradiography. The second was mass spectrometric analysis of the output from the *in vitro* kinase assay, or immunoprecipitated transiently transfected GFP-ANCHR. Together, these methods can give an indication of which phosphorylation events are biologically relevant. However, as shown in **paper II**, peptide phosphorylation in vitro does not imply a similar event in vivo (Aurora B-mediated phosphorylation of ANCHR), highlighting the importance of data verification.

Conclusions and future perspectives

The work presented in this thesis has contributed to our understanding of how key signalling events are controlled during regulation of the cell division cycle. We have shown that a specific PI3K-III sub-complex is involved in the control of degradative endocytic traffic and cytokinesis (**paper I**), and identified ANCHR as a novel cell cycle checkpoint regulator (**paper II** and **III**), as summarized in figure 13.

Differential regulation of the PI3K-III complex is a topic of wide interest, especially given its diverse functions in many essential biological processes. Future research will determine additional aspects of PI3K-III regulation that control its context-specific functions. While the role of its catalytic product, PtdIns3P, in autophagy and endosomal membrane trafficking has been studied in some detail, its role in regulation of cytokinesis is only beginning to be unravelled. Furthermore, the nature of the tumour suppressive functions of PI3K-III and PtdIns3P needs to be further dissected, understanding of which could potentially be exploited therapeutically.

Since ANCHR is a previously uncharacterized protein, much is yet to be learned about its roles in checkpoint control. How does ANCHR induce G2 arrest? What are the upstream regulators of ANCHR and do different cellular processes rely on similar ANCHR-mediated mechanisms? Does ANCHR control other cell cycle checkpoints or cell signalling events? What are the roles of the different structural elements of ANCHR? Is PtdIns3P-binding involved in the regulation of ANCHR? What comprises the MIM-MIT interaction network and how is this differentially regulated? How does VPS4 translocate from the midbody to the abscission zone? How does ANCHR deregulation impact on chromosomal stability and tumourigenesis? Can ANCHR provide a candidate target or prognostic marker for cancer diagnostics or therapy? These and many other questions remain to be answered. Nevertheless, our findings outline many exciting avenues of potential future research.

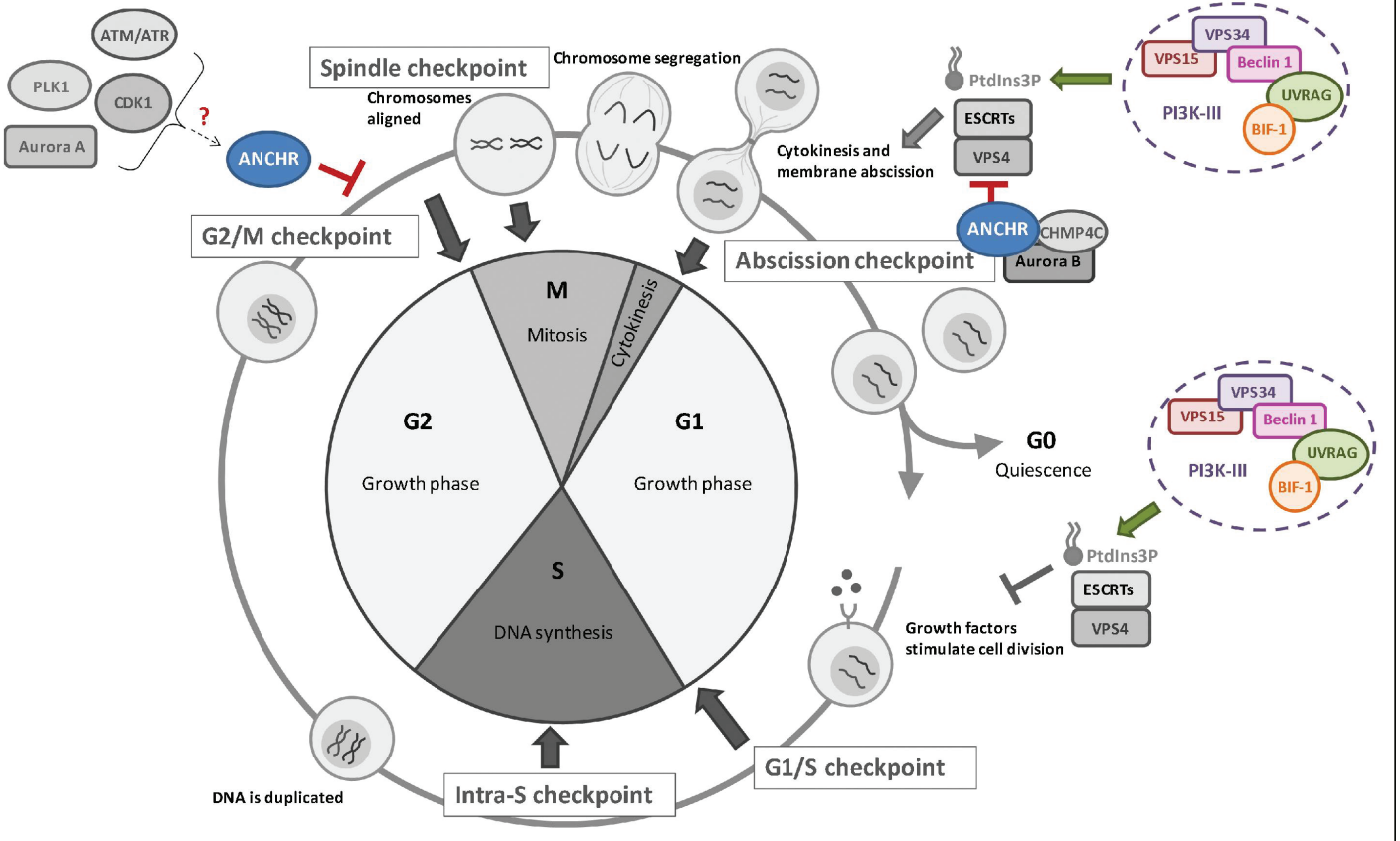

Figure 13: Summary. The PI3K-III complex consisting of VPS15, VPS34, Beclin 1, UVRAG and BIF-1 controls growth factor receptor degradation and cytokinesis. ANCHR is required for G2/M checkpoint function and abscission checkpoint-mediated arrest during cytokinesis.

Reference List

Adell,M.A. and Teis,D. (2011). Assembly and disassembly of the ESCRT-III membrane scission complex. FEBS Lett. *585*, 3191-3196.

Andersen,S.S. (1999). Balanced regulation of microtubule dynamics during the cell cycle: a contemporary view. Bioessays *21*, 53-60.

Babst,M., Davies,B.A., and Katzmann,D.J. (2011). Regulation of Vps4 during MVB sorting and cytokinesis. Traffic. *12*, 1298-1305.

Babst,M., Katzmann,D.J., Estepa-Sabal,E.J., Meerloo,T., and Emr,S.D. (2002). Escrt-III: an endosome-associated heterooligomeric protein complex required for mvb sorting. Dev. Cell *3*, 271-282.

Babst,M., Sato,T.K., Banta,L.M., and Emr,S.D. (1997). Endosomal transport function in yeast requires a novel AAA-type ATPase, Vps4p. EMBO J. *16*, 1820-1831.

Backer,J.M. (2008). The regulation and function of Class III PI3Ks: novel roles for Vps34. Biochem. J. *410*, 1-17.

Bajorek,M., Morita,E., Skalicky,J.J., Morham,S.G., Babst,M., and Sundquist,W.I. (2009). Biochemical analyses of human IST1 and its function in cytokinesis. Mol. Biol. Cell *20*, 1360-1373.

Bekri,S., Adelaide,J., Merscher,S., Grosgeorge,J., Caroli-Bosc,F., Perucca-Lostanlen,D., Kelley,P.M., Pebusque,M.J., Theillet,C., Birnbaum,D., and Gaudray,P. (1997). Detailed map of a region commonly amplified at 11q13-->q14 in human breast carcinoma. Cytogenet. Cell Genet. *79*, 125-131.

Booher,R.N., Holman,P.S., and Fattaey,A. (1997). Human Myt1 is a cell cycle-regulated kinase that inhibits Cdc2 but not Cdk2 activity. J. Biol. Chem. *272*, 22300-22306.

Bunz,F., Dutriaux,A., Lengauer,C., Waldman,T., Zhou,S., Brown,J.P., Sedivy,J.M., Kinzler,K.W., and Vogelstein,B. (1998). Requirement for p53 and p21 to sustain G2 arrest after DNA damage. Science *282*, 1497-1501.

Burd,C.G. and Emr,S.D. (1998). Phosphatidylinositol(3)-phosphate signaling mediated by specific binding to RING FYVE domains. Mol. Cell *2*, 157-162.

Capalbo,L., Montembault,E., Takeda,T., Bassi,Z.I., Glover,D.M., and D'Avino,P.P. (2012). The chromosomal passenger complex controls the function of endosomal

sorting complex required for transport-III Snf7 proteins during cytokinesis. Open. Biol. *2*, 120070.

Cardozo,T. and Pagano,M. (2004). The SCF ubiquitin ligase: insights into a molecular machine. Nat. Rev. Mol. Cell Biol. *5*, 739-751.

Carlton,J.G., Caballe,A., Agromayor,M., Kloc,M., and Martin-Serrano,J. (2012). ESCRT-III governs the Aurora B-mediated abscission checkpoint through CHMP4C. Science *336*, 220-225.

Carlton,J.G. and Martin-Serrano,J. (2007). Parallels between cytokinesis and retroviral budding: a role for the ESCRT machinery. Science *316*, 1908-1912.

Cheever,M.L., Sato,T.K., de,B.T., Kutateladze,T.G., Emr,S.D., and Overduin,M. (2001). Phox domain interaction with PtdIns(3)P targets the Vam7 t-SNARE to vacuole membranes. Nat. Cell Biol. *3*, 613-618.

Chinwalla,V., Chien,A., Odero,M., Neilly,M.B., Zeleznik-Le,N.J., and Rowley,J.D. (2003). A t(11;15) fuses MLL to two different genes, AF15q14 and a novel gene MPFYVE on chromosome 15. Oncogene *22*, 1400-1410.

Chow,J. and Poon,R.Y. (2010). DNA damage and polyploidization. Adv. Exp. Med. Biol. *676*, 57-71.

Christoforidis,S., Miaczynska,M., Ashman,K., Wilm,M., Zhao,L., Yip,S.C., Waterfield,M.D., Backer,J.M., and Zerial,M. (1999). Phosphatidylinositol-3-OH kinases are Rab5 effectors. Nat. Cell Biol. *1*, 249-252.

Cimini,D., Mattiuzzo,M., Torosantucci,L., and Degrassi,F. (2003). Histone hyperacetylation in mitosis prevents sister chromatid separation and produces chromosome segregation defects. Mol. Biol. Cell *14*, 3821-3833.

Dimaano,C., Jones,C.B., Hanono,A., Curtiss,M., and Babst,M. (2008). Ist1 regulates Vps4 localization and assembly. Mol. Biol. Cell *19*, 465-474.

Donzelli,M. and Draetta,G.F. (2003). Regulating mammalian checkpoints through Cdc25 inactivation. EMBO Rep. *4*, 671-677.

Elia,N., Sougrat,R., Spurlin,T.A., Hurley,J.H., and Lippincott-Schwartz,J. (2011). Dynamics of endosomal sorting complex required for transport (ESCRT) machinery during cytokinesis and its role in abscission. Proc. Natl. Acad. Sci. U. S. A *108*, 4846-4851.

Eriksson,D. and Stigbrand,T. (2010). Radiation-induced cell death mechanisms. Tumour. Biol. *31*, 363-372.

Fabrikant,G., Lata,S., Riches,J.D., Briggs,J.A., Weissenhorn,W., and Kozlov,M.M. (2009). Computational model of membrane fission catalyzed by ESCRT-III. PLoS. Comput. Biol. *5*, e1000575.

Fenech,M., Kirsch-Volders,M., Natarajan,A.T., Surralles,J., Crott,J.W., Parry,J., Norppa,H., Eastmond,D.A., Tucker,J.D., and Thomas,P. (2011). Molecular mechanisms of micronucleus, nucleoplasmic bridge and nuclear bud formation in mammalian and human cells. Mutagenesis *26*, 125-132.

Fernandez-Borja,M., Wubbolts,R., Calafat,J., Janssen,H., Divecha,N., Dusseljee,S., and Neefjes,J. (1999). Multivesicular body morphogenesis requires phosphatidyl-inositol 3-kinase activity. Curr. Biol. *9*, 55-58.

Florenes,V.A., Maelandsmo,G.M., Forus,A., Andreassen,A., Myklebost,O., and Fodstad,O. (1994). MDM2 gene amplification and transcript levels in human sarcomas: relationship to TP53 gene status. J. Natl. Cancer Inst. *86*, 1297-1302.

Fu,J., Bian,M., Jiang,Q., and Zhang,C. (2007). Roles of Aurora kinases in mitosis and tumorigenesis. Mol. Cancer Res. *5*, 1-10.

Furuya,N., Yu,J., Byfield,M., Pattingre,S., and Levine,B. (2005). The evolutionarily conserved domain of Beclin 1 is required for Vps34 binding, autophagy and tumor suppressor function. Autophagy. *1*, 46-52.

Furuya,T., Kim,M., Lipinski,M., Li,J., Kim,D., Lu,T., Shen,Y., Rameh,L., Yankner,B., Tsai,L.H., and Yuan,J. (2010). Negative regulation of Vps34 by Cdk mediated phosphorylation. Mol. Cell *38*, 500-511.

Futter,C.E., Collinson,L.M., Backer,J.M., and Hopkins,C.R. (2001). Human VPS34 is required for internal vesicle formation within multivesicular endosomes. J. Cell Biol. *155*, 1251-1264.

Gaullier,J.M., Simonsen,A., D'Arrigo,A., Bremnes,B., Stenmark,H., and Aasland,R. (1998). FYVE fingers bind PtdIns(3)P. Nature *394*, 432-433.

Gillooly,D.J., Morrow,I.C., Lindsay,M., Gould,R., Bryant,N.J., Gaullier,J.M., Parton,R.G., and Stenmark,H. (2000). Localization of phosphatidylinositol 3-phosphate in yeast and mammalian cells. EMBO J. *19*, 4577-4588.

Gisselsson,D., Pettersson,L., Hoglund,M., Heidenblad,M., Gorunova,L., Wiegant,J., Mertens,F., Dal,C.P., Mitelman,F., and Mandahl,N. (2000). Chromosomal breakage-fusion-bridge events cause genetic intratumor heterogeneity. Proc. Natl. Acad. Sci. U. S. A *97*, 5357-5362.

Goi,T., Kawasaki,M., Yamazaki,T., Koneri,K., Katayama,K., Hirose,K., and Yamaguchi,A. (2003). Ascending colon cancer with hepatic metastasis and

cholecystolithiasis in a patient with situs inversus totalis without any expression of UVRAG mRNA: report of a case. Surg. Today *33*, 702-706.

Gordon,D.J., Resio,B., and Pellman,D. (2012). Causes and consequences of aneuploidy in cancer. Nat. Rev. Genet. *13*, 189-203.

Goss,J.W. and Toomre,D.K. (2008). Both daughter cells traffic and exocytose membrane at the cleavage furrow during mammalian cytokinesis. J. Cell Biol. *181*, 1047-1054.

Gromley,A., Yeaman,C., Rosa,J., Redick,S., Chen,C.T., Mirabelle,S., Guha,M., Sillibourne,J., and Doxsey,S.J. (2005). Centriolin anchoring of exocyst and SNARE complexes at the midbody is required for secretory-vesicle-mediated abscission. Cell *123*, 75-87.

Guizetti,J., Schermelleh,L., Mantler,J., Maar,S., Poser,I., Leonhardt,H., Muller-Reichert,T., and Gerlich,D.W. (2011). Cortical constriction during abscission involves helices of ESCRT-III-dependent filaments. Science *331*, 1616-1620.

Hadders,M.A., Agromayor,M., Obita,T., Perisic,O., Caballe,A., Kloc,M., Lamers,M.H., Williams,R.L., and Martin-Serrano,J. (2012). ESCRT-III binding protein MITD1 is involved in cytokinesis and has an unanticipated PLD fold that binds membranes. Proc. Natl. Acad. Sci. U. S. A *109*, 17424-17429.

Hanahan,D. and Weinberg,R.A. (2011). Hallmarks of cancer: the next generation. Cell *144*, 646-674.

Hanson,P.I., Roth,R., Lin,Y., and Heuser,J.E. (2008). Plasma membrane deformation by circular arrays of ESCRT-III protein filaments. J. Cell Biol. *180*, 389-402.

Hanson,P.I. and Whiteheart,S.W. (2005). AAA+ proteins: have engine, will work. Nat. Rev. Mol. Cell Biol. *6*, 519-529.

Hartwell,L.H. and Weinert,T.A. (1989). Checkpoints: controls that ensure the order of cell cycle events. Science *246*, 629-634.

He,C., Wei,Y., Sun,K., Li,B., Dong,X., Zou,Z., Liu,Y., Kinch,L.N., Khan,S., Sinha,S., Xavier,R.J., Grishin,N.V., Xiao,G., Eskelinen,E.L., Scherer,P.E., Whistler,J.L., and Levine,B. (2013). Beclin 2 functions in autophagy, degradation of G protein-coupled receptors, and metabolism. Cell *154*, 1085-1099.

Heald,R. and McKeon,F. (1990). Mutations of phosphorylation sites in lamin A that prevent nuclear lamina disassembly in mitosis. Cell *61*, 579-589.

Herman,P.K., Stack,J.H., DeModena,J.A., and Emr,S.D. (1991). A novel protein kinase homolog essential for protein sorting to the yeast lysosome-like vacuole. Cell *64*, 425-437.

Hierro,A., Sun,J., Rusnak,A.S., Kim,J., Prag,G., Emr,S.D., and Hurley,J.H. (2004). Structure of the ESCRT-II endosomal trafficking complex. Nature *431*, 221-225.

Hofmann,K. and Falquet,L. (2001). A ubiquitin-interacting motif conserved in components of the proteasomal and lysosomal protein degradation systems. Trends Biochem. Sci. *26*, 347-350.

Hurley,J.H. and Hanson,P.I. (2010). Membrane budding and scission by the ESCRT machinery: it's all in the neck. Nat. Rev. Mol. Cell Biol. *11*, 556-566.

Ionov,Y., Nowak,N., Perucho,M., Markowitz,S., and Cowell,J.K. (2004). Manipulation of nonsense mediated decay identifies gene mutations in colon cancer Cells with microsatellite instability. Oncogene *23*, 639-645.

Itakura,E., Kishi,C., Inoue,K., and Mizushima,N. (2008). Beclin 1 forms two distinct phosphatidylinositol 3-kinase complexes with mammalian Atg14 and UVRAG. Mol. Biol. Cell *19*, 5360-5372.

Itakura,E. and Mizushima,N. (2009). Atg14 and UVRAG: mutually exclusive subunits of mammalian Beclin 1-PI3K complexes. Autophagy. *5*, 534-536.

Jackson,S.P. and Bartek,J. (2009). The DNA-damage response in human biology and disease. Nature *461*, 1071-1078.

Janssen,A., van der Burg,M., Szuhai,K., Kops,G.J., and Medema,R.H. (2011). Chromosome segregation errors as a cause of DNA damage and structural chromosome aberrations. Science *333*, 1895-1898.

Karlsson-Rosenthal,C. and Millar,J.B. (2006). Cdc25: mechanisms of checkpoint inhibition and recovery. Trends Cell Biol. *16*, 285-292.

Katzmann,D.J., Odorizzi,G., and Emr,S.D. (2002). Receptor downregulation and multivesicular-body sorting. Nat. Rev. Mol. Cell Biol. *3*, 893-905.

Kieffer,C., Skalicky,J.J., Morita,E., De,D., I, Ward,D.M., Kaplan,J., and Sundquist,W.I. (2008). Two distinct modes of ESCRT-III recognition are required for VPS4 functions in lysosomal protein targeting and HIV-1 budding. Dev. Cell *15*, 62-73.

Kihara,A., Kabeya,Y., Ohsumi,Y., and Yoshimori,T. (2001a). Beclin-phosphatidylinositol 3-kinase complex functions at the trans-Golgi network. EMBO Rep. *2*, 330-335.

Kihara,A., Noda,T., Ishihara,N., and Ohsumi,Y. (2001b). Two distinct Vps34 phosphatidylinositol 3-kinase complexes function in autophagy and carboxypeptidase Y sorting in Saccharomyces cerevisiae. J. Cell Biol. *152*, 519-530.

Kim,J., Kim,Y.C., Fang,C., Russell,R.C., Kim,J.H., Fan,W., Liu,R., Zhong,Q., and Guan,K.L. (2013). Differential regulation of distinct Vps34 complexes by AMPK in nutrient stress and autophagy. Cell *152*, 290-303.

Kim,M.S., Jeong,E.G., Ahn,C.H., Kim,S.S., Lee,S.H., and Yoo,N.J. (2008). Frameshift mutation of UVRAG, an autophagy-related gene, in gastric carcinomas with microsatellite instability. Hum. Pathol. *39*, 1059-1063.

Kimura,K., Hirano,M., Kobayashi,R., and Hirano,T. (1998). Phosphorylation and activation of 13S condensin by Cdc2 in vitro. Science *282*, 487-490.

Knaevelsrud,H., Ahlquist,T., Merok,M.A., Nesbakken,A., Stenmark,H., Lothe,R.A., and Simonsen,A. (2010). UVRAG mutations associated with microsatellite unstable colon cancer do not affect autophagy. Autophagy. *6*, 863-870.

Kostelansky,M.S., Schluter,C., Tam,Y.Y., Lee,S., Ghirlando,R., Beach,B., Conibear,E., and Hurley,J.H. (2007). Molecular architecture and functional model of the complete yeast ESCRT-I heterotetramer. Cell *129*, 485-498.

Kutateladze,T. and Overduin,M. (2001). Structural mechanism of endosome docking by the FYVE domain. Science *291*, 1793-1796.

Landsberg,M.J., Vajjhala,P.R., Rothnagel,R., Munn,A.L., and Hankamer,B. (2009). Three-dimensional structure of AAA ATPase Vps4: advancing structural insights into the mechanisms of endosomal sorting and enveloped virus budding. Structure. *17*, 427-437.

Lee,H.H., Elia,N., Ghirlando,R., Lippincott-Schwartz,J., and Hurley,J.H. (2008a). Midbody targeting of the ESCRT machinery by a noncanonical coiled coil in CEP55. Science *322*, 576-580.

Lee,J.H. and Paull,T.T. (2004). Direct activation of the ATM protein kinase by the Mre11/Rad50/Nbs1 complex. Science *304*, 93-96.

Lee,M.Y., Kim,H.J., Kim,M.A., Jee,H.J., Kim,A.J., Bae,Y.S., Park,J.I., Chung,J.H., and Yun,J. (2008b). Nek6 is involved in G2/M phase cell cycle arrest through DNA damage-induced phosphorylation. Cell Cycle *7*, 2705-2709.

Lee,S., Chang,J., Renvoise,B., Tipirneni,A., Yang,S., and Blackstone,C. (2012). MITD1 is recruited to midbodies by ESCRT-III and participates in cytokinesis. Mol. Biol. Cell *23*, 4347-4361.

Lee,Y.C., Que,J., Chen,Y.C., Lin,J.T., Liou,Y.C., Liao,P.C., Liu,Y.P., Lee,K.H., Lin,L.C., Hsiao,M., Hung,L.Y., Huang,C.Y., and Lu,P.J. (2013). Pin1 acts as a negative regulator of the G2/M transition by interacting with the Aurora-A-Bora complex. J. Cell Sci. *126*, 4862-4872.

Lens,S.M., Voest,E.E., and Medema,R.H. (2010). Shared and separate functions of polo-like kinases and aurora kinases in cancer. Nat. Rev. Cancer *10*, 825-841.

Liang,C., Feng,P., Ku,B., Dotan,I., Canaani,D., Oh,B.H., and Jung,J.U. (2006). Autophagic and tumour suppressor activity of a novel Beclin1-binding protein UVRAG. Nat. Cell Biol. *8*, 688-699.

Liang,X.H., Jackson,S., Seaman,M., Brown,K., Kempkes,B., Hibshoosh,H., and Levine,B. (1999). Induction of autophagy and inhibition of tumorigenesis by beclin 1. Nature *402*, 672-676.

Liang,Y., Lin,S.Y., Brunicardi,F.C., Goss,J., and Li,K. (2009). DNA damage response pathways in tumor suppression and cancer treatment. World J. Surg. *33*, 661-666.

Lindas,A.C., Karlsson,E.A., Lindgren,M.T., Ettema,T.J., and Bernander,R. (2008). A unique cell division machinery in the Archaea. Proc. Natl. Acad. Sci. U. S. A *105*, 18942-18946.

Lobrich,M. and Jeggo,P.A. (2007). The impact of a negligent G2/M checkpoint on genomic instability and cancer induction. Nat. Rev. Cancer *7*, 861-869.

Lottridge,J.M., Flannery,A.R., Vincelli,J.L., and Stevens,T.H. (2006). Vta1p and Vps46p regulate the membrane association and ATPase activity of Vps4p at the yeast multivesicular body. Proc. Natl. Acad. Sci. U. S. A *103*, 6202-6207.

Lu,L.Y., Wood,J.L., Ye,L., Minter-Dykhouse,K., Saunders,T.L., Yu,X., and Chen,J. (2008). Aurora A is essential for early embryonic development and tumor suppression. J. Biol. Chem. *283*, 31785-31790.

Mackay,D.R., Makise,M., and Ullman,K.S. (2010). Defects in nuclear pore assembly lead to activation of an Aurora B-mediated abscission checkpoint. J. Cell Biol. *191*, 923-931.

Macurek,L., Lindqvist,A., Lim,D., Lampson,M.A., Klompmaker,R., Freire,R., Clouin,C., Taylor,S.S., Yaffe,M.B., and Medema,R.H. (2008). Polo-like kinase-1 is activated by aurora A to promote checkpoint recovery. Nature *455*, 119-123.

Mall,M., Walter,T., Gorjanacz,M., Davidson,I.F., Nga Ly-Hartig,T.B., Ellenberg,J., and Mattaj,I.W. (2012). Mitotic lamin disassembly is triggered by lipid-mediated signaling. J. Cell Biol. *198*, 981-990.

Marina,O., Hainz,U., Biernacki,M.A., Zhang,W., Cai,A., Duke-Cohan,J.S., Liu,F., Brusic,V., Neuberg,D., Kutok,J.L., Alyea,E.P., Canning,C.M., Soiffer,R.J., Ritz,J., and Wu,C.J. (2010). Serologic markers of effective tumor immunity against chronic lymphocytic leukemia include nonmutated B-cell antigens. Cancer Res. *70*, 1344-1355.

Marino,G., Salvador-Montoliu,N., Fueyo,A., Knecht,E., Mizushima,N., and Lopez-Otin,C. (2007). Tissue-specific autophagy alterations and increased tumorigenesis in mice deficient in Atg4C/autophagin-3. J. Biol. Chem. *282*, 18573-18583.

Mathew,R., Kongara,S., Beaudoin,B., Karp,C.M., Bray,K., Degenhardt,K., Chen,G., Jin,S., and White,E. (2007). Autophagy suppresses tumor progression by limiting chromosomal instability. Genes Dev. *21*, 1367-1381.

Matsuoka,S., Ballif,B.A., Smogorzewska,A., McDonald,E.R., III, Hurov,K.E., Luo,J., Bakalarski,C.E., Zhao,Z., Solimini,N., Lerenthal,Y., Shiloh,Y., Gygi,S.P., and Elledge,S.J. (2007). ATM and ATR substrate analysis reveals extensive protein networks responsive to DNA damage. Science *316*, 1160-1166.

McCullough,J., Row,P.E., Lorenzo,O., Doherty,M., Beynon,R., Clague,M.J., and Urbe,S. (2006). Activation of the endosome-associated ubiquitin isopeptidase AMSH by STAM, a component of the multivesicular body-sorting machinery. Curr. Biol. *16*, 160-165.

Mendoza,M., Norden,C., Durrer,K., Rauter,H., Uhlmann,F., and Barral,Y. (2009). A mechanism for chromosome segregation sensing by the NoCut checkpoint. Nat. Cell Biol. *11*, 477-483.

Menzel,T., Nahse-Kumpf,V., Kousholt,A.N., Klein,D.K., Lund-Andersen,C., Lees,M., Johansen,J.V., Syljuasen,R.G., and Sorensen,C.S. (2011). A genetic screen identifies BRCA2 and PALB2 as key regulators of G2 checkpoint maintenance. EMBO Rep. *12*, 705-712.

Moberg,K.H., Schelble,S., Burdick,S.K., and Hariharan,I.K. (2005). Mutations in erupted, the Drosophila ortholog of mammalian tumor susceptibility gene 101, elicit non-cell-autonomous overgrowth. Dev. Cell *9*, 699-710.

Morita,E., Colf,L.A., Karren,M.A., Sandrin,V., Rodesch,C.K., and Sundquist,W.I. (2010). Human ESCRT-III and VPS4 proteins are required for centrosome and spindle maintenance. Proc. Natl. Acad. Sci. U. S. A *107*, 12889-12894.

Morita,E., Sandrin,V., Chung,H.Y., Morham,S.G., Gygi,S.P., Rodesch,C.K., and Sundquist,W.I. (2007). Human ESCRT and ALIX proteins interact with proteins of the midbody and function in cytokinesis. EMBO J. *26*, 4215-4227.

Morrison,H.A., Dionne,H., Rusten,T.E., Brech,A., Fisher,W.W., Pfeiffer,B.D., Celniker,S.E., Stenmark,H., and Bilder,D. (2008). Regulation of early endosomal entry by the Drosophila tumor suppressors Rabenosyn and Vps45. Mol. Biol. Cell *19*, 4167-4176.

Murray,J.T., Panaretou,C., Stenmark,H., Miaczynska,M., and Backer,J.M. (2002). Role of Rab5 in the recruitment of hVps34/p150 to the early endosome. Traffic. *3*, 416-427.

Nassirpour,R., Shao,L., Flanagan,P., Abrams,T., Jallal,B., Smeal,T., and Yin,M.J. (2010). Nek6 mediates human cancer cell transformation and is a potential cancer therapeutic target. Mol. Cancer Res. *8*, 717-728.

Nielsen,E., Christoforidis,S., Uttenweiler-Joseph,S., Miaczynska,M., Dewitte,F., Wilm,M., Hoflack,B., and Zerial,M. (2000). Rabenosyn-5, a novel Rab5 effector, is complexed with hVPS45 and recruited to endosomes through a FYVE finger domain. J. Cell Biol. *151*, 601-612.

Nigg,E.A. (1995). Cyclin-dependent protein kinases: key regulators of the eukaryotic cell cycle. Bioessays *17*, 471-480.

Norbury,C. and Nurse,P. (1992). Animal cell cycles and their control. Annu. Rev. Biochem. *61*, 441-470.

Obara,K., Noda,T., Niimi,K., and Ohsumi,Y. (2008). Transport of phosphatidylinositol 3-phosphate into the vacuole via autophagic membranes in Saccharomyces cerevisiae. Genes Cells *13*, 537-547.

Olivier,M., Hollstein,M., and Hainaut,P. (2010). TP53 mutations in human cancers: origins, consequences, and clinical use. Cold Spring Harb. Perspect. Biol. *2*, a001008.

Olsen,J.V., Vermeulen,M., Santamaria,A., Kumar,C., Miller,M.L., Jensen,L.J., Gnad,F., Cox,J., Jensen,T.S., Nigg,E.A., Brunak,S., and Mann,M. (2010). Quantitative phosphoproteomics reveals widespread full phosphorylation site occupancy during mitosis. Sci. Signal. *3*, ra3.

Panaretou,C., Domin,J., Cockcroft,S., and Waterfield,M.D. (1997). Characterization of p150, an adaptor protein for the human phosphatidylinositol (PtdIns) 3-kinase. Substrate presentation by phosphatidylinositol transfer protein to the p150.Ptdins 3-kinase complex. J. Biol. Chem. *272*, 2477-2485.

Parker,L.L. and Piwnica-Worms,H. (1992). Inactivation of the p34cdc2-cyclin B complex by the human WEE1 tyrosine kinase. Science *257*, 1955-1957.

Patki,V., Lawe,D.C., Corvera,S., Virbasius,J.V., and Chawla,A. (1998). A functional PtdIns(3)P-binding motif. Nature *394*, 433-434.

Qu,X., Yu,J., Bhagat,G., Furuya,N., Hibshoosh,H., Troxel,A., Rosen,J., Eskelinen,E.L., Mizushima,N., Ohsumi,Y., Cattoretti,G., and Levine,B. (2003). Promotion of tumorigenesis by heterozygous disruption of the beclin 1 autophagy gene. J. Clin. Invest *112*, 1809-1820.

Raiborg,C., Bache,K.G., Mehlum,A., Stang,E., and Stenmark,H. (2001). Hrs recruits clathrin to early endosomes. EMBO J. *20*, 5008-5021.

Raiborg,C. and Stenmark,H. (2009). The ESCRT machinery in endosomal sorting of ubiquitylated membrane proteins. Nature *458*, 445-452.

Reid,E., Connell,J., Edwards,T.L., Duley,S., Brown,S.E., and Sanderson,C.M. (2005). The hereditary spastic paraplegia protein spastin interacts with the ESCRT-III complex-associated endosomal protein CHMP1B. Hum. Mol. Genet. *14*, 19-38.

Rue,S.M., Mattei,S., Saksena,S., and Emr,S.D. (2008). Novel Ist1-Did2 complex functions at a late step in multivesicular body sorting. Mol. Biol. Cell *19*, 475-484.

Russell,R.C., Tian,Y., Yuan,H., Park,H.W., Chang,Y.Y., Kim,J., Kim,H., Neufeld,T.P., Dillin,A., and Guan,K.L. (2013). ULK1 induces autophagy by phosphorylating Beclin-1 and activating VPS34 lipid kinase. Nat. Cell Biol. *15*, 741-750.

Sagona,A.P., Nezis,I.P., Bache,K.G., Haglund,K., Bakken,A.C., Skotheim,R.I., and Stenmark,H. (2011). A tumor-associated mutation of FYVE-CENT prevents its interaction with Beclin 1 and interferes with cytokinesis. PLoS. One. *6*, e17086.

Sagona,A.P., Nezis,I.P., Pedersen,N.M., Liestol,K., Poulton,J., Rusten,T.E., Skotheim,R.I., Raiborg,C., and Stenmark,H. (2010). PtdIns(3)P controls cytokinesis through KIF13A-mediated recruitment of FYVE-CENT to the midbody. Nat. Cell Biol. *12*, 362-371.

Sagona,A.P. and Stenmark,H. (2010). Cytokinesis and cancer. FEBS Lett. *584*, 2652-2661.

Samson,R.Y., Obita,T., Freund,S.M., Williams,R.L., and Bell,S.D. (2008). A role for the ESCRT system in cell division in archaea. Science *322*, 1710-1713.

Sarkes,D. and Rameh,L.E. (2010). A novel HPLC-based approach makes possible the spatial characterization of cellular PtdIns5P and other phosphoinositides. Biochem. J. *428*, 375-384.

Schiel,J.A., Simon,G.C., Zaharris,C., Weisz,J., Castle,D., Wu,C.C., and Prekeris,R. (2012). FIP3-endosome-dependent formation of the secondary ingression mediates ESCRT-III recruitment during cytokinesis. Nat. Cell Biol. *14*, 1068-1078.

Schu,P.V., Takegawa,K., Fry,M.J., Stack,J.H., Waterfield,M.D., and Emr,S.D. (1993). Phosphatidylinositol 3-kinase encoded by yeast VPS34 gene essential for protein sorting. Science *260*, 88-91.

Scott,A., Chung,H.Y., Gonciarz-Swiatek,M., Hill,G.C., Whitby,F.G., Gaspar,J., Holton,J.M., Viswanathan,R., Ghaffarian,S., Hill,C.P., and Sundquist,W.I. (2005). Structural and mechanistic studies of VPS4 proteins. EMBO J. *24*, 3658-3669.

Seki,A., Coppinger,J.A., Du,H., Jang,C.Y., Yates,J.R., III, and Fang,G. (2008a). Plk1- and beta-TrCP-dependent degradation of Bora controls mitotic progression. J. Cell Biol. *181*, 65-78.

Seki,A., Coppinger,J.A., Jang,C.Y., Yates,J.R., and Fang,G. (2008b). Bora and the kinase Aurora a cooperatively activate the kinase Plk1 and control mitotic entry. Science *320*, 1655-1658.

Shabbeer,S., Omer,D., Berneman,D., Weitzman,O., Alpaugh,A., Pietraszkiewicz,A., Metsuyanim,S., Shainskaya,A., Papa,M.Z., and Yarden,R.I. (2013). BRCA1 targets G2/M cell cycle proteins for ubiquitination and proteasomal degradation. Oncogene *32*, 5005-5016.

Simon,G.C. and Prekeris,R. (2008). The role of FIP3-dependent endosome transport during cytokinesis. Commun. Integr. Biol. *1*, 132-133.

Simonsen,A., Lippe,R., Christoforidis,S., Gaullier,J.M., Brech,A., Callaghan,J., Toh,B.H., Murphy,C., Zerial,M., and Stenmark,H. (1998). EEA1 links PI(3)K function to Rab5 regulation of endosome fusion. Nature *394*, 494-498.

Sjoblom,T., Jones,S., Wood,L.D., Parsons,D.W., Lin,J., Barber,T.D., Mandelker,D., Leary,R.J., Ptak,J., Silliman,N., Szabo,S., Buckhaults,P., Farrell,C., Meeh,P., Markowitz,S.D., Willis,J., Dawson,D., Willson,J.K., Gazdar,A.F., Hartigan,J., Wu,L., Liu,C., Parmigiani,G., Park,B.H., Bachman,K.E., Papadopoulos,N., Vogelstein,B., Kinzler,K.W., and Velculescu,V.E. (2006). The consensus coding sequences of human breast and colorectal cancers. Science *314*, 268-274.

Skalicky,J.J., Arii,J., Wenzel,D.M., Stubblefield,W.M., Katsuyama,A., Uter,N.T., Bajorek,M., Myszka,D.G., and Sundquist,W.I. (2012). Interactions of the human LIP5 regulatory protein with endosomal sorting complexes required for transport. J. Biol. Chem. *287*, 43910-43926.

Slagsvold,T., Aasland,R., Hirano,S., Bache,K.G., Raiborg,C., Trambaiolo,D., Wakatsuki,S., and Stenmark,H. (2005). Eap45 in mammalian ESCRT-II binds ubiquitin via a phosphoinositide-interacting GLUE domain. J. Biol. Chem. *280*, 19600-19606.

Stauffer,D.R., Howard,T.L., Nyun,T., and Hollenberg,S.M. (2001). CHMP1 is a novel nuclear matrix protein affecting chromatin structure and cell-cycle progression. J. Cell Sci. *114*, 2383-2393.

Steigemann,P., Wurzenberger,C., Schmitz,M.H., Held,M., Guizetti,J., Maar,S., and Gerlich,D.W. (2009). Aurora B-mediated abscission checkpoint protects against tetraploidization. Cell *136*, 473-484.

Stuchell-Brereton,M.D., Skalicky,J.J., Kieffer,C., Karren,M.A., Ghaffarian,S., and Sundquist,W.I. (2007). ESCRT-III recognition by VPS4 ATPases. Nature *449*, 740-744.

Stucki,M. and Jackson,S.P. (2006). gammaH2AX and MDC1: anchoring the DNA-damage-response machinery to broken chromosomes. DNA Repair (Amst) *5*, 534-543.

Su,A.I., Wiltshire,T., Batalov,S., Lapp,H., Ching,K.A., Block,D., Zhang,J., Soden,R., Hayakawa,M., Kreiman,G., Cooke,M.P., Walker,J.R., and Hogenesch,J.B. (2004). A gene atlas of the mouse and human protein-encoding transcriptomes. Proc. Natl. Acad. Sci. U. S. A *101*, 6062-6067.

Syljuasen,R.G., Jensen,S., Bartek,J., and Lukas,J. (2006). Adaptation to the ionizing radiation-induced G2 checkpoint occurs in human cells and depends on checkpoint kinase 1 and Polo-like kinase 1 kinases. Cancer Res. *66*, 10253-10257.

Takahashi,Y., Coppola,D., Matsushita,N., Cualing,H.D., Sun,M., Sato,Y., Liang,C., Jung,J.U., Cheng,J.Q., Mule,J.J., Pledger,W.J., and Wang,H.G. (2007). Bif-1 interacts with Beclin 1 through UVRAG and regulates autophagy and tumorigenesis. Nat. Cell Biol. *9*, 1142-1151.

Takahashi,Y., Karbowski,M., Yamaguchi,H., Kazi,A., Wu,J., Sebti,S.M., Youle,R.J., and Wang,H.G. (2005). Loss of Bif-1 suppresses Bax/Bak conformational change and mitochondrial apoptosis. Mol. Cell Biol. *25*, 9369-9382.

Taylor,W.R. and Stark,G.R. (2001). Regulation of the G2/M transition by p53. Oncogene *20*, 1803-1815.

Theis-Febvre,N., Filhol,O., Froment,C., Cazales,M., Cochet,C., Monsarrat,B., Ducommun,B., and Baldin,V. (2003). Protein kinase CK2 regulates CDC25B phosphatase activity. Oncogene *22*, 220-232.

Vaccari,T. and Bilder,D. (2005). The Drosophila tumor suppressor vps25 prevents nonautonomous overproliferation by regulating notch trafficking. Dev. Cell *9*, 687-698.

Vaccari,T., Rusten,T.E., Menut,L., Nezis,I.P., Brech,A., Stenmark,H., and Bilder,D. (2009). Comparative analysis of ESCRT-I, ESCRT-II and ESCRT-III function in Drosophila by efficient isolation of ESCRT mutants. J. Cell Sci. *122*, 2413-2423.

van Vugt,M.A., Bras,A., and Medema,R.H. (2004). Polo-like kinase-1 controls recovery from a G2 DNA damage-induced arrest in mammalian cells. Mol. Cell *15*, 799-811.

Villa,L.L. (1997). Human papillomaviruses and cervical cancer. Adv. Cancer Res. *71*, 321-341.

Vitale,I., Galluzzi,L., Castedo,M., and Kroemer,G. (2011). Mitotic catastrophe: a mechanism for avoiding genomic instability. Nat. Rev. Mol. Cell Biol. *12*, 385-392.

Ward,J.F. (1990). The yield of DNA double-strand breaks produced intracellularly by ionizing radiation: a review. Int. J. Radiat. Biol. *57*, 1141-1150.

Wollert,T., Wunder,C., Lippincott-Schwartz,J., and Hurley,J.H. (2009). Membrane scission by the ESCRT-III complex. Nature *458*, 172-177.

Wood,L.D., Parsons,D.W., Jones,S., Lin,J., Sjoblom,T., Leary,R.J., Shen,D., Boca,S.M., Barber,T., Ptak,J., Silliman,N., Szabo,S., Dezso,Z., Ustyanksky,V., Nikolskaya,T., Nikolsky,Y., Karchin,R., Wilson,P.A., Kaminker,J.S., Zhang,Z., Croshaw,R., Willis,J., Dawson,D., Shipitsin,M., Willson,J.K., Sukumar,S., Polyak,K., Park,B.H., Pethiyagoda,C.L., Pant,P.V., Ballinger,D.G., Sparks,A.B., Hartigan,J., Smith,D.R., Suh,E., Papadopoulos,N., Buckhaults,P., Markowitz,S.D., Parmigiani,G., Kinzler,K.W., Velculescu,V.E., and Vogelstein,B. (2007). The genomic landscapes of human breast and colorectal cancers. Science *318*, 1108-1113.

Wu,C., Orozco,C., Boyer,J., Leglise,M., Goodale,J., Batalov,S., Hodge,C.L., Haase,J., Janes,J., Huss,J.W., III, and Su,A.I. (2009). BioGPS: an extensible and customizable portal for querying and organizing gene annotation resources. Genome Biol. *10*, R130.

Xiao,J., Chen,X.W., Davies,B.A., Saltiel,A.R., Katzmann,D.J., and Xu,Z. (2009). Structural basis of Ist1 function and Ist1-Did2 interaction in the multivesicular body pathway and cytokinesis. Mol. Biol. Cell *20*, 3514-3524.

Yang,D., Rismanchi,N., Renvoise,B., Lippincott-Schwartz,J., Blackstone,C., and Hurley,J.H. (2008). Structural basis for midbody targeting of spastin by the ESCRT-III protein CHMP1B. Nat. Struct. Mol. Biol. *15*, 1278-1286.

Yu,Z., Gonciarz,M.D., Sundquist,W.I., Hill,C.P., and Jensen,G.J. (2008). Cryo-EM structure of dodecameric Vps4p and its 2:1 complex with Vta1p. J. Mol. Biol. *377*, 364-377.

Yue,Z., Jin,S., Yang,C., Levine,A.J., and Heintz,N. (2003). Beclin 1, an autophagy gene essential for early embryonic development, is a haploinsufficient tumor suppressor. Proc. Natl. Acad. Sci. U. S. A *100*, 15077-15082.

Zhao,Z., Oh,S., Li,D., Ni,D., Pirooz,S.D., Lee,J.H., Yang,S., Lee,J.Y., Ghozalli,I., Costanzo,V., Stark,J.M., and Liang,C. (2012). A dual role for UVRAG in maintaining chromosomal stability independent of autophagy. Dev. Cell *22*, 1001-1016.

Zhong,Y., Wang,Q.J., Li,X., Yan,Y., Backer,J.M., Chait,B.T., Heintz,N., and Yue,Z. (2009). Distinct regulation of autophagic activity by Atg14L and Rubicon associated with Beclin 1-phosphatidylinositol-3-kinase complex. Nat. Cell Biol. *11*, 468-476.

Zwicker,F., Ebert,M., Huber,P.E., Debus,J., and Weber,K.J. (2011). A specific inhibitor of protein kinase CK2 delays gamma-H2Ax foci removal and reduces clonogenic survival of irradiated mammalian cells. Radiat. Oncol. *6*, 15.

I

II

ANCHR mediates Aurora B-dependent abscission checkpoint control via retention of VPS4

Sigrid B. Thoresen[1,2], Coen Campsteijn[1,2], Marina Vietri[1,2], Kay O. Schink[1,2], Knut Liestøl[1,3], Jens S. Andersen[4], Camilla Raiborg[1,2] & Harald Stenmark[1,2,5]

[1]Centre for Cancer Biomedicine, Faculty of Medicine, Oslo University Hospital, Montebello, Norway

[2]Department of Biochemistry, Institute for Cancer Research, Oslo University Hospital, Montebello, Norway

[3]Department of Informatics, University of Oslo, Norway.

[4]Department of Biochemistry and Molecular Biology, University of Southern Denmark, Odense, Denmark

[5]Correspondence: stenmark@ulrik.uio.no, telephone: +47 22781818, fax: +47 22781845

Cytokinesis is the final stage of cell division where two daughter cells and their genetic content are physically separated. The final membrane abscission event is mediated by the endosomal sorting complex required for transport (ESCRT) machinery through the activity of the ATPase VPS4 [1-4], and occurs at an abscission zone that is spatially separated from the protein-rich midbody ring at the center of the intercellular bridge. Pioneering work in both yeast and mammalian cells has identified the existence of an Aurora B-dependent abscission checkpoint (also termed NoCut) that delays abscission to avoid DNA damage and aneuploidy in cells with chromosome segregation defects[5-9]. Although Aurora B-dependent phosphorylation of the ESCRT-III component CHMP4C[8] has been implicated as a regulatory event, how abscission delay occurs on a mechanistic level is largely unknown. Here we show that VPS4 is a key effector of the abscission checkpoint, and that its activity is controlled by the previously uncharacterized protein ZFYVE19, here renamed ANCHR (Abscission/NoCut Checkpoint Regulator) in concert with CHMP4C. ANCHR localizes to centrosomes and the midbody ring, inhibits the accumulation of multinucleate cells and controls abscission timing in an Aurora B-dependent manner. ANCHR-mediated abscission delay is specifically dependent on its ability to bind VPS4. Importantly, we show that ANCHR and CHMP4C associate with VPS4 at the midbody ring and cooperate to prevent VPS4 relocalization to the abscission zone, and this retention is relieved upon inactivation of Aurora B to allow abscission. Taken together, we propose a model where Aurora B-induced abscission checkpoint is mediated by CHMP4C and ANCHR via retention of VPS4 at the midbody ring.

Previous work identified the lipid phosphatidylinositol 3-phosphate (PtdIns3P) as a regulator of cytokinesis[10, 11]. In an siRNA screen targeting PtdIns3P-binding proteins, depletion of the previously uncharacterised 471 amino acid protein ANCHR (ZFYVE19; transcript accession NM_001077268.1) significantly increased the fraction of multinucleated HeLa cells compared to cells transfected with non-targeting siRNA

(Fig. S1), indicative of cleavage furrow regression and failed abscission. This was validated using two individual siRNA oligonucleotides targeting ANCHR, and the phenotype could be rescued by stably expressing moderate levels of siRNA resistant GFP-ANCHR that did not induce any obvious phenotypes on its own (Fig. 1A, 1B and 1C). Interestingly, depletion of ANCHR also caused a moderate decrease in cytokinetic profiles (Fig. 1A), indicating that it is dispensable for completion of abscission but potentially involved in controlling abscission timing. To more accurately determine abscission dynamics, we monitored microtubule disassembly, which correlates strongly with abscission[7], in normally segregating HeLaK cells stably expressing GFP-α-tubulin (microtubule marker) and mCherry-Histone 2B (H2B, chromatin marker). Of note, in ANCHR-depleted cells, the time from complete cleavage furrow ingression to abscission was decreased from about 75 min to less than 60 min, as compared with control-treated cells (non-targeting siRNA: 75.2 ± 13.8 min; siANCHR-1: 58.4 ± 8.3 min; siANCHR-2: 55.8 ± 6.7 min; siANCHR-2+GFP-ANCHR^{R}: 69.2 ± 8 min)(Fig. 1D and Fig. S2A). This suggests that ANCHR could be a negative regulator of abscission. In further support of this conclusion, depletion of ANCHR caused cleavage furrow regression and multinucleation predominantly in cells with missegregating chromatin, indicating a potential role for ANCHR cytokinesis delay specifically in the presence of chromatin bridges (Fig. 1E and Fig. S2B).

To further investigate a role for ANCHR in control of cytokinesis, we studied the localization of endogenous ANCHR throughout the cell cycle, and found it to reside mainly on centrosomes in interphase and early mitosis, and also at the cleavage furrow and midbody ring in late mitosis and cytokinesis (Fig. 1F). These structures are central regulatory hubs during cell cycle progression and checkpoint signalling[12-15]. Overexpressed GFP-ANCHR similarly localized to centrosomes and to the midbody ring (Fig. 1G).

Since ANCHR can bind PtdIns3P though its FYVE domain *in vitro* (Fig. S3A and S3B), we assessed whether PtdIns3P is required for ANCHR localization to the midbody ring.

Even though expression of a FYVE-domain-containing N-terminal fragment ($ANCHR_{1-133}$) was sufficient to confer localization to the midbody ring (Fig. S3C), this occurred irrespective of PtdIns3P-binding as a PtdIns3P-binding-deficient mutant of ANCHR ($ANCHR_{R101A}$) equally localized to the midbody ring (Fig. S3B). Interestingly, we observed that high overexpression of ANCHR induced a significant delay in abscission, as judged by a marked increase in cytokinetic profiles 24 hours after transfection as compared to control transfected cells (Fig. 1H). Moreover, the PtdIns3P-binding deficient mutant of ANCHR, but not the N-terminal fragment, induced this arrest at least as strongly. Thus, our data suggest that PtdIns3P binding is not essential for positive regulation of ANCHR function during cytokinesis, but it may still contribute to ANCHR function or localization, consistent with the finding that PtdIns3P depletion causes cytokinesis arrest[10, 11]. Together, our data identify ANCHR as a novel regulator of abscission timing.

The phenotypes caused by aberrant expression of ANCHR were reminiscent of previously published phenotypes resulting from deregulation of the abscission checkpoint[7, 8]. Thus, we speculated that ANCHR could be involved in abscission checkpoint regulation. One way of activating the abscission checkpoint is by depletion of nucleoporin 153 (NUP153) which interferes with nuclear pore complex assembly and causes an Aurora B mediated delay in cytokinesis[16]. Co-depletion with ANCHR strongly reduced NUP153-depletion-induced cytokinetic delay, while exhibiting an increase in multinucleated cells similar to ANCHR depletion alone (Fig. 2A and B). As Aurora B has been identified as a master regulator of cytokinesis and the abscission checkpoint[7, 8, 16, 17], we wanted to ascertain whether this ANCHR-dependent abscission delay requires Aurora B signalling. Indeed, adding the specific Aurora B inhibitor AZD1152[18] released GFP-ANCHR-transfected cells from cytokinesis arrest and allowed abscission in a time-dependent manner (Fig. 2C, 2D and S4), showing that ANCHR-dependent abscission checkpoint activation is regulated by

Aurora B. Taken together, our data indicate that ANCHR is an essential regulator of the Aurora B-dependent abscission checkpoint.

To identify possible mechanisms explaining how ANCHR regulates the abscission checkpoint, we performed mass spectrometry on GFP-ANCHR immunoprecipitates (Fig. S5A). The prominent co-purifying factor was VPS4 (Table S1), an AAA ATPase known to be essential for completion of cytokinesis [1, 2]. This interaction was confirmed by further co-immunoprecipitation experiments followed by probing immunoblots for endogenous VPS4 (Fig. 3A), and mass spectrometry on immunoprecipitates from cell lines stably expressing moderate levels of GFP-ANCHR and GFP-VPS4A which do not arrest in cytokinesis (Fig. S5B and C and Table S2). ANCHR and VPS4 also colocalized at centrosomes during interphase and the early stages of mitosis (Fig. S6). During mitotic exit and cytokinesis they showed distinctive localization at the ingressed cleavage furrow, with ANCHR localizing to the midbody ring and VPS4 at the midzone spindle flanking the midbody (Fig. 3B). Importantly, VPS4 could occasionally be detected colocalizing with ANCHR at the midbody ring during late cytokinesis in normally segregating cells, but this frequency was dramatically higher in cytokinetic cells displaying lagging chromatin in the intercellular bridge (Fig. 3B and C, Fig. S7). Strikingly, VPS4 was visibly localized at high levels on the midbody ring upon overexpression of GFP-ANCHR, regardless of chromatin segregation status (Fig. 3D and Fig. S8A). In contrast, VPS4 was barely detected on the midbody ring in ANCHR-depleted cells, even in the presence of chromatin bridges (Fig. 3D), and this was not due to disruption of midbodies upon depletion of ANCHR (Fig. S9) Quantification confirmed that VPS4 intensity on the midbody ring in the presence of chromatin bridges is dependent on ANCHR levels (Fig. 3D). Live and confocal imaging of HeLa cells stably expressing GFP-VPS4A and mCherry-CEP55 (a midbody ring marker) also showed that VPS4 localized to the CEP55-positive ring prior to abscission (Fig. S8B and S8C and Supplementary Movie S1).

Bioinformatic analyses of the ANCHR amino acid sequence revealed the presence of two putative type-1 MIT-interacting motifs (MIMs), denoted MIM1-A and MIM1-B, that conform to the consensus sequence shown to mediate interaction between ESCRT-III proteins and the VPS4 MIT (microtubule interacting and transport) domain (Fig. S8D). These were both deleted in the N-terminal fragment ($ANCHR_{1-133}$) that was unable to induce an abscission delay (see Fig. 1H). Interestingly, deleting either the VPS4A MIT-domain or the ANCHR MIM1-A, but not MIM1-B, abolished their interaction (Fig. 3E and F), showing that these proteins engage in a classical MIM-MIT interaction. Moreover, the ANCHR MIM1-A was essential for the increased intensity of VPS4 at the midbody ring in cells overexpressing GFP-ANCHR (Fig. 3G). We conclude that VPS4 interacts with the ANCHR MIM1-A via its MIT-domain, and is present at the midbody ring in an ANCHR-dependent manner during late cytokinesis.

Taking into consideration that abscission is accelerated or delayed in ANCHR-depleted or -overexpressing cells, respectively, and that the amount of VPS4 on the midbody ring is dependent on ANCHR levels, ANCHR-dependent retention of VPS4 at the midbody ring could provide a possible mechanism for abscission timing. Strikingly, deletion of the MIM1-A completely abolished ANCHR-dependent cytokinetic delay (Fig. 4A and S10A). Moreover, the fraction of cytokinetic cells visibly containing VPS4 on the midbody ring (late cytokinetic cells) was significantly increased upon overexpression of GFP-ANCHR compared to non-transfected cells, and this increase was dependent on the presence of the MIM1-A (Fig. 4B). This reflects the concurrent increased retention of VPS4 on the midbody ring with the delay at late cytokinesis, both of which are dependent on the interaction between ANCHR and VPS4. Conversely, ANCHR depletion resulted in a decrease in the frequency of late cytokinetic cells containing VPS4 on the midbody ring, reflecting the requirement for VPS4 retention on the midbody ring to delay cytokinesis, irrespective of chromatin segregation status.

To monitor directly whether ANCHR retains VPS4 at the midbody ring, we generated cells stably expressing VPS4 fused to the photoconvertable fluorescent protein mEOS2. The retention time of a midbody-specific pool of photoconverted mEOS2-VPS4A was more than doubled in cells overexpressing ANCHR (half-time 45.9±6.4 sec, n=20) compared to control cells (half-time 20.9±2.4 sec, n=17) (Fig. 4C and Fig. S10B), further supporting the notion that ANCHR interacts with VPS4 at the midbody ring. As VPS4 activation requires other MIM containing ESCRT-III subunits, ANCHR-dependent VPS4 retention could affect VPS4 interactions with its activators. Because we had already shown that ANCHR-mediated abscission delay is Aurora B-dependent, we set out to determine whether termination of checkpoint signalling by Aurora B inhibition would result in release of VPS4 from the midbody ring. Indeed, the fraction of late cytokinetic cells visibly containing VPS4 on the midbody ring was strongly reduced after 1 hour of AZD1152 treatment in ANCHR-overexpressing cells, with a redistribution of VPS4 to the abscission zone (Fig. 4D and E). This suggests that Aurora B inhibition facilitates release of VPS4 from the midbody ring and subsequently normal abscission. Together, our data indicate that ANCHR exerts its effects on abscission checkpoint regulation through its interaction with and retention of VPS4 at the midbody ring until Aurora B-mediated checkpoint signalling is terminated.

As it has recently been shown that the ESCRT-III component CHMP4C is a key regulator of the abscission checkpoint, we assessed any epistatic or cooperative relationship between CHMP4C and ANCHR. Interestingly, co-depletion of ANCHR and CHMP4C did not aggravate cytokinetic profile or multinucleation phenotypes compared to depletion of either component individually (Fig. 5A). Moreover, depletion of ANCHR resulted in significant decrease in cytokinetic arrest induced by over-expression of CHMP4C, and vice versa (Fig. 5B). Together these results argue against an epistatic relationship, but rather suggest a cooperative role for ANCHR and CHMP4C in abscission checkpoint regulation. Such cooperativity was supported by a

synergistic effect on cytokinesis arrest induced by expression of moderate levels of ANCHR and CHMP4C together, where expression of either induced only a marginal increase in the cytokinetic fraction (Fig. 5C). Since CHMP4C possesses a type-2 MIM that can bind VPS4 in a yeast-2-hybrid setting[19], we set out to further explore this interaction. Firstly, GFP-CHMP4C colocalized with endogenous VPS4 as well as ANCHR at the midbody ring in late cytokinesis (Fig. 5D, 5G and 5H). Secondly, CHMP4C levels affected VPS4 abundance at the midbody ring (Fig. 5E), much like ANCHR. Thirdly, endogenous VPS4 coimmunoprecipitated with transfected CHMP4C (Fig. 5F).

Importantly, in cells arrested in cytokinesis by overexpression of ANCHR and CHMP4C, immunoprecipitation experiments showed that ANCHR could associate with CHMP4C in addition to VPS4, arguing that these form a ternary complex on the midbody ring (Fig. 5I). As it has been shown that CHMP4C function in the abscission checkpoint depends on its phosphorylation by Aurora B, we explored the effect of Aurora B inhibition on the interaction of CHMP4C with VPS4 and ANCHR. Inhibition of Aurora B resulted in dissociation of VPS4 from CHMP4C, with levels reduced by approximately 40% (Fig. 5F and Fig S11A). Similarly, CHMP4C dissociated from ANCHR upon Aurora B inhibition (Fig. 5I). We assessed whether such phospho-regulation extended to ANCHR, but even though ANCHR could be phosphorylated on Serine-22 by Aurora B *in vitro*, there was no evidence supporting this phosphorylation event *in vivo* (Fig. S12 and Table S3). Thus, Aurora B appears to sustain the ANCHR/CHMP4C/VPS4 ternary complex specifically by targeting CHMP4C.

Based on our findings we propose a model where a subset of VPS4 localizes transiently to the midbody ring towards the end of cytokinesis and is retained there by ANCHR and CHMP4C in an Aurora B-dependent manner while abscission checkpoint signalling persists. Termination of Aurora B-mediated signalling results in dephosphorylation of CHMP4C, dissociation of the ANCHR/CHMP4C/VPS4 ternary complex, and, although the mechanistic details are not fully elucidated, presumably release of this pool of VPS4 which is then activated to complete abscission at the

abscission zone (Fig. 5J). Ternary complex formation is likely mediated by cooperativity between the different ANCHR and CHMP4C MIM subtypes, MIM-1 and MIM-2 respectively, which are known to bind on the diametrically opposite surface of a MIT domain. This has been elegantly shown for proteins such as IST1, which contains both a MIM-1 and a MIM-2 that wrap around the VPS4 MIT domain to keep it in an inactive state[20], and cooperative binding of both IST1 MIMs to MITD1, another MIT domain protein, has been reported[21]. This highlights the complex nature of competition between ESCRT proteins for MIT domains, and lends credence to a model where dual interaction involving ANCHR and CHMP4C could counteract VPS4 association with other ESCRT-III subunits implicated in its activation. It is interesting that Borealin, a subunit of the Aurora B-containing chromosomal passenger complex, interacts directly with CHMP4 proteins in both fruit flies and human cells[8, 9], suggesting a conserved mechanism for recruitment of Aurora B to CHMP4 and its interacting proteins. In a significant fraction of ANCHR-depleted cytokinetic cells with chromatin segregation errors, VPS4 could not be detected on the midbody or the spindle midzone, rather displaying a partially regressed cleavage furrow (Fig. 4B). As this fraction is proportional to the increased frequency of binuclear cells observed earlier (Fig. 1A), it is possible that prematurely attempted abscission at a stage that is incompatible with abscission (due to the presence of lagging chromatin) leads to cleavage furrow regression. Future work may shed further light on how ANCHR-mediated abscission checkpoint regulation protects against multinucleation.

Previous research suggests that the recruitment of VPS4 to the midbody is dependent on CEP55, and, in part, the ESCRT-interacting protein ALIX[2], which is in accordance with our data indicating that ANCHR and CHMP4C function to tether and retain rather than recruit VPS4 to the midbody ring. It is intriguing that VPS4 emerges as a main regulatory checkpoint target node since it is known to interact with several factors implicated in control and execution of abscission, including IST1, CHMP1B, CHMP2A, CHMP4B, CHMP4C and CHMP6[19, 20, 22]. Furthermore, VPS4 is the last known

component to be recruited to the abscission zone, about 10 minutes prior to abscission[4]. The proposed models explains how abscission can be delayed despite high levels of soluble VPS4 present in the cytokinetic bridge, where only a subset of VPS4 that transiently localizes to the midbody ring will become abscission-competent. It will be interesting to further develop the model as future work may reveal how the different components interlink to govern the abscission checkpoint. Because aberrant expression of ANCHR has been linked to cancer[23, 24], it will be of great interest to understand the mechanistic details of abscission checkpoint regulation in protecting against DNA damage and multinucleation, both of which are critical contributors to cancer.

References

1. Carlton,J.G. & Martin-Serrano,J. Parallels between cytokinesis and retroviral budding: a role for the ESCRT machinery. *Science* **316**, 1908-1912 (2007).

2. Morita,E. *et al.* Human ESCRT and ALIX proteins interact with proteins of the midbody and function in cytokinesis. *EMBO J.* **26**, 4215-4227 (2007).

3. Guizetti,J. *et al.* Cortical constriction during abscission involves helices of ESCRT-III-dependent filaments. *Science* **331**, 1616-1620 (2011).

4. Elia,N., Sougrat,R., Spurlin,T.A., Hurley,J.H., & Lippincott-Schwartz,J. Dynamics of endosomal sorting complex required for transport (ESCRT) machinery during cytokinesis and its role in abscission. *Proc. Natl. Acad. Sci. U. S. A* **108**, 4846-4851 (2011).

5. Norden,C. *et al.* The NoCut pathway links completion of cytokinesis to spindle midzone function to prevent chromosome breakage. *Cell* **125**, 85-98 (2006).

6. Mendoza,M. *et al.* A mechanism for chromosome segregation sensing by the NoCut checkpoint. *Nat. Cell Biol.* **11**, 477-483 (2009).

7. Steigemann,P. *et al.* Aurora B-mediated abscission checkpoint protects against tetraploidization. *Cell* **136**, 473-484 (2009).

8. Carlton,J.G., Caballe,A., Agromayor,M., Kloc,M., & Martin-Serrano,J. ESCRT-III governs the Aurora B-mediated abscission checkpoint through CHMP4C. *Science* **336**, 220-225 (2012).

9. Capalbo,L. *et al.* The chromosomal passenger complex controls the function of endosomal sorting complex required for transport-III Snf7 proteins during cytokinesis. *Open Biol.* **2**, 120070 (2012).

10. Sagona,A.P. *et al.* A tumor-associated mutation of FYVE-CENT prevents its interaction with Beclin 1 and interferes with cytokinesis. *PLoS. One.* **6**, e17086 (2011).

11. Thoresen,S.B., Pedersen,N.M., Liestol,K., & Stenmark,H. A phosphatidylinositol 3-kinase class III sub-complex containing VPS15, VPS34, Beclin 1, UVRAG and BIF-1 regulates cytokinesis and degradative endocytic traffic. *Exp. Cell Res.* **316**, 3368-3378 (2010).

12. Doxsey,S.J. Molecular links between centrosome and midbody. *Mol. Cell* **20**, 170-172 (2005).

13. Doxsey,S., McCollum,D., & Theurkauf,W. Centrosomes in cellular regulation. *Annu. Rev. Cell Dev. Biol.* **21**, 411-434 (2005).

14. Caballe,A. & Martin-Serrano,J. ESCRT machinery and cytokinesis: the road to daughter cell separation. *Traffic.* **12**, 1318-1326 (2011).

15. Agromayor,M. & Martin-Serrano,J. Knowing when to cut and run: mechanisms that control cytokinetic abscission. *Trends Cell Biol.*(2013).

16. Mackay,D.R., Makise,M., & Ullman,K.S. Defects in nuclear pore assembly lead to activation of an Aurora B-mediated abscission checkpoint. *J. Cell Biol.* **191**, 923-931 (2010).

17. Carmena,M., Ruchaud,S., & Earnshaw,W.C. Making the Auroras glow: regulation of Aurora A and B kinase function by interacting proteins. *Curr. Opin. Cell Biol.* **21**, 796-805 (2009).

18. Kettenbach,A.N. *et al.* Quantitative phosphoproteomics identifies substrates and functional modules of Aurora and Polo-like kinase activities in mitotic cells. *Sci. Signal.* **4**, rs5 (2011).

19. von Schwedler,U.K. *et al.* The protein network of HIV budding. *Cell* **114**, 701-713 (2003).

20. Bajorek,M. *et al.* Biochemical analyses of human IST1 and its function in cytokinesis. *Mol. Biol. Cell* **20**, 1360-1373 (2009).

21. Lee,S. *et al.* MITD1 is recruited to midbodies by ESCRT-III and participates in cytokinesis. *Mol. Biol. Cell* **23**, 4347-4361 (2012).

22. Morita,E. *et al.* Human ESCRT-III and VPS4 proteins are required for centrosome and spindle maintenance. *Proc. Natl. Acad. Sci. U. S. A* **107**, 12889-12894 (2010).

23. Chinwalla,V. *et al.* A t(11;15) fuses MLL to two different genes, AF15q14 and a novel gene MPFYVE on chromosome 15. *Oncogene* **22**, 1400-1410 (2003).

24. Marina,O. *et al.* Serologic markers of effective tumor immunity against chronic lymphocytic leukemia include nonmutated B-cell antigens. *Cancer Res.* **70**, 1344-1355 (2010).

Acknowledgements

Anne Engen and Heidi Plum Bjønnes are acknowledged for expert handling of cell cultures, and Torill Høiby and Carolina Herrmann for invaluable technical assistance. Olav Mjaavatten at the Proteomics Unit at the University of Bergen (PROBE) and Gustavo de Souza at the Proteomics Core Facility Unit at Oslo University Hospital are acknowledged for performing mass spectrometry analysis of GFP-ANCHR and GFP-VPS4 immunoprecipitates. We also thank Prof. Daniel Gerlich at the Institute of Molecular Biotechnology (IMBA), Vienna, for supplying plasmids for the generation of GFP-α-tubulin/mCherry-H2B stable cell lines, and Prof. Juan Martin-Serrano, King's College London, UK, for advice on NoCut activation. S.B.T. and M.V. are PhD students and C.R. a senior researcher of the South-Eastern Norway Regional Health Authority. C.C. is a postdoctoral fellow of the Norwegian Cancer Society. H.S. was supported by an Advanced Grant from the European Research Council. This work was partly supported by the Research Council of Norway through its Centres of Excellence funding scheme, project number 179571.

Author contributions

S.B.T. generated plasmid constructs, performed confocal, high-content and live imaging, biochemical work, cell transfections, image processing, data analysis, statistical analyses and preparation of figures. C.C. generated plasmid constructs and stable cell lines, performed live microscopy, photoconversion experiments, image processing, *in vitro* kinase assays and data analysis. C.R. carried out and analysed the siRNA screen targeting PtdIns3P-binding proteins, and performed cell transfections for epistasis studies. M.V. performed cell transfections, biochemical work and image analysis. K.O.S. generated plasmid constructs and stable cell lines, perfomed photoconversion experiments and image processing. K.L. did the statistical analysis of the siRNA screen. J.S.A. performed mass spectrometry analysis of Aurora B-

phosphorylated ANCHR. H.S. coordinated the study and oversaw experiments. S.B.T., C.C. and H.S. wrote the paper. All authors discussed the results and assisted in revising the manuscript.

Competing financial interests

The authors declare no competing financial interests.

METHODS:

Cell culture, plasmid transfections and small molecule inhibitor treatments

HeLa and HeLa'Kyoto' (HeLaK) cells were maintained in Dulbecco's modified Eagle's medium (DMEM; Gibco) supplemented with 10% foetal bovine serum (FBS), 5 U ml^{-1} penicillin and 50 μg ml^{-1} streptomycin. DNA plasmid constructs are listed in table 1. Cloning of ANCHR was based on the canonical sequence for ZFYVE19; accession NM_001077268.1. For plasmid transfection, DNA was complexed with FUGENE-6 transfection reagent (Promega) in DMEM without serum, penicillin and streptomycin, and added to cells at 50% confluency in complete DMEM for 24 hours. The concentrations of DNA used were 1 μg for immunofluorescence, 3 μg for general GFP-trap immunoprecipitations and 32 μg for GFP-trap immunoprecipitations analysed by mass spectrometry. The AuroraB inhibitor AZD1152 (Selleckchem) was used at a concentration of 1 μM.

Table 1: Plasmids used for transient tranfections:

Plasmid name	Relevant characteristics
pEGFP-ANCHR	Full length, Resistant to siANCHR-2
pEGFP-ANCHR R101A	Mutation in the FYVE-domain
pEGFP-ANCHR$_{1-133}$	N-terminal fragment containing the FYVE-domain
pEGFP-ANCHRΔMIM1-A	MIM1-A deleted (Δaa172-185)
pEGFP-ANCHRΔMIM1-B	MIM1-B deleted (Δaa321-337)
Myc-ANCHR$_{1-133}$	N-terminal fragment containing the FYVE-domain
Myc-ANCHR$_{1-133}$R101A	N-terminal fragment containing the FYVE-domain Mutation in the FYVE-domain
pcDNA3.1-V5-VPS4A	Full length
pcDNA3.1-V5-VPS4AΔMIT	MIT-domain deletion (Δaa1-80)
pcDNA3.1-eGFP-CHMP4C	Full length
pcDNA3.1-V5-CHMP4C	Full length
pcDNA3.1_PGK-eGFP-ANCHR	GFP-ANCHR expression driven by weak PGK promoter
pcDNA3.1_PGK-V5-CHMP4C	V5-CHMP4C expression driven by weak PGK promoter

siRNA treatments

For the screen targeting PtdIns3P-binding proteins, an siRNA library consisting of 91 pooled siRNAs (each pool consisting of four different siRNAs) was constructed (On-Target Plus library, custom made by Dharmacon). ON-Target Plus individual siRNA oligonucleotides were from Dharmacon, which included pre-designed non-targeting siRNA (D-001810-01), and siRNAs specific for ANCHR/ZFYVE19 (Oligo 1: J-017961-05 and Oligo 2: J-017961-08). siRNA against CHMP4C (AATCGAATCCAGAGAGAAA), VPS4 (CCGAGAAGCTGAAGGATTA) and Nup153 (GGACTTGTTAGATCTAGTT) from Ambion have been described previously[8, 22, 25]. Ambion non-targeting control siRNA was pre-designed (Cat. No. 4390844). siRNA oligonucleotides were complexed with Lipofectamine RNAiMAX transfection reagent (Invitrogen) in DMEM without serum, penicillin and streptomycin, and added to cells at 50% confluency in penicillin- and streptomycin-free DMEM, at a final siRNA concentration of 100 nM (screen), 70nM (non-targeting, ZFYVE19 and CHMP4C siRNAs), 10nM (Nup153 siRNA), and 50nM (CHMP4C and VPS4 siRNAs). After 16 hours, cells were washed twice in DMEM and maintained in DMEM for a total of 72 hours post-transfection.

ANCHR and CHMP4C siRNA and plasmid transfection combination treatments

HeLa cells were seeded into 6 well plates and transfected the same day with 75 nM siRNA oligos using Lipofectamine RNAiMAX (Invitrogen) according to the manufacturer's instructions. The next day the siRNA treated cells were trypsinized and split onto coverslips. 48 hours post siRNA transfection the cells were transfected with plasmid cDNA using FUGENE-6 (Promega) according to the manufacturer's instructions. 72 hours post siRNA transfection and 24 hours post cDNA transfection, the cells were fixed in 3% PFA prior to immunostaining and image analysis.

Antibodies

Rabbit anti-ZFYVE19/ANCHR (Bethyl Laboratories, WB 1:1000, IF 1:1000), mouse anti-ZFYVE19/ANCHR (Sigma-Aldrich, IF 1:50), rabbit anti-VPS4 (Sigma-Aldrich, WB 1:500, IF 1:200), mouse anti-α-tubulin (Sigma-Aldrich, WB 1:10000, IF 1:1000), mouse anti-β-actin (Sigma, WB 1:20000), rabbit anti-γ-tubulin (Abcam, IF 1:1000), mouse anti-Nup153 (Covance, MMS-102P, WB 1:1000), goat anti-V5 (Abcam, WB 1:1000, IF 1:200), mouse anti-GFP (Living Colors, WB 1:1000), rabbit anti-phospho-T232 AuroraB (Rockland, IF 1:200), goat anti-RacGAP1 (Abcam, IF 1:500), Human anti-EEA1 antiserum (gift from Ban-Hock Toh, Monash University, Melbourne, Australia, IF 1:100) were used as primary antibodies. Secondary antibodies included anti-mouse-, anti-rabbit- and anti-goat- Alexa488 (Jackson), Alexa555 (Molecular Probes) Cy5 (Jackson), and phalloidin-conjugated Alexa647 (Molecular Probes).

High-content microscopy and analysis of cytokinesis profiles and multinuclear cells

For the screen, cells pre-seeded on flat glass-bottomed 96-well plates (Nunc) coated with Fibronectin were fixed with 3% paraformaldehyde and stained using antibodies against α-tubulin, Aurora B kinase and DNA (Hoechst). For other experiments cells seeded on coverslips were fixed in 3% paraformaldehyde and stained for DNA (Hoechst), α-tubulin and, in the case of knock-down studies, pT232 Aurora B. Cells were then imaged using an Olympus ScanR automated microscope equipped with an ULSAPO 40x objective. 81 images (siRNA screen) or 64 images (other experiments) from each well/coverslip were then scored manually to give the fraction of multinuclear cells and cells in cytokinesis (profiles showing two daughter cells connected by an Aurora B-positive midbody structure with unsevered microtubule filaments). Images shown in figures are representative of ≥ three independent experiments.

Confocal fluorescence microscopy for localisation studies

HeLa cells grown on coverslips were fixed in 3% paraformaldehyde for 15 minutes, permeabilized with 0.05% saponin in PEM buffer (80 mM PIPES, 5 mM EGTA, 1 mM $MgCl_2$ [pH 6.8]) and washed twice in PBS containing 0.05% saponin. The cells were then stained using the indicated primary antibodies for 1 hour, washed three times in PBS/saponin, stained with secondary antibodies for 1 hour, and washed three times in PBS. The cells were mounted in Mowiol containing 1 $\mu g\ ml^{-1}$ Hoechst and examined with a Zeiss LSM 710 or 780 confocal microscope (Carl Zeiss MicroImaging GmbH, Jena, Germany) equipped with an Ar-Laser Multiline (458/488/514nm), a DPSS-561 10 (561nm), a Laser diode 405-30 CW (405nm), and a HeNe-laser (633nm). The objective used was a Zeiss Plan-Apochromat 63x/1.40 Oil DIC M27. Image processing was performed with basic software ZEN 2009 (Carl Zeiss MicroImaging GmbH, Jena, Germany) and Photoshop CS4 (Adobe, Mountain View, CA). ImageJ software (National Institutes of Health, Bethesda, MD, USA) was used for determination of mean fluorescence intensity of VPS4 staining at the midbody, where the region of interest (ROI) was defined as the ANCHR-positive midbody ring at the plane of lagging chromatin. Here, intensity settings for the relevant channels were kept constant during imaging. Images shown in figures are representative of ≥ three independent experiments.

Co-immunoprecipitation

Cells were transfected with plasmid DNA as indicated previously. After 24 hours, cells were lysed in lysis buffer (10 mM Tris-HCl pH7.5, 150 mM NaCl, 0.5 mM EDTA, 0.5% NP40, 1:100 protease inhibitor mix (Roche Applied Science) and 1:100 phosphatase inhibitor cocktails 2 & 3 (Sigma-Aldrich)) for 30 minutes on ice with mixing every 10 minutes. The lysate was collected by centrifugation at 20000g for 10 minutes, and subjected to GFP-trap pull down (Chromotek) as specified by the manufacturer's

instructions. Briefly, lysates were diluted in 500 µl dilution buffer (10mM Tris-HCl pH7.5, 150mM NaCl, 0.5mM EDTA, 1:100 protease inhibitor mix (Roche Applied Science) and 1:100 phosphatase inhibitor cocktails 2 & 3 (Sigma-Aldrich)), and incubated with pre-washed beads for 2 hours rotating at 4 °C. After washing three times, the beads were boiled at 100 °C in SDS-sample buffer for 10 minutes, and SDS-PAGE was performed with the supernatant.

Immunoblotting

Cells were lysed in lysis buffer (25 mM HEPES pH 7.2, 125 mM potassium acetate, 2.5 mM magnesium acetate, 5 mM EGTA, 1 mM DTT, 0.5% Nonidet P40, 1:100 protease inhibitor mix (Roche Applied Science)). After centrifugation for 5 min at 20000g the whole cell lysate was collected and subjected to SDS-PAGE on a 4-20% gradient gel. The proteins were transferred to Immobilon-P membrane (Millipore) and visualized by immunoblotting using the Supersignal West Dura Extended Duration Substrate kit (Pierce). Imaging was performed using the Syngene gel documentation unit. Blots shown in figures are representative of ≥ three independent experiments.

Purification of GST-tagged ANCHR

GST-ANCHR was purified from transformed BL21 cells, where protein expression was induced with 0.3 mM isopropyl β-D-1-thiogalactopyranoside (IPTG) for 3 h at 37 °C. The bacterial pellet was lysed in B-PER buffer (Pierce) containing 1:25 protease inhibitor mix (Roche) and 1 mM dithiothreitol (DTT), with sonication (5 min twice). Following incubation of lysate with Glutathione-sepharose beads (GE Healthcare) for 30 min at room temperature, the protein was eluted in purification buffer (20 mM Tris-HCl, 60 mM NaCl, pH = 7.6) containing 10 mM reduced Glutathione on a column. Finally, the eluted protein was dialysed overnight.

Live microscopy

Cells seeded in Lab-Tek eight-well chamber slides with coverslip bottom (Nunc) were imaged on a Deltavision microscope (Applied Precision) equipped with Elite TruLight Illumination System, a CoolSNAP HQ2camera and a 60× Plan Apochromat (1.42 NA) lens. For temperature control during live observation, the microscope stage was kept at 37°C by a temperature-controlled incubation chamber. Time-lapse images (12 z-sections 0.8 µm apart) were acquired every 5 minutes over a total time period of 12 hours, and deconvolved using the softWoRx software (Applied Precision).

Photoconversion

Photoconversion of mEOS2-VPS4 was performed on a Zeiss LSM 710 confocal microscope. Stable cell lines expressing mEOS2-VPS4 were transfected with GFF-ANCHR. Non-transfected cells were measured as control. Cytokinetic cells were identified by the connecting bridge and the VPS4 / ANCHR-positive midbodies. Midbody-localized VPS4 was photoconverted by illuminating a small region of interest (ROI) at the midbody with a 405 nm diode laser (30 mW, AOTF set to 3% transmission, 75 bleach cycles). The residence time of the red fluorescent form of mEOS2 inside the bleaching ROI was measured every 7.5 s for a total of 225 s. In case the midbody was moving out of the ROI, a new ROI covering the whole range of movement was used. All post-acquisition analysis was performed with Graphpad Prism software. First, each photoconversion measurement was normalized. Then, curve fitting using a model for monoexponential decay was performed for each measurement and the half-life of the fluorescence residence time was calculated. Half-life values were plotted and statistical significance between the control and GFP-ANCHR-transfected cells was tested using the Student's T-Test function of Graphpad Prism. For visualisation of the photoconversion kinetics, as shown in Figure S9B, the

mean values of all control and GFP-ANCHR measurements were plotted. The arrow indicates the time of photoconversion.

Stable cell lines

Stable cell lines expressing eGFP-Tubulin and H2B-mCherry were created by transfection of Hela "Kyoto" cells with pmEGFP-Tubulin-IRES-Puro and pH2B-mCherry-IRES-Neo vectors[7] (Addgene plasmids # 21042, 21044). Stable clones were selected after antibiotic selection (0,5 µg /ml Puromycin; 500 µg/ml Geneticin). All other stable cell lines were lentivirus-generated pools. To archieve low expression levels, the weak PGK promoter was used for transgene expression. 3rd generation Lentivirus was generated using procedures and plasmids as previously described[26]. Briefly, eGFP/mCherry/mEOS2 fusions were generated as Gateway ENTRY plasmids using standard molecular biology techniques. From these vectors, Lentiviral transfer vectors were generated by recombination into pLenti Destination vectors (Addgene # 19067, 19068) using a Gateway LR reaction. VSV-G pseudotyped lentiviral particles were packaged using a 3rd generation packaging system[27] (Addgene plasmids # 12251, 12253, 12259). Cells were then transduced with low virus titers (MOI ≈<1) and stable expressing populations were generated by antibiotic selection. Detailed cloning procedures can be requested from the authors. The stable cell lines used in this study are listed in table 2.

Table 2: Stable cell lines:

Background	Cell line name	Plasmids
HeLa 'Kyoto'	EGFP-a-tubulin and mCherry-H2B	pmEGFP_a_tubulin_IRES_puro2b[7] pH2B_mCherry_IRES_neo3[7]
HeLa	HA-eGFP-VPS4A	pLenti-PGK_HA-eGFP-VPS4A_Puro
HeLa 'Kyoto'	HA-eGFP-VPS4A and mCherry-CEP55	pLenti-PGK_HA-eGFP-VPS4A_Puro pLenti-PGK_mCherry-CEP55_Neo
HeLa	HA-eGFP- ANCHR^R	pLenti-PGK_HA-eGFP-ANCHR^R_Puro
HeLa	mEOS2-VPS4A	pLenti-PGK_mEos2-VPS4A_Puro
HeLa	HA-eGFP- ANCHR^R and H2B-mCherry	pLenti-CMV_H2B-mCherry_Neo pLenti-PGK_HA-eGFP-ANCHR^R_Bsd
HeLa 'Kyoto' eGFP-α-tubulin H2B-mCherry	eGFP-α-tubulin, mCherry-H2B and HA-eGFP-ANCHR^R	pLenti-PGK_HA-eGFP-ANCHR^R_Bsd

Statistical analyses

Values are expressed as means ± S.D for bar charts. In box-plots, medians are denoted by a solid black line while the edges of the boxes represent the first and third quartile. Whiskers denote minimum and maximum values. For the dot plot in Fig. 4C, error bars show the 95% confidence interval. Fig S9B shows means of all experiments ± S.E.M. For Fig. 1E, significance was determined using Fisher's exact test. Testing of differences between wells in the siRNA screen (PtdIns3P-binding proteins regulating cytokinesis), taking into account the experimental design, was based on analysis of variance and was performed with the JMP 7.0 statistical system. Dunnett's correction for multiple testing was used. For other experiments, significance was determined using two-tailed students t-tests for paired samples or unpaired samples with equal variance, where appropriate.

Methods references:

7. Steigemann,P. *et al.* Aurora B-mediated abscission checkpoint protects against tetraploidization. *Cell* **136**, 473-484 (2009).

8. Carlton,J.G., Caballe,A., Agromayor,M., Kloc,M., & Martin-Serrano,J. ESCRT-III governs the Aurora B-mediated abscission checkpoint through CHMP4C. *Science* **336**, 220-225 (2012).

22. Morita,E. *et al.* Human ESCRT-III and VPS4 proteins are required for centrosome and spindle maintenance. *Proc. Natl. Acad. Sci. U. S. A* **107**, 12889-12894 (2010).

25. Mackay,D.R., Elgort,S.W., & Ullman,K.S. The nucleoporin Nup153 has separable roles in both early mitotic progression and the resolution of mitosis. *Mol. Biol. Cell* **20**, 1652-1660 (2009).

26. Campeau,E. *et al.* A versatile viral system for expression and depletion of proteins in mammalian cells. *PLoS. One.* **4**, e6529 (2009).

27. Dull,T. *et al.* A third-generation lentivirus vector with a conditional packaging system. *J. Virol.* **72**, 8463-8471 (1998).

FIGURE LEGENDS

Figure 1: ANCHR (ZFYVE19) localizes to centrosomes and the midbody and negatively regulates abscission in a PtdIns3P-independent manner. (A) Parental HeLa cells or HeLa cells stably expressing moderate levels of siRNA-resistant GFP-ANCHR (GFP-ANCHR^R) were transfected with siRNAs as indicated, and after 72 hours fixed and stained for α-tubulin, Aurora B and DNA (Hoechst). Images collected on a high-content ScanR microscope were then scored manually to quantify cells in cytokinesis and multinuclear cells. Values are given as the mean fraction of the total cell population from three independent experiments ± SD, n>200 per experiment, **p<0.01. **(B and C)** Representative western blots of lysates from the same cell populations used in (A), blotted for ANCHR and α-tubulin (loading control). IB, Immunoblot. Arrowheads in (C) denote GFP-ANCHR^R (upper) and endogenous ANCHR (lower). **(D)** Asynchronous HeLa cells stably expressing GFP-α-tubulin and mCherry-H2B with or without GFP-ANCHR^R were treated with siRNAs as indicated, and the duration of cytokinesis was determined by calculating the time from complete cleavage furrow ingression to microtubule disassembly (abscission) from live imaging. n=41, 22, 16, 25 and 25 respectively for non-targeting siRNA, siANCHR-1, siANCHR-2, non-targeting siRNA + GFP-ANCHR^R and siANCHR-2 + GFP-ANCHR^R, ** p<0.01. **(E)** Asynchronous HeLa cells stably expressing GFP-α-tubulin and mCherry-H2B with or without GFP-ANCHR^R were treated with siRNAs as indicated, imaged live, and the incidence of cleavage furrow regression in cells containing anaphase lagging chromatin were scored. n=19, 26, 19 and 15 respectively for non-targeting siRNA, siANCHR-2, non-targeting siRNA + GFP-ANCHR^R and siANCHR-2 + GFP-ANCHR^R, ** p<0.01 (Fisher's exact test). **(F and G)** Representative confocal images showing the localization of ANCHR (F) and GFP-ANCHR (G) through the cell cycle. The cells were co-stained with antibodies against γ-tubulin, α-tubulin and DNA (Hoechst). Scale bar = 10 μm. **(H)** HeLa cells were transiently transfected with the indicated fusion protein

expression constructs, and after 24 hours fixed and stained for α-tubulin and DNA (Hoechst). Images collected on a high-content ScanR microscope were then scored manually to quantify cells in cytokinesis. Values are given as the mean fraction of the transfected (GFP-positive) cell population from three independent experiments ± SD, n>50 per experiment, *p<0.05, n.s. = non-significant. A representative image showing GFP-ANCHR-transfected cells arrested in cytokinesis. Arrowheads indicate intercellular bridge with GFP-ANCHR positive midbody ring. Scale bar = 10 μm.

Figure 2: ANCHR regulates the Aurora B-dependent abscission checkpoint. (A and B) HeLa cells were transfected with siRNAs as indicated, and after 72 hours fixed and stained for α-tubulin, pT232 Aurora B and DNA (Hoechst). Images collected on a high-content ScanR microscope were then scored manually to quantify cells in cytokinesis and multinuclear cells. Images in (A) are confocal images showing representative cell populations. Closed arrowheads indicate cytokinetic bridge. Open arrowheads indicate multinuclear cells. Scale bar= 10 μm. Values in (B) are given as the mean fraction of the total cell population from three independent experiments ± SD, n>100 per experiment. **p<0.01 and *p<0.05. A representative western blot of lysates from the same cell populations used for imaging is shown below, blotted for ANCHR, NUP153 and α-tubulin (loading control). IB = Immunoblot. **(C and D)** HeLa cells were transiently transfected with GFP-ANCHR expression construct, and after 24 hours treated with 1 μM AZD1152 (Aurora B inhibitor) for 0, 1 or 2 hours or left untreated and fixed and stained for α-tubulin and DNA (Hoechst). Images collected on a high-content ScanR microscope were then scored manually to quantify cells in cytokinesis. Images in (C) are confocal images showing representative cell populations. Closed arrowheads indicate cytokinetic bridges. Scale bar = 10 μm. Values in (D) are given as the mean fraction of the transfected (GFP-positive) cell population in cytokinesis from three independent experiments ± SD, n>50 per experiment, **p<0.01.

Figure 3: ANCHR interacts with VPS4 at the midbody. **(A)** GFP-trap immunoprecipitates (IP) from HeLa cells expressing GFP or GFP-ANCHR analysed by western blotting using antibodies against GFP and VPS4. **(B)** Representative confocal images showing the localization of ANCHR and VPS4 at the midbody/cytokinetic bridge at early and late cytokinesis in the presence and absence of chromatin bridges (indicated by arrowheads). Scale bar = 10 μm. **(C)** The mean fraction of cytokinetic cells visibly positive for VPS4 at the midbody ring (scored manually) from three independent experiments ± SD, n=100 per experiment, **p<0.01. **(D)** Representative confocal images showing the intensity of VPS4 at the midbody ring in GFP-ANCHR-transfected, untransfected, or ANCHR-depleted cells in the presence of chromatin bridges (arrowheads). Scale bar = 10 μm. The green channel shows GFP (top panel) or endogenous ANCHR (bottom two panels), respectively. The relative VPS4 intensities (percentage) at the ANCHR-positive midbody ring normalized to the mean intensity in untransfected cells and midbody ring levels of RacGAP1 are represented by box plots. Medians are denoted by a solid black line while the edges of the boxes represent the first and third quartile. Whiskers denote minimum and maximum values. n=15, **p<0.01. **(E)** GFP-trap immunoprecipitates (IP) from HeLa cells expressing GFP or GFP-ANCHR with either V5-VPS4A or V5-VPS4AΔMIT analysed by western blotting using antibodies against GFP and V5. **(F)** GFP-trap immunoprecipitates (IP) from HeLa cells expressing GFP, GFP-ANCHR, GFP-ANCHRΔMIM1-A or GFP-ANCHRΔMIM1-B analysed by western blotting using antibodies against GFP and VPS4. **(G)** Representative confocal images showing the intensity of VPS4 at the midbody ring in cells expressing GFP-ANCHR, GFP-ANCHRΔMIM1-A or GFP-ANCHRΔMIM1-B in the presence of chromatin bridges (arrowheads). Scale bar = 10 μm. The relative VPS4 intensities (percentage) at the ANCHR-positive midbody ring normalized to the mean intensity in untransfected cells and midbody ring levels of RacGAP1 are represented by box plots. Medians are denoted by a solid black line while the edges of the boxes represent the first and third quartile. Whiskers denote minimum and maximum values. n=15, *p<0.05.

Figure 4: ANCHR-mediated cytokinetic arrest is dependent on its interaction with and retention of VPS4 at the midbody ring. (A) HeLa cells were transiently transfected with the indicated fusion protein expression constructs, and after 24 hours fixed and stained for α-tubulin and DNA (Hoechst). Images collected on a high-content ScanR microscope were then scored manually to quantify cells in cytokinesis. Values are given as the mean fraction of the transfected (GFP-positive) cell population from three independent experiments ± SD, n>50 per experiment, *p<0.05. **(B)** Classification of ANCHR-depleted, untransfected, GFP-ANCHR-transfected or GFP-ANCHRΔMIM1-A-transfected cytokinetic cells according to the visible localization of VPS4 to the mitotic spindle (early cytokinetic cells), the midbody ring (late cytokinetic cells), or neither, from three independent experiments ± SD, n=100 per experiment. **p<0.01 and *p<0.05. Representative confocal images showing ANCHR, VPS4 and DNA (Hoechst) are included as illustrations. Scale bar = 2 μm. **(C)** Untransfected or GFP-ANCHR-transfected HeLa cells stably expressing mEOS2-VPS4A were photoconverted at the midbody, and the residence time of the red fluorescent form of mEOS2 inside the bleaching ROI was measured every 7.5 seconds for a total of 225 seconds. The half-life of the fluorescence residence time is shown, with error bars denoting the 95% confidence interval. Untransfected: n=17, GFP-ANCHR-transfected: n=20. **p<0.01. **(D and E)** Quantification of untreated or AZD1152-treated (1 μM for 1 hour) GFP-ANCHR-transfected cytokinetic cells according to the visible localization of VPS4 to the midbody ring or abscission zone, from three independent experiments ± SD, n=100 per experiment, **p<0.01 and *p<0.05. Representative confocal images (E) showing GFP-ANCHR, VPS4 and α-tubulin. Open arrowhead = abscission zone. Scale bar = 2 μm.

Figure 5: ANCHR and CHMP4C function in a cooperative and Aurora B-dependent manner to retain VPS4 at the midbody. (A) HeLa cells were transfected with siRNAs as indicated, and after 72 hours fixed and stained for α-tubulin, Aurora B and DNA

(Hoechst). Images collected on a high-content ScanR microscope were then scored manually to quantify cells in cytokinesis and multinuclear cells. Values are given as the mean fraction of the total cell population from four independent experiments ± SD, normalized to the respective non-targeting siRNA control, n>200 per experiment, n.s. = non-significant. **(B)** HeLa cells were transfected with siRNAs as indicated, and after 48 hours transfected with DNA as indicated. After another 24 hours, cells were fixed and stained for α-tubulin and DNA (Hoechst). Images collected on a high-content ScanR microscope were then scored manually to quantify cells in cytokinesis. Values are given as the mean fraction of the total cell population from three independent experiments ± SD, n>50 per experiment, **p<0.01, *p<0.05. **(C)** HeLa cells were transfected with DNA as indicated, where transgenes were expressed by a weak PGK promoter. After 24 hours, cells were fixed and stained for α-tubulin and DNA (Hoechst). Images collected on a high-content ScanR microscope were then scored manually to quantify cells in cytokinesis. Values are given as the mean fraction of the total cell population from three sets of images per condition ± SD, n>50. **p<0.01, *p<0.05. **(D)** Representative confocal images showing the localization of GFP-CHMP4C and VPS4 at the midbody ring during late cytokinesis. The cells were co-stained for DNA (Hoechst). Scale bar = 10 μm. **(E)** The relative VPS4 intensities (percentage) at the midbody ring normalized to the mean intensity in untransfected cells are represented by box plots. Medians are denoted by a solid black line while the edges of the boxes represent the first and third quartile. Whiskers denote minimum and maximum values. n=15, **p<0.01. **(F)** GFP-trap immunoprecipitates (IP) from HeLa cells expressing GFP or GFP-CHMP4C ± AZD1152 (2 μM for 2.5 hours) analysed by western blotting using antibodies against GFP and VPS4. **(G)** Representative confocal images showing the localization of GFP-CHMP4C and endogenous ANCHR at the midbody ring during late cytokinesis. The cells were co-stained with anti-α-tubulin and for DNA (Hoechst). Scale bar = 10 μm. **(H)** Representative confocal images showing the localization of GFP-ANCHR, V5-CHMP4C

and endogenous VPS4 at the midbody ring during late cytokinesis. The cells were co-stained for DNA (Hoechst). Scale bar = 10 μm. **(I)** GFP-trap immunoprecipitates (IP) from HeLa cells expressing GFP or GFP-ANCHR with V5-CHMP4C ± AZD1152 (2 μM for 2.5 hours) analysed by western blotting using antibodies against GFP and V5. **(J)** Model for the ANCHR-mediated regulation of VPS4 upon abscission checkpoint activation. At late cytokinesis, until abscission checkpoint signalling is terminated, ANCHR and CHMP4C retain abscission-competent VPS4 at the midbody ring. Upon deactivation of Aurora B, dephosphorylation of CHMP4C results in dissociation of the ANCHR/CHMP4C/VPS4 ternary complex. Consequently, VPS4 can presumably migrate to the abscission zone to mediate the final stages of abscission through its effects on ESCRT-III.

Figure 1

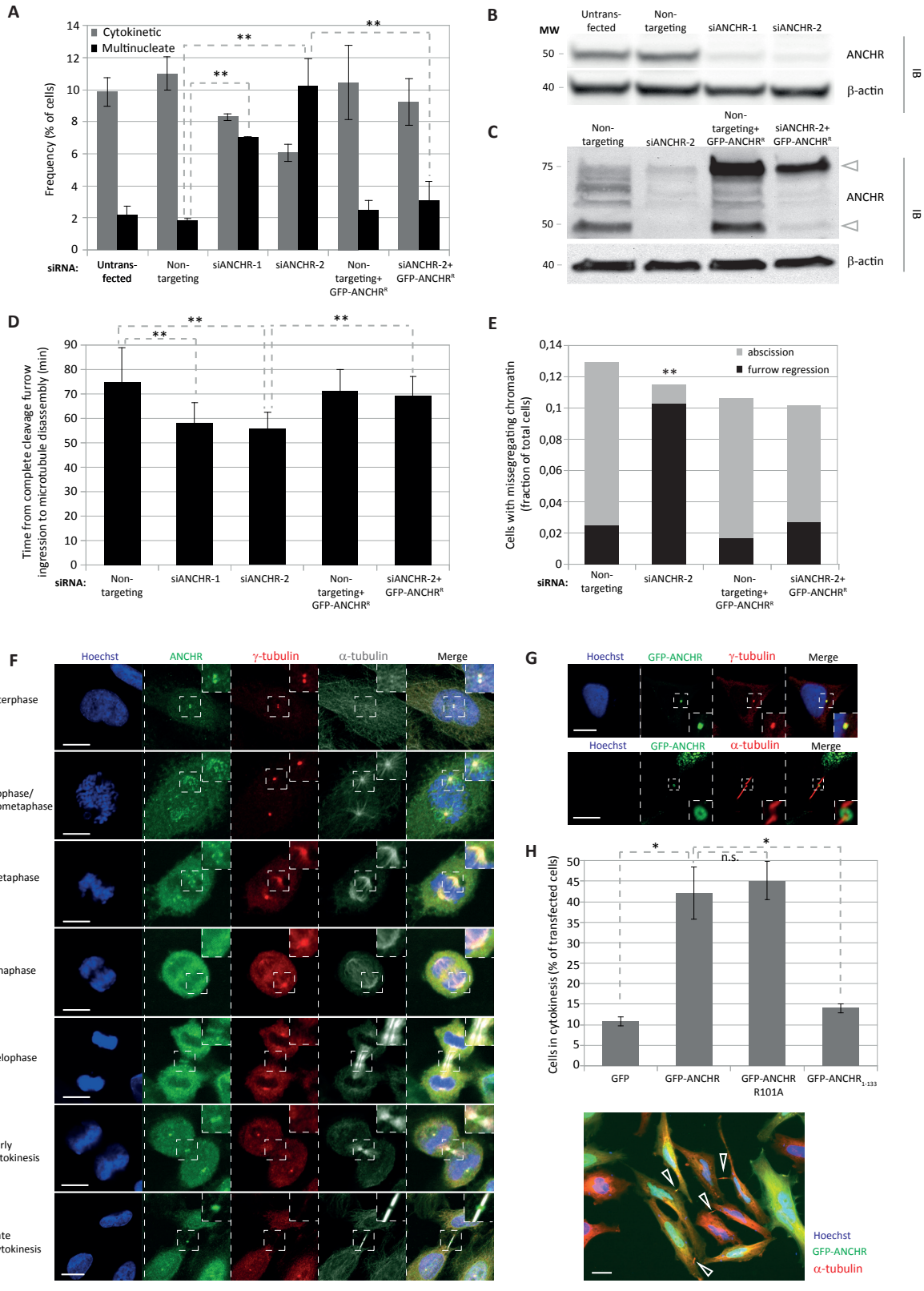
A
Cytokinetic
Multinucleate
Frequency (% of cells)
siRNA:
Untrans-fected
Non-targeting
siANCHR-1
siANCHR-2
Non-targeting+ GFP-ANCHR^R
siANCHR-2+ GFP-ANCHR^R
B
MW
Untrans-fected
Non-targeting
siANCHR-1
siANCHR-2
ANCHR
β-actin
IB
C
Non-targeting
siANCHR-2
Non-targeting+ GFP-ANCHR^R
siANCHR-2+ GFP-ANCHR^R
ANCHR
β-actin
IB
D
Time from complete cleavage furrow ingression to microtubule disassembly (min)
siRNA:
Non-targeting
siANCHR-1
siANCHR-2
Non-targeting+ GFP-ANCHR^R
siANCHR-2+ GFP-ANCHR^R
E
Cells with missegregating chromatin (fraction of total cells)
abscission
furrow regression
siRNA:
Non-targeting
siANCHR-2
Non-targeting+ GFP-ANCHR^R
siANCHR-2+ GFP-ANCHR^R
F
Hoechst
ANCHR
γ-tubulin
α-tubulin
Merge
Interphase
Prophase/ Prometaphase
Metaphase
Anaphase
Telophase
Early cytokinesis
Late cytokinesis
G
Hoechst
GFP-ANCHR
γ-tubulin
Merge
Hoechst
GFP-ANCHR
α-tubulin
Merge
H
Cells in cytokinesis (% of transfected cells)
n.s.
GFP
GFP-ANCHR
GFP-ANCHR R101A
GFP-ANCHR 1-133
Hoechst
GFP-ANCHR
α-tubulin

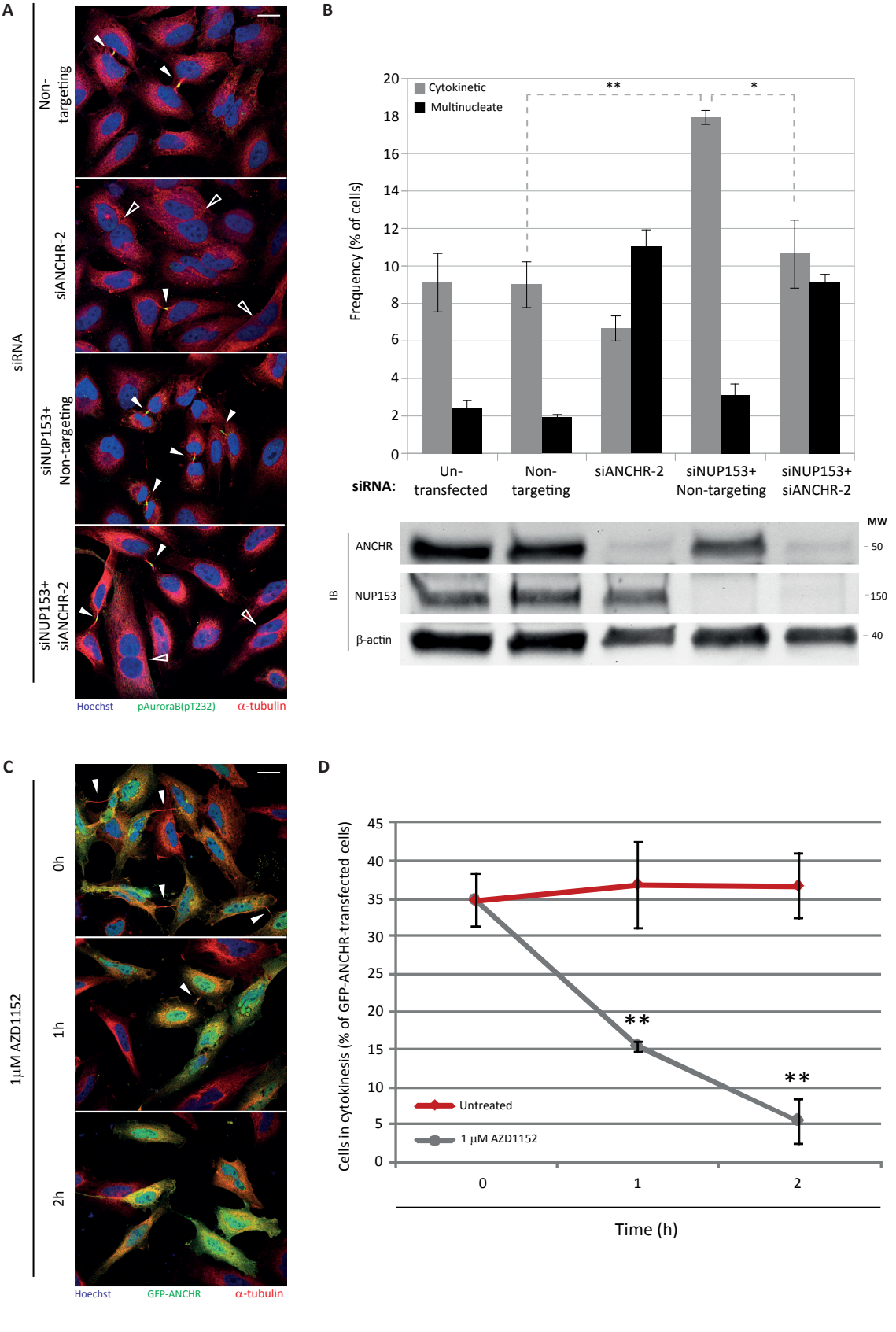
A
siRNA
Non-targeting
siANCHR-2
siNUP153+ Non-targeting
siNUP153+ siANCHR-2
Hoechst
pAuroraB(pT232)
α-tubulin
B
Cytokinetic
Multinucleate
**
*
Frequency (% of cells)
siRNA:
Un-transfected
Non-targeting
siANCHR-2
siNUP153+ Non-targeting
siNUP153+ siANCHR-2
IB
ANCHR
NUP153
β-actin
MW
50
150
40
C
1μM AZD1152
0h
1h
2h
Hoechst
GFP-ANCHR
α-tubulin
D
Cells in cytokinesis (% of GFP-ANCHR-transfected cells)
Untreated
1 μM AZD1152
Time (h)

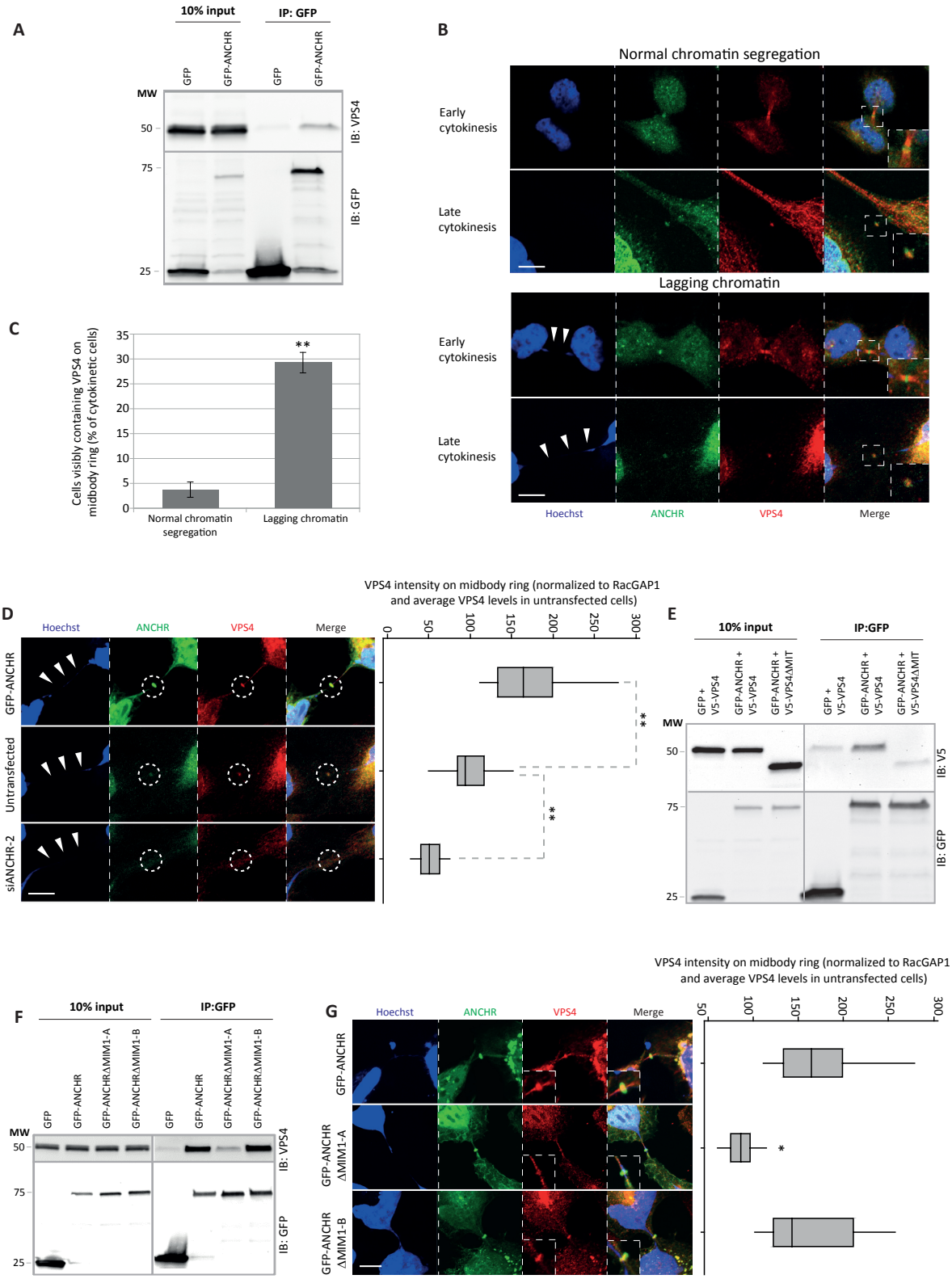
A
10% input
IP: GFP
GFP
GFP-ANCHR
GFP
GFP-ANCHR
MW
50
75
25
IB: VPS4
IB: GFP
B
Normal chromatin segregation
Early cytokinesis
Late cytokinesis
Lagging chromatin
Early cytokinesis
Late cytokinesis
Hoechst
ANCHR
VPS4
Merge
C
Cells visibly containing VPS4 on midbody ring (% of cytokinetic cells)
35
30
25
20
15
10
5
0
**
Normal chromatin segregation
Lagging chromatin
D
Hoechst
ANCHR
VPS4
Merge
GFP-ANCHR
Untransfected
siANCHR-2
VPS4 intensity on midbody ring (normalized to RacGAP1 and average VPS4 levels in untransfected cells)
0
50
100
150
200
250
300
**
**
E
10% input
IP:GFP
GFP + V5-VPS4
GFP-ANCHR + V5-VPS4
GFP-ANCHR + V5-VPS4ΔMIT
GFP + V5-VPS4
GFP-ANCHR + V5-VPS4
GFP-ANCHR + V5-VPS4ΔMIT
MW
50
75
25
IB: V5
IB: GFP
F
10% input
IP:GFP
GFP
GFP-ANCHR
GFP-ANCHRΔMIM1-A
GFP-ANCHRΔMIM1-B
GFP
GFP-ANCHR
GFP-ANCHRΔMIM1-A
GFP-ANCHRΔMIM1-B
MW
50
75
25
IB: VPS4
IB: GFP
G
Hoechst
ANCHR
VPS4
Merge
GFP-ANCHR
GFP-ANCHR ΔMIM1-A
GFP-ANCHR ΔMIM1-B
VPS4 intensity on midbody ring (normalized to RacGAP1 and average VPS4 levels in untransfected cells)
50
100
150
200
250
300
*

Figure 4

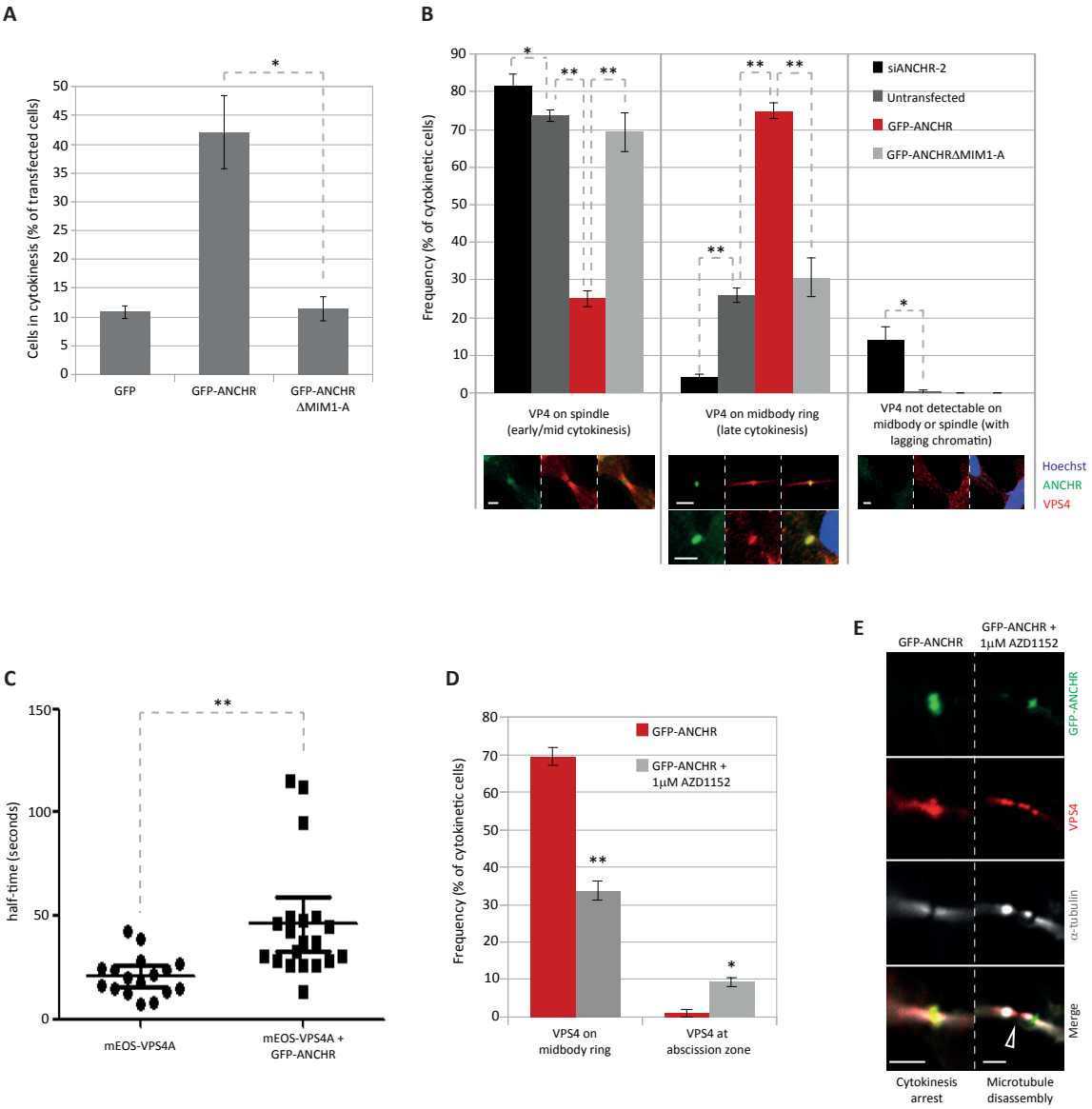
A
Cells in cytokinesis (% of transfected cells)
GFP
GFP-ANCHR
GFP-ANCHR ΔMIM1-A
B
Frequency (% of cytokinetic cells)
siANCHR-2
Untransfected
GFP-ANCHR
GFP-ANCHRΔMIM1-A
VP4 on spindle (early/mid cytokinesis)
VP4 on midbody ring (late cytokinesis)
VP4 not detectable on midbody or spindle (with lagging chromatin)
Hoechst
ANCHR
VPS4
C
Normalized fluorescence residence half-time (seconds)
mEOS-VPS4A
mEOS-VPS4A + GFP-ANCHR
D
Frequency (% of cytokinetic cells)
GFP-ANCHR
GFP-ANCHR + 1μM AZD1152
VPS4 on midbody ring
VPS4 at abscission zone
E
GFP-ANCHR
GFP-ANCHR + 1μM AZD1152
GFP-ANCHR
VPS4
α-tubulin
Merge
Cytokinesis arrest
Microtubule disassembly

Figure 5

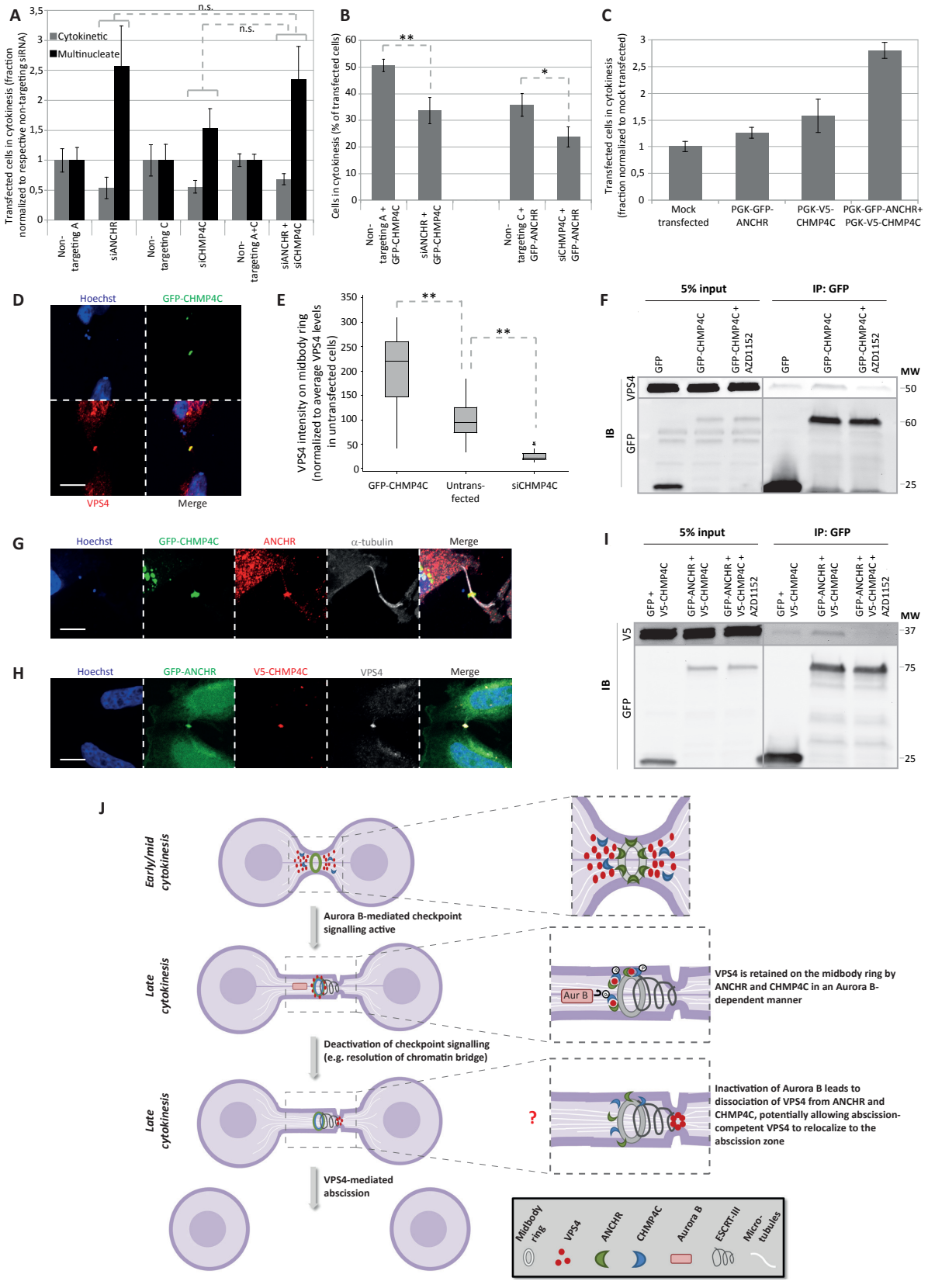
A
Transfected cells in cytokinesis (fraction normalized to respective non-targeting siRNA)
Cytokinetic
Multinucleate
n.s.
n.s.
Non-targeting A
siANCHR
Non-targeting C
siCHMP4C
Non-targeting A+C
siANCHR + siCHMP4C
B
Cells in cytokinesis (% of transfected cells)
**
*
Non-targeting A + GFP-CHMP4C
siANCHR + GFP-CHMP4C
Non-targeting C + GFP-ANCHR
siCHMP4C + GFP-ANCHR
C
Transfected cells in cytokinesis (fraction normalized to mock transfected)
Mock transfected
PGK-GFP-ANCHR
PGK-V5-CHMP4C
PGK-GFP-ANCHR+ PGK-V5-CHMP4C
D
Hoechst
GFP-CHMP4C
VPS4
Merge
E
VPS4 intensity on midbody ring (normalized to average VPS4 levels in untransfected cells)
**
**
*
GFP-CHMP4C
Untrans-fected
siCHMP4C
F
5% input
IP: GFP
GFP
GFP-CHMP4C
GFP-CHMP4C + AZD1152
MW
IB
VPS4
GFP
50
60
25
G
Hoechst
GFP-CHMP4C
ANCHR
α-tubulin
Merge
H
Hoechst
GFP-ANCHR
V5-CHMP4C
VPS4
Merge
I
5% input
IP: GFP
GFP + V5-CHMP4C
GFP-ANCHR + V5-CHMP4C
GFP-ANCHR + V5-CHMP4C + AZD1152
MW
IB
V5
GFP
37
75
25
J
Early/mid cytokinesis
Aurora B-mediated checkpoint signalling active
Late cytokinesis
Aur B
VPS4 is retained on the midbody ring by ANCHR and CHMP4C in an Aurora B-dependent manner
Deactivation of checkpoint signalling (e.g. resolution of chromatin bridge)
Late cytokinesis
?
Inactivation of Aurora B leads to dissociation of VPS4 from ANCHR and CHMP4C, potentially allowing abscission-competent VPS4 to relocalize to the abscission zone
VPS4-mediated abscission
Midbody ring
VPS4
ANCHR
CHMP4C
Aurora B
ESCRT-III
Micro-tubules

SUPPLEMENTARY METHODS:

Liposome binding assay

Biotin-labelled PolyPIPosomes (Echelon Biosciences) were incubated with GST-ANCHR protein and reaction buffer (1 mM dithiothreitol (DTT), 2% protease inhibitor cocktail, 0.1% BSA, 10 μM $ZnCl_2$ in 30 mM Tris-HCl / 150 mM NaCl buffer) for 1 h with rotation at 4 °C. Thereafter, pre-washed streptavidin beads from Dynabeads (Dynal, Invitrogen) were added to the reaction and incubated for further 1 h, rotating at 4 °C. After washing, the samples were boiled in SDS-sample buffer for 10 min and analysed by SDS-PAGE on a 4–20% gradient gel and immunoblotting using anti-GST horseradish peroxidase (HRP)-conjugated antibody.

Recombinant protein expression, *in vitro* and *in vivo* kinase assays

GST-ANCHR and GST alone were expressed overnight at 12 ˚C in ArcticExpress (BL21 derived) bacteria. Cells were lysed and GST fusions were purified using glutathione-sepharose beads, eluted with 10mM reduced glutathione, and dialyzed overnight against 50mM HEPES KOH (pH 7.5), 150mM NaCl and 0.2mM EGTA.

In vitro kinase assays were performed by incubating 5μg of purified recombinant protein with 50ng active Aurora B (Millipore) and 5μCi of g ^{33}P-ATP in reaction buffer (25mM HEPES KOH (pH 7.5), 125mM NaCl, 10mM $MgCl_2$, 10mM sodium pyrophosphate and 2mM DTT) for 15 minutes at 30˚C. Reactions were terminated by addition of 2x Laemmli buffer, boiled and subjected to SDS-PAGE electrophoresis. For determination of radioactivity incorporation, proteins were transferred to PVDF, exposed to a phospho-imager screen (KODAK) and visualized using a Pharos. Total protein content was determined by coomassie staining.

For in vivo phopshorylation assays, following transfection, cells were incubated in phosphate-free medium, complemented with dialyzed FBS and 25μCi/ml [33P]-phosphate for 16 hours, followed by treatment for 2.5 hours with 1μM AZD1152 where indicated.

Mass spectrometry

For mass spectrometry analysis of ANCHR interactors, approximately 2x10^7 cells were transfected with 32 mg DNA per condition, and after 24 hours the resulting lysate was subjected to GFP-trap immunoprecipitation and SDS-PAGE followed by coomassie staining. Visible bands were excised and sent for mass spectrometric analysis performed by Probe (Bergen, Norway).

For mass spectrometry analysis of moderate level ANCHR-VPS4 interactions, immunoprecipitates from whole lysates from HeLa cell lines stably expressing GFP-ANCHR or GFP-VPS4A (approx. 5*10^7cells per sample) were analysed by the Proteomics Core Facility (Oslo University Hospital).

For phosphorylation of ANCHR, the reaction output from in vitro kinase assays were analysed by mass spectrometry by J.S.A. at the Department of Biochemistry and Molecular Biology, University of Southern Denmark, Odense, Denmark.

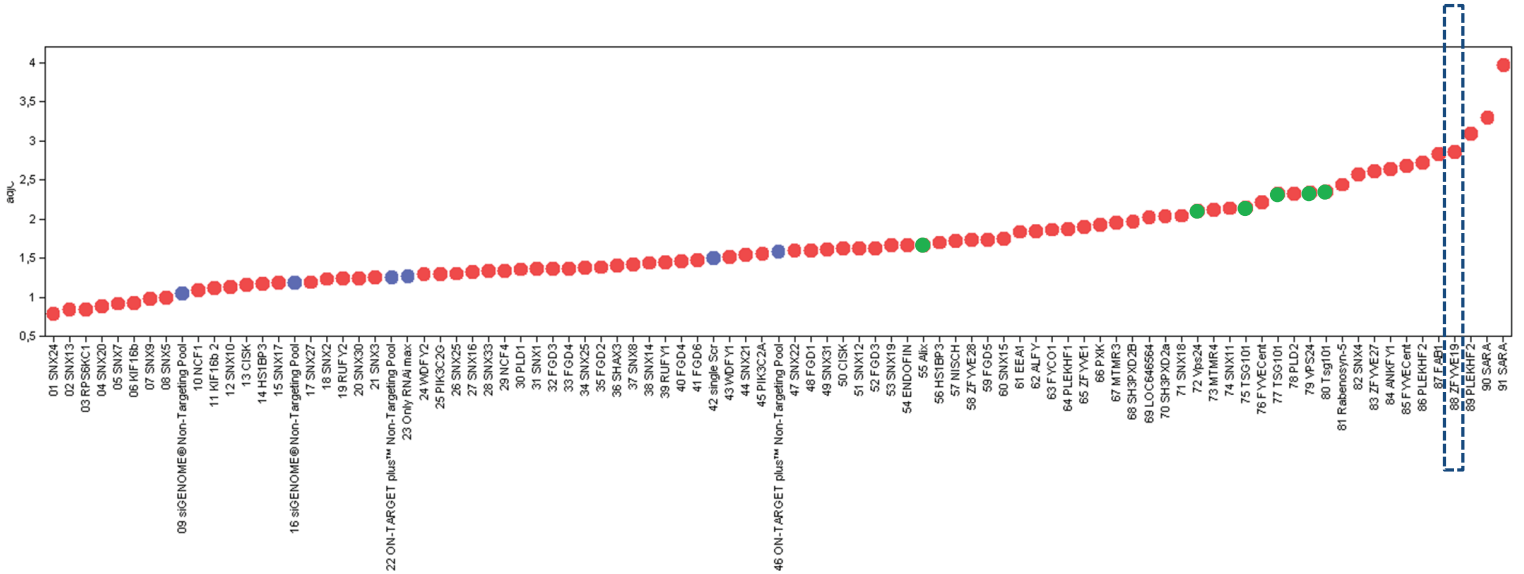

Figure S1: The FYVE domain protein ANCHR (ZFYVE19) regulates abscission. HeLa cells were transfected with smart-pool siRNAs targeting thePtdIns(3)P-binding FYVE- and PX- domain families of proteins, and after 72 or 96 hours fixed and stained for a-tubulin, Aurora B and DNA (Hoechst). Images collected on a high-content ScanR microscope were then scored manually to quantify multinuclear cells. The values obtained are ranked in ascending order according to the frequency of multinuclear cells. Each dot represents the average of four individual observations. Red dots represent PtdIns(3)P-binding proteins, while green and blue dots represent positive and negative controls, respectively. Dashed box highlights ANCHR (ZFYVE19).

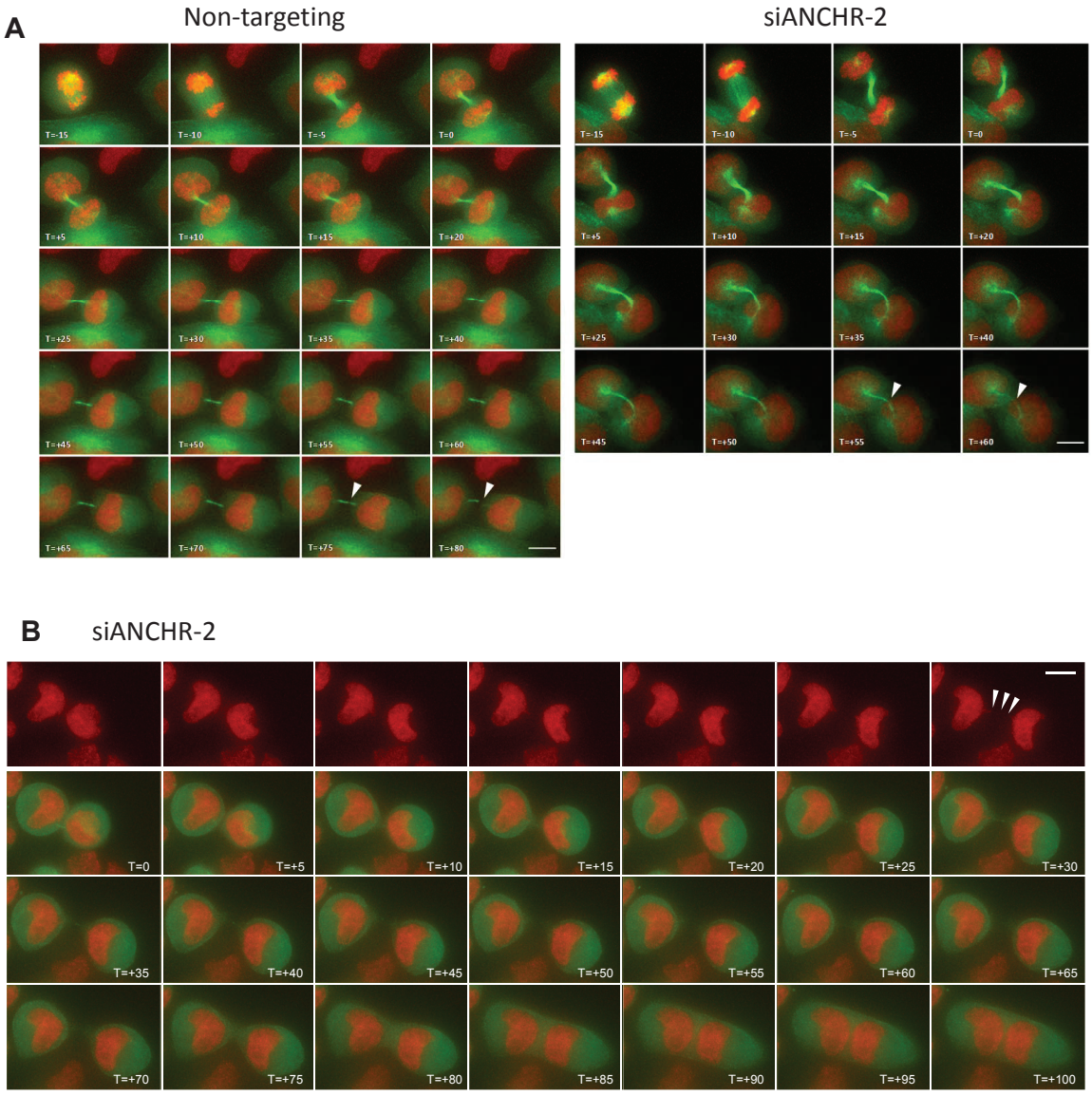

Figure S2: ANCHR (ZFYVE19) regulates abscission timing and prevents cleavage furrow regression in the presence of lagging chromatin. Montage showing sequential images of asynchronous HeLa cells expressing GFP-a-tubulin and mCherry-H2B treated with siRNAs through cytokinesis, with a time interval of 5 min. T=time, T=0 defined as the point of complete cleavage furrow ingression. Scale bar = 10 uM. **(A)** Arrows indicate microtubule disassembly **(B)** Arrows indicate lagging anaphase chromatin.

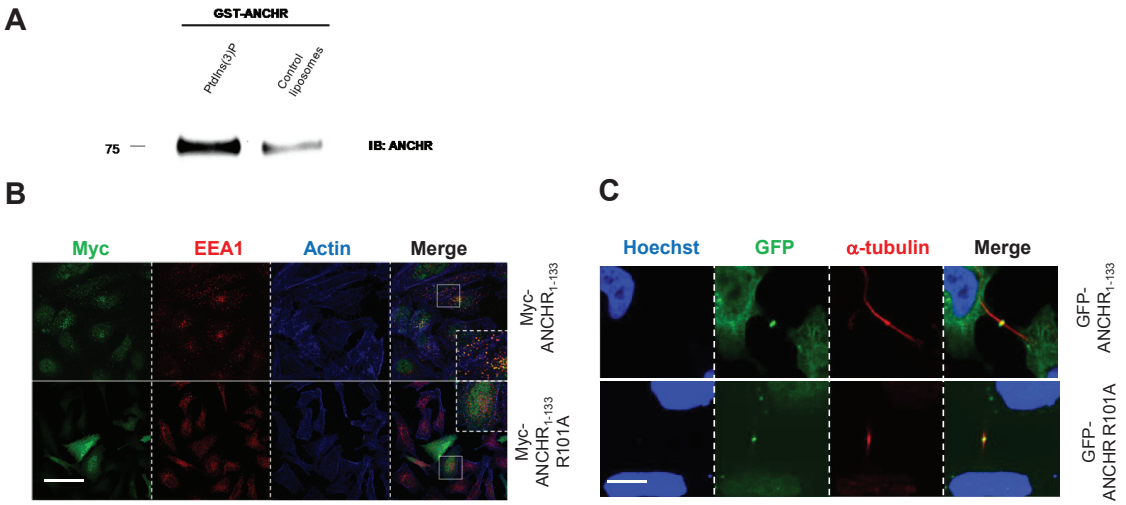

Figure S3: ANCHR (ZFYVE19) binds PtdIns(3)P. (A) Immunoblot showing GST alone or GST-ANCHR incubated with PtdIns(3)P-liposomes. **(B)** Representative confocal images showing the localization of Myc-ANCHR$_{1-133,}$ but not Myc-ANCHR$_{1-133}$R101A to PtdIns(3)P-rich early endosomes. The cells were co-stained with antibodies against the early endosome marker EEA1 and Actin. Scale bar = 20 uM. **(C)** Representative confocal images showing the localization of GFP-ANCHR$_{1-133}$ and GFP-ANCHR R101A to the midbody. The cells were co-stained with antibodies against a-tubulin and DNA (Hoechst). Scale bar = 10 uM.

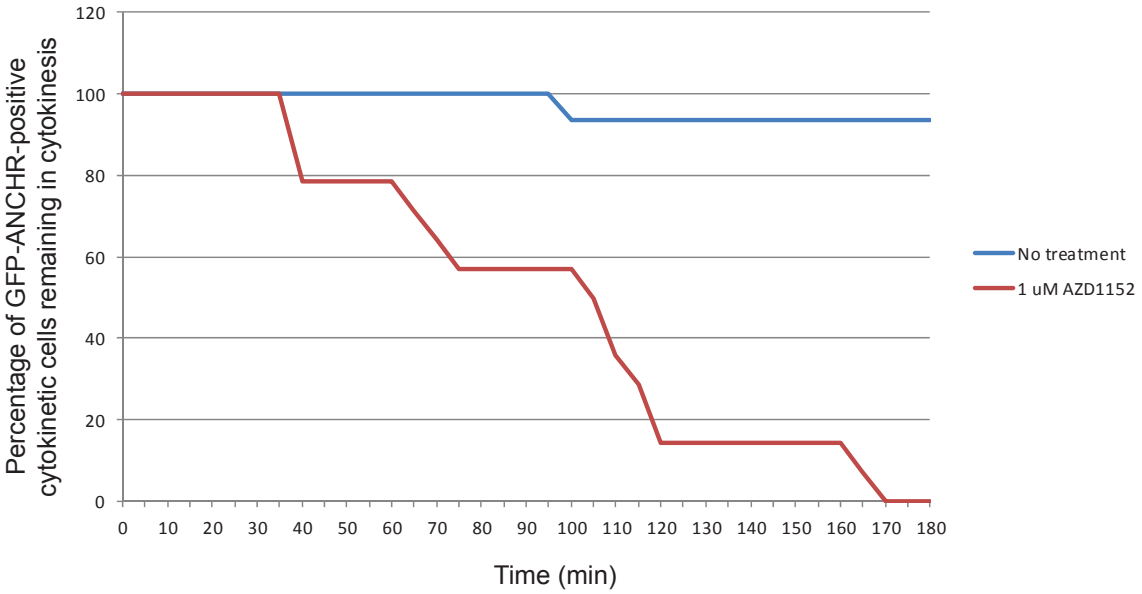

Figure S4: ANCHR-overexpression-induced cytokinetic arrest requires Aurora B activity. HeLa cells stably expressing mCherry-H2B (Histone/DNA marker) were transiently transfected with GFP-ANCHR and after 24 hours cells arrested in cytokinesis were either treated with 1 μM AZD1152 or left untreated and imaged live for a total of 3 hours. The graph shows the fraction of arrested cells remaining in cytokinesis as a function of time (min).

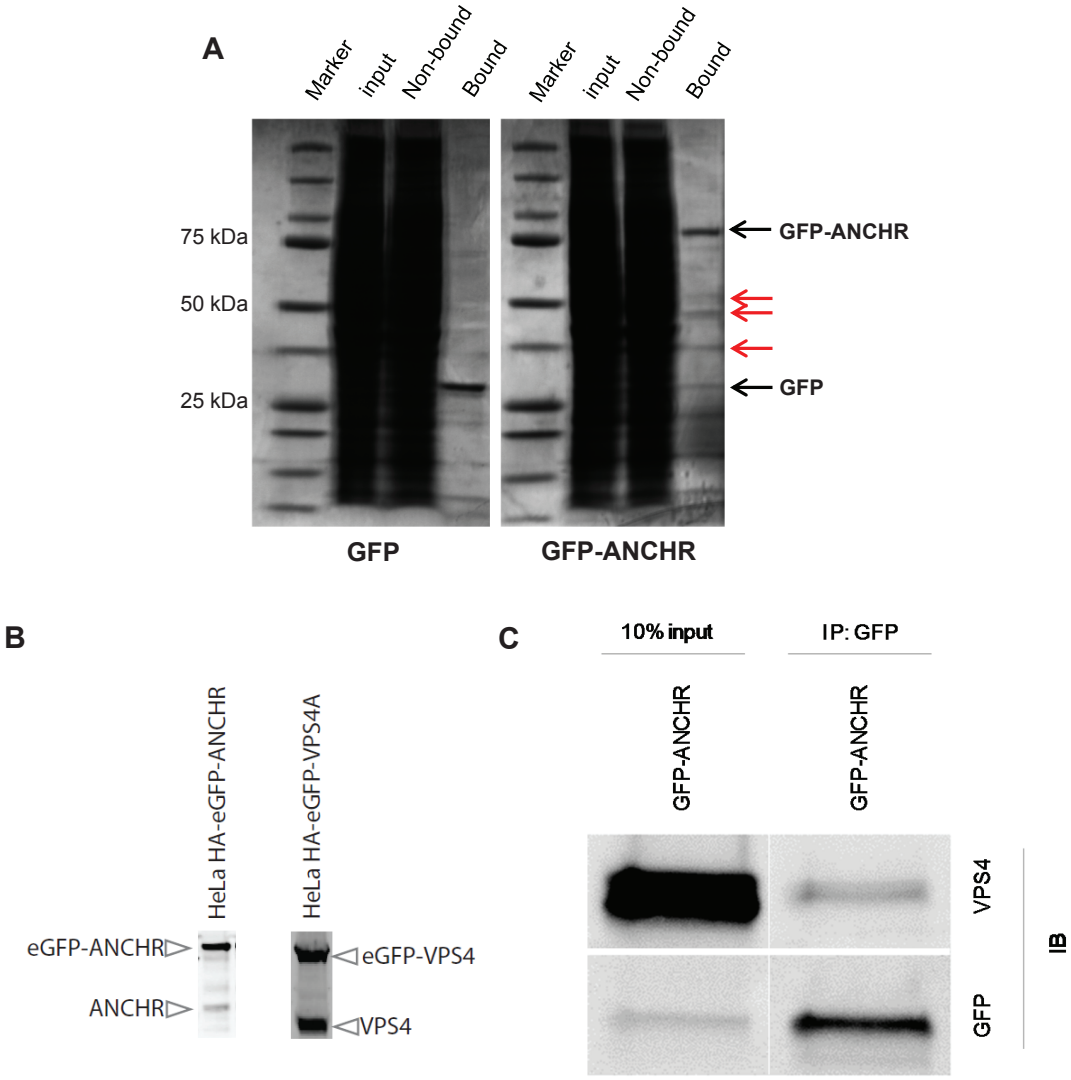

Figure S5: ANCHR interacts with VPS4 at overexpressed and moderate, non-arresting levels. (A) Coomassie-stained gel of GFP-trap lysates used for mass spectromeric analysis of proteins interacting with overexpressed GFP or GFP-ANCHR. Black arrows indicate GFP and GFP-ANCHR. Red arrows indicate bands specifically detected in the GFP-ANCHR pull down which were excised and sent for mass spec analysis. **(B)** Western blot analysis of lysates from stable transgenic HeLa lines used for mass spec analysis presented in supplementary table S2, probed with anti-ANCHR (left panel) or anti-VPS4 (right panel) antibodies to determine the expression level of transgene compared to endogenous allele. Quantification indicated that the eGFP-ANCHR transgene was overexpressed 6 fold compared to endogenous, whereas eGFP-VPS4 levels were equal to endogenous. **(C)** GFP-trap immunoprecipitates (IP) from HeLa cells stably expressing GFP-ANCHR analysed by western blotting using antibodies against GFP and VPS4.

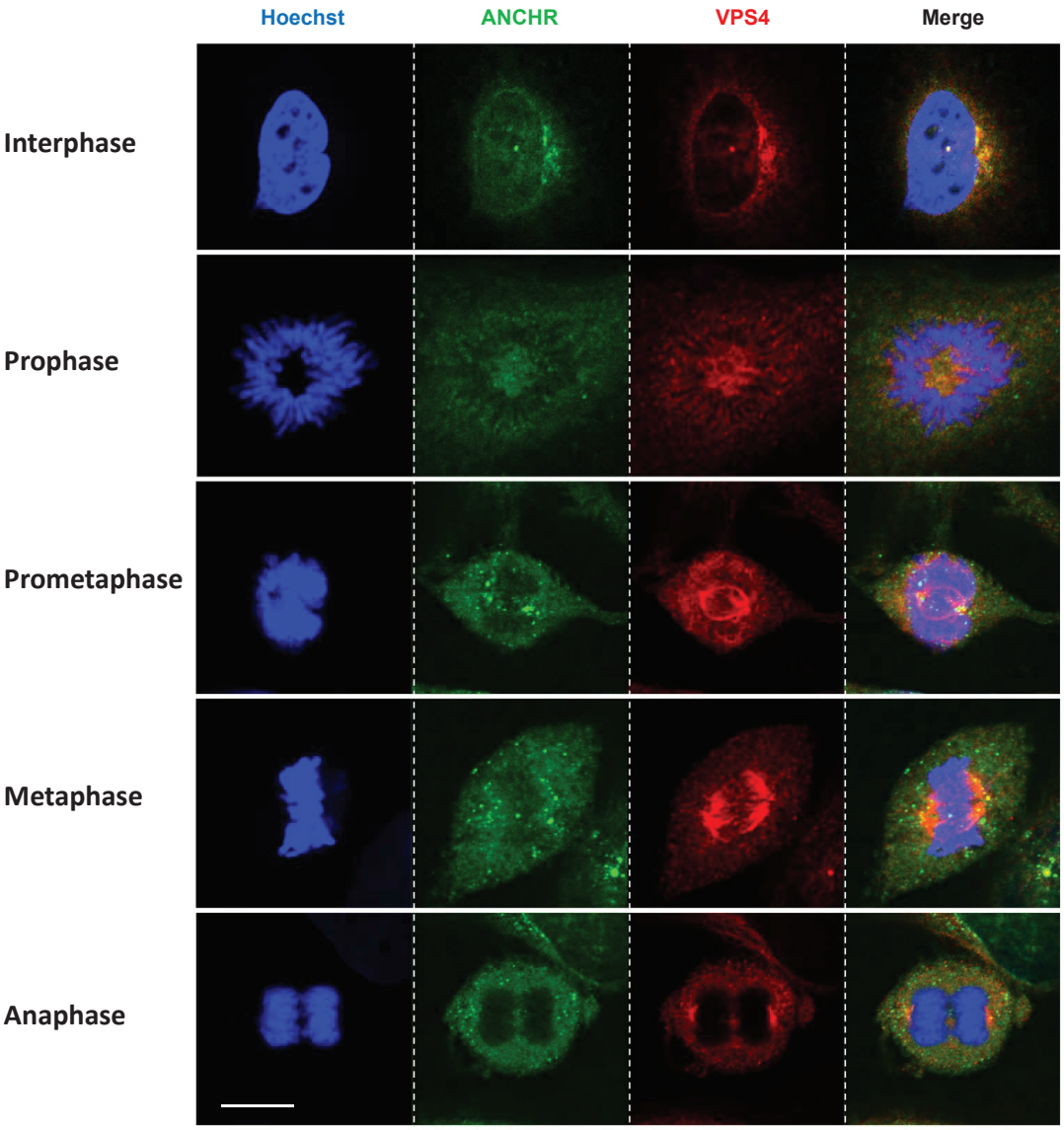

Figure S6: Localization of ANCHR and VPS4 during interphase and early mitosis. Representative confocal images showing HeLa cells stained with antibodies against endogenous ANCHR and VPS4, and DNA (Hoechst). Scale bar = 10 uM.

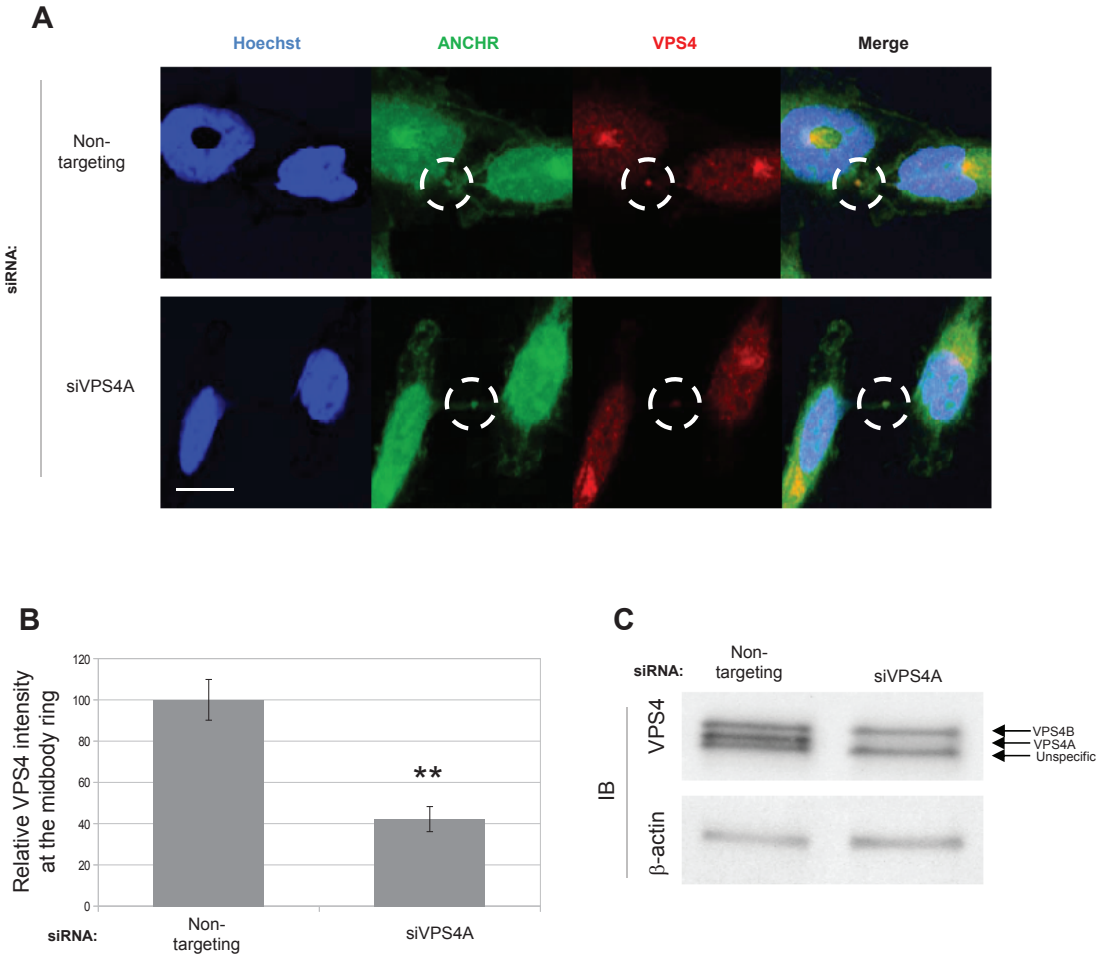

Figure S7: Specificity of the VPS4 antibody. HeLa cells were treated with either non-targeting siRNA or VPS4A siRNA for 72 hours and stained with antibodies against endogenous ANCHR and VPS4, and DNA (Hoechst). **(A)** Representative confocal images showing late cytokinetic cells containing chromatin bridges. Circles highlight the midbody ring. Scale bar = 10 uM. **(B)** Quantitation of VPS4 intensities on midbody rings. **(C)** Western blot from whole cell lysates blotted for VPS4 and β-actin. Arrows indicate VPS4B (top), VPS4A (middle) and an unspecific band (bottom).

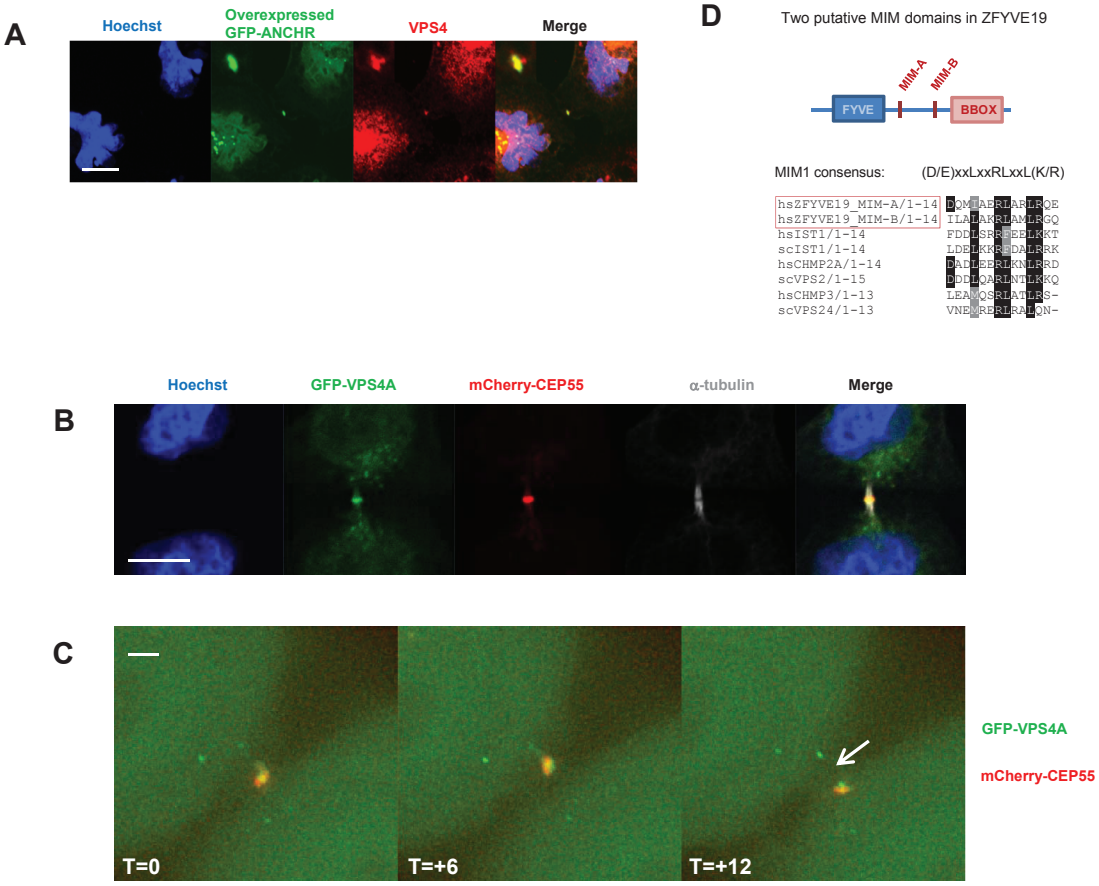

Figure S8: ANCHR interacts with VPS4 at the midbody (A) Representative confocal images showing GFP-ANCHR and endogenous VPS4 at the midbody in a normally segregating cell. The cells were co-stained with Hoechst (DNA). Scale bar = 10 uM. **(B)** Representative confocal images from HeLa cells stably expressing GFP-VPS4A and mCherry-CEP55 showing their colocalization at the Flemming body/midbody ring. The cells were co-stained with antibodies against a-tubulin and DNA (Hoechst). Scale bar = 10 uM **(C)** Montage showing sequential images of a HeLa cell expressing GFP-VPS4 and mCherry-CEP55, with a time interval of 5 min. GFP-VPS4 co-localizes with the mCherry-CEP55-positive Flemming body/midbody ring prior to abscission. Arrow indicates severed cytokinetic bridge. Scale bar = 2 uM. **(D)** The structure of ANCHR showing the defined domains, including the MIM-A and MIM-B. Alignment of the ANCHR MIM-A and MIM-B with other type-1 MIMs from different ESCRTs.

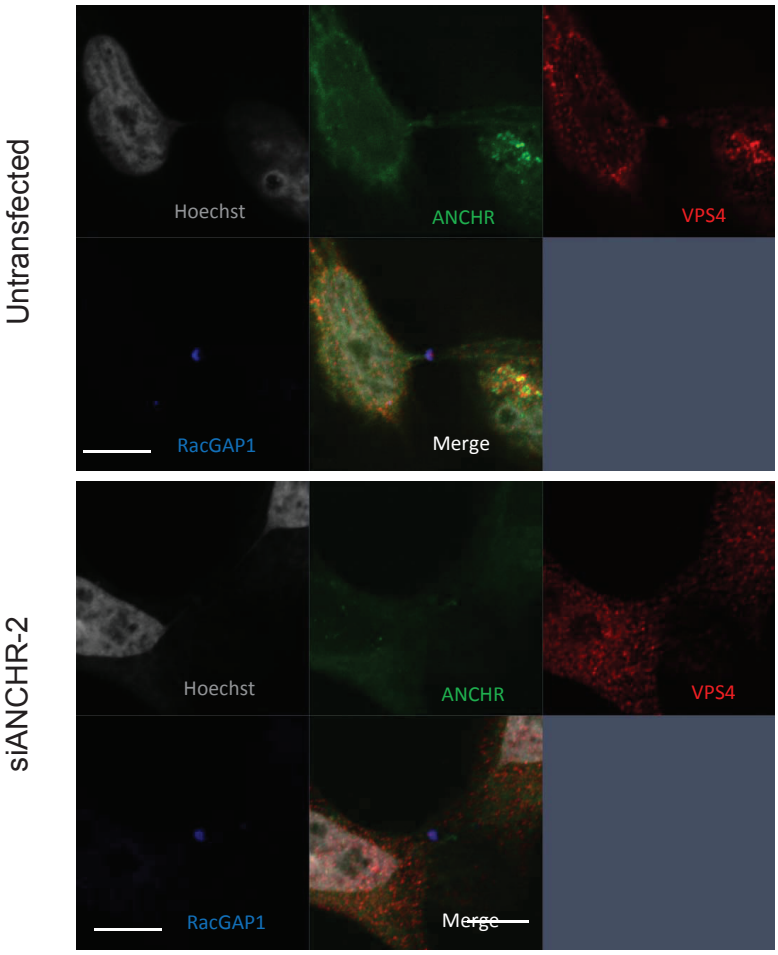

Figure S9: The midbody is intact in ANCHR-depleted cells. Representative confocal images showing ANCHR, VPS4 and RacGAP1 at the midbody in untransfected (left panel) or ANCHR-depleted (right panel) cells. The cells were co-stained with Hoechst (DNA). Scale bar = 10 uM.

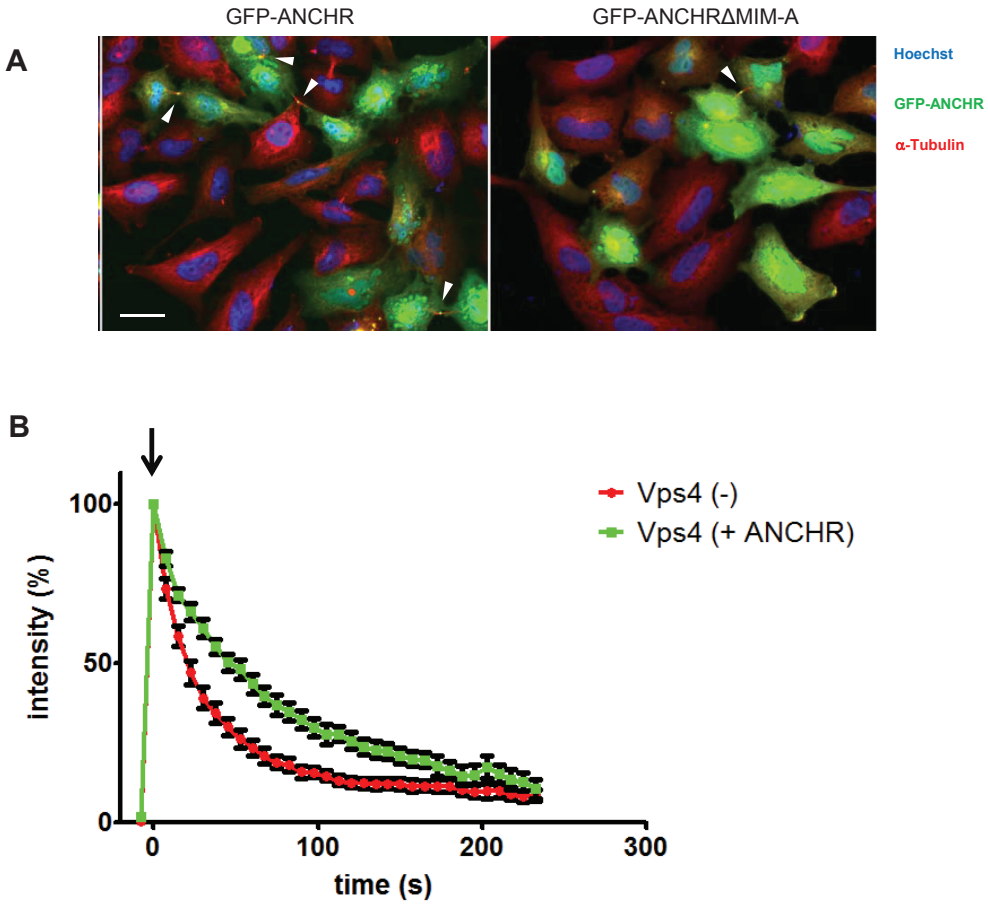

Figure S10: ANCHR-mediated cytokinetic arrest is dependent on its interaction with and retention of VPS4 at the midbody ring. (A) Representative images collected on a high-content ScanR microscope showing HeLa cells 24 hours after being transiently transfected with the indicated fusion protein expression constructs, and fixed and stained for a-tubulin and DNA (Hoechst). Deletion of the MIM-A abolishes GFP-ANCHR induced cytokinetic arrest. Scale bar = 10 uM. **(B)** Photoconversion of mEOS2-VPS4 in untransfected or GFP-ANCHR-transfected HeLa cells. Midbody-localized VPS4 was photoconverted by illuminating a small region of interest (ROI) at the midbody and the residence time of the red fluorescent form of mEOS2 inside the bleaching ROI was measured every 7.5 s for a total of 225 s. Photoconversion kinetics are plotted showing means of all experiments ± S.E.M. (untransfected: n=17, GFP-ANCHR-transfected: n=20). The arrow indicates the time of photoconversion.

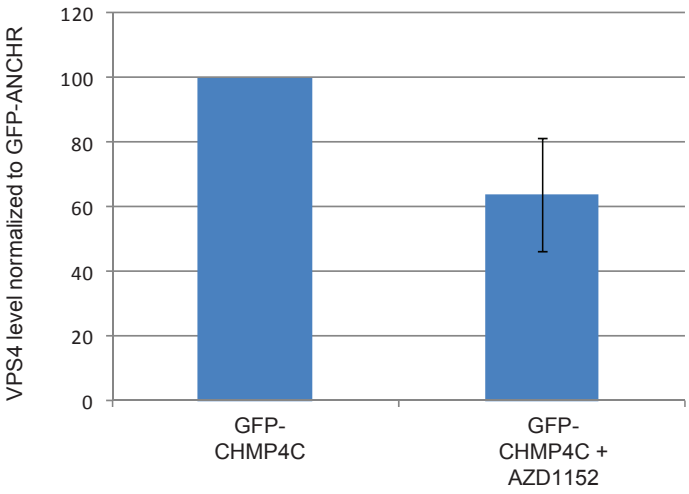

Figure S11: VPS4 interaction with CHMP4C is reduced upon Aurora B inhibition. Quantitation of VPS4 from GFP-trap blots illustrated in Fig. 5F. Values are averaged from three independent experiments.

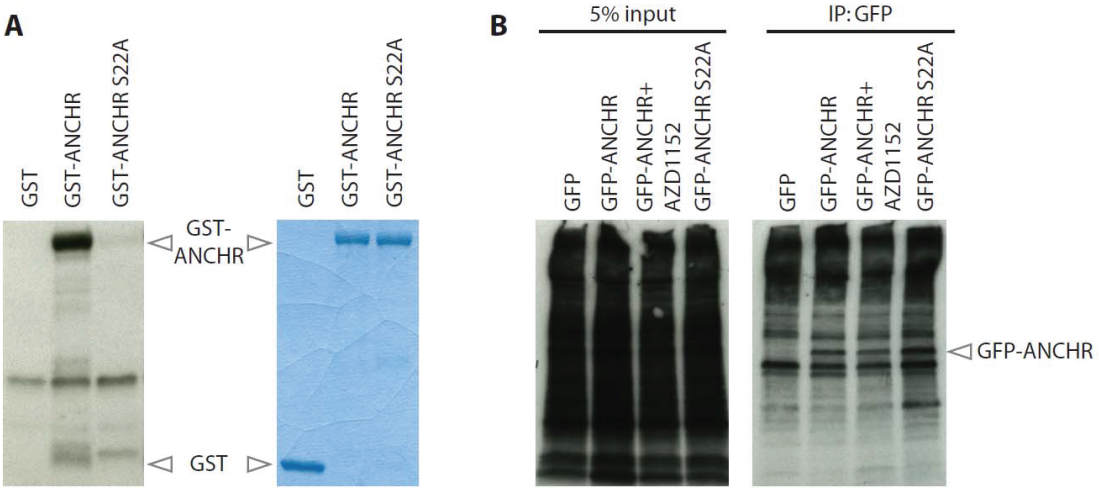

Figure S12: *In vitro* and *in vivo* phosphorylation of ANCHR. (A) ANCHR can be phosphorylated by Aurora B at S22 *in vitro*. *In vitro* kinase assays using purified recombinant GST or GST-ANCHR, incubated with active Aurora B kinase in the presence of 33P. Incorporation of 33P was visualized by autoradiography, protein loading was assessed by coomassie staining. Mass spectrometry analysis (supplementary table S3) of *in vitro* phosphorylated GST-ANCHR using the non-radioactive phosphorus isotope identified S22 as the dominant phosphorylation site. Subsequent in vitro kinase assays using mutated GST-ANCHR S22A abolished phosphorylation by Auorora B, indicating that S22 is the sole Aurora B target in ANCHR *in vitro*. **(B)** ANCHR is not a prominent Aurora B target *in vivo*. HeLa cells transfected with the indicated constructs were labelled with ^{33}P overnight, and treated with 1 μM AZD1152 for 2.5 hours where indicated. Following lysis, GFP-fusions were immunoprecipitated using GFP antibodies. Incorporation of ^{33}P was evaluated by autoradiography.

III